NUREG/CR-3295
MEA-2017
Vol. 2

Light Water Reactor Pressure Vessel Surveillance Dosimetry Improvement Program

Postirradiation Notch Ductility and Tensile Strength Determinations for PSF Simulated Surveillance and Through-Wall Specimen Capsules

Prepared by J. R. Hawthorne, B. H. Menke

Materials Engineering Associates, Inc.

ENSA, Inc.

Prepared for
U.S. Nuclear Regulatory Commission

NOTICE

This rep[illegible]s prepared as an account of work sponsored by an agency of the United States Government. Neither the United States Government nor any agency thereof, or any of their employees, makes any warranty, expressed or implied, or assumes any legal liability of responsibility for any third party's use, or the results of such use, of any information, apparatus, product or process disclosed in this report, or represents that its use by such third party would not infringe privately owned rights.

NOTICE

Availability of Reference Materials Cited in NRC Publications

Most documents cited in NRC publications will be available from one of the following sources:

1. The NRC Public Document Room, 1717 H Street, N.W.
   Washington, DC 20555
2. The NRC/GPO Sales Program, U.S. Nuclear Regulatory Commission,
   Washington, DC 20555
3. The National Technical Information Service, Springfield, VA 22161

Although the listing that follows represents the majority of documents cited in NRC publications, it is not intended to be exhaustive.

Referenced documents available for inspection and copying for a fee from the NRC Public Document Room include NRC correspondence and internal NRC memoranda; NRC Office of Inspection and Enforcement bulletins, circulars, information notices, inspection and investigation notices; Licensee Event Reports; vendor reports and correspondence; Commission papers; and applicant and licensee documents and correspondence.

The following documents in the NUREG series are available for purchase from the NRC/GPO Sales Program: formal NRC staff and contractor reports, NRC-sponsored conference proceedings, and NRC booklets and brochures. Also available are Regulatory Guides, NRC regulations in the *Code of Federal Regulations*, and *Nuclear Regulatory Commission Issuances*.

Documents available from the National Technical Information Service include NUREG series reports and technical reports prepared by other federal agencies and reports prepared by the Atomic Energy Commission, forerunner agency to the Nuclear Regulatory Commission.

Documents available from public and special technical libraries include all open literature items, such as books, journal and periodical articles, and transactions. *Federal Register* notices, federal and state legislation, and congressional reports can usually be obtained from these libraries.

Documents such as theses, dissertations, foreign reports and translations, and non-NRC conference proceedings are available for purchase from the organization sponsoring the publication cited.

Single copies of NRC draft reports are available free, to the extent of supply, upon written request to the Division of Technical Information and Document Control, U.S. Nuclear Regulatory Commission, Washington, DC 20555.

Copies of industry codes and standards used in a substantive manner in the NRC regulatory process are maintained at the NRC Library, 7920 Norfolk Avenue, Bethesda, Maryland, and are available there for reference use by the public. Codes and standards are usually copyrighted and may be purchased from the originating organization or, if they are American National Standards, from the American National Standards Institute, 1430 Broadway, New York, NY 10018.

GPO Printed copy price: $5.50

NUREG/CR-3295
MEA-2017
Vol. 2
RF, R5

Light Water Reactor Pressure Vessel Surveillance Dosimetry Improvement Program

Postirradiation Notch Ductility and Tensile Strength Determinations for PSF Simulated Surveillance and Through-Wall Specimen Capsules

Manuscript Completed: August 1983
Date Published: April 1984

Prepared by
J. R. Hawthorne, B. H. Menke

Materials Engineering Associates, Inc.
9700 B George Palmer Highway
Lanham, MD 20706

Under Contract to:
ENSA, Inc.
3320 Bailey Avenue
Buffalo, NY 14215

Prepared for
Division of Engineering Technology
Office of Nuclear Regulatory Research
U.S. Nuclear Regulatory Commission
Washington, D.C. 20555
NRC FIN B8133

ABSTRACT

The Light Water Reactor-Pressure Vessel Surveillance Dosimetry Improvement Program of the Nuclear Regulatory Commission (NRC) has irradiated mechanical property test specimens of several steels in a pressure vessel wall/thermal shield mock-up facility. The investigation is part of a broad NRC effort to develop key neutron physics-dosimetry-metallurgy correlations for making highly accurate projections of radiation-induced embrittlement to reactor vessels. The steels studied represent a wide range of radiation embrittlement sensitivities and include plates, forgings and submerged arc weld deposits (two each).

This report presents notch ductility and tensile properties information developed with specimen irradiations at simulated surveillance and in-wall locations. The irradiations were conducted at 288°C; neutron fluences were typical of vessel end-of-life conditions. Data comparisons are used to illustrate the toughness gradient produced by irradiation and to assess the relative irradiation effect at surveillance vs. through-wall positions.

The postirradiation toughness gradient between vessel surface and midwall locations, indexed to the 41 J transition temperature, was found to be small (31°C or less) for five of the six materials. Tensile test observations support the notch ductility trend indications. Simulated surveillance capsule irradiations reproduced reasonably well the embrittlement at vessel inner surface and quarter wall thickness positions in almost all cases. The primary exceptions to both trends were provided by the steel having the highest embrittlement sensitivity (0.23% Cu, 1.58% Ni weld deposit). Aggregate results for this material suggest an independent contribution of high (>1%) nickel contents to radiation sensitivity development and a weld susceptibility to long term time-at-temperature effects.

Candidate areas for future research study are indicated.

CONTENTS

LIST OF FIGURES

Figure		Page

Figure		Page

LIST OF TABLES

ACKNOWLEDGMENTS

The authors express their appreciation to M. Vagins for helpful discussions in the planning of postirradiation tests to best meet the needs of PTS analyses. The authors also thank C.Z. Serpan for his advice on overall PSF program objectives and his encouragement during the conduct of the material evaluations.

The contributions of W. E. Hagel and L. LaMont to the experimental test phase and the assistance of A. L. Hiser, Jr., M. Mayfield and E. D'Ambrosio in report preparation are acknowledged with appreciation. The authors also thank Dr. F. J. Loss for his review and useful comments on the report and its presentation.

1. INTRODUCTION

One objective of the Light Water Reactor-Pressure Vessel (LWR-PV) Surveillance Dosimetry Improvement Program established by the Nuclear Regulatory Commission (NRC), is the development of key information for the accurate projection of radiation-induced mechanical properties changes in reactor vessel walls (Refs. 1,2). The total effort represents a multi-laboratory program with international participation. MEA was given responsibility for the development and analysis of mechanical properties data required for the study.

This report is a sequel to Reference 3 which presented the initial set of postirradiation mechanical properties data from the Program. The initial determinations were for two reference plates irradiated in the form of Charpy-V (C_V), compact tension (CT) and tension (T) test specimens. The plates are known as the ASTM A 302-B Correlation-Monitor Plate and the Heavy Section Steel Technology (HSST) Program A 533-B Plate 03 (Refs. 4,5). For the remaining materials reported upon here, irradiation assembly space was too limited to permit inclusion of CT specimens for parallel fracture toughness determinations. That is, only C_V and T specimens of these materials were irradiated. For simplicity and because of testing schedules, the results were not included in the initial report. The present report, on the other hand, provides a complete compilation of C_V and T data for all of the materials.

Reference 3 provides additional background on the objectives and the approach of the Program. In brief, the investigations were designed to study through-wall toughness gradients produced by 288°C irradiation and to determine the relative irradiation effect at surveillance capsule vs. in-wall locations. Additionally, the study was designed to explore the correspondence of C_V and CT fracture toughness test methods in their independent descriptions of radiation-induced embrittlement for the reactor service case. Six materials (steel plates, forgings, and submerged arc weld deposits) were provided by U.S.A. and overseas laboratories. As will be evident here, the materials represent a broad range of radiation embrittlement sensitivities.

Typically, the task of mechanical properties prediction for vessels reduces to three key components: proper and accurate definition of the neutron field, accurate projection of field attenuation to and through the vessel wall, and proper estimation of the steel's response to the local neutron field. For the conduct of through-wall neutron dosimetry investigations and for through-wall neutron exposures of mechanical test specimens, a pressure vessel mock-up was constructed for the Program at the Oak Ridge Research Reactor (ORR). The facility, known as the Pool Side Facility (PSF), simulates a large segment of a reactor thermal shield and vessel wall (Ref. 2). Here, specimens can be irradiated in sealed capsules under closely controlled temperature conditions at simulated surveillance and through-wall locations.

Figures 1 and 2 are schematic illustrations showing the spatial relationship of the PSF to the ORR fuel core and the locations of individual capsule assemblies. Note that the simulated surveillance capsules are posi-

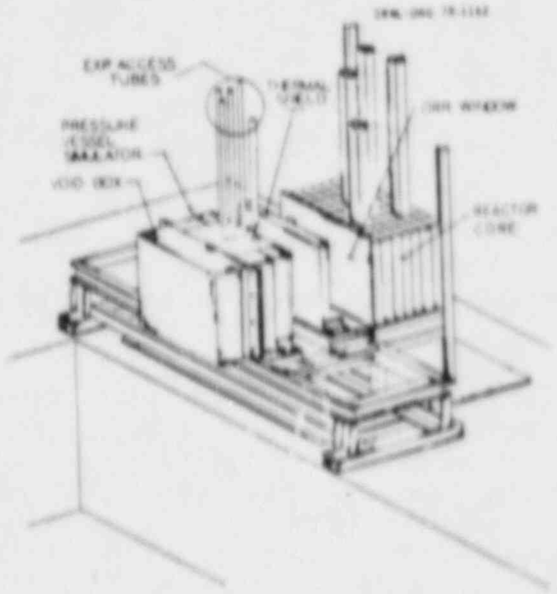

Fig. 1 Schematic illustration of PSF Facility. The pressure vessel simulator and the thermal shield are located outside of the aluminum pressure vessel (not shown) housing the reactor core (courtesy ORNL).

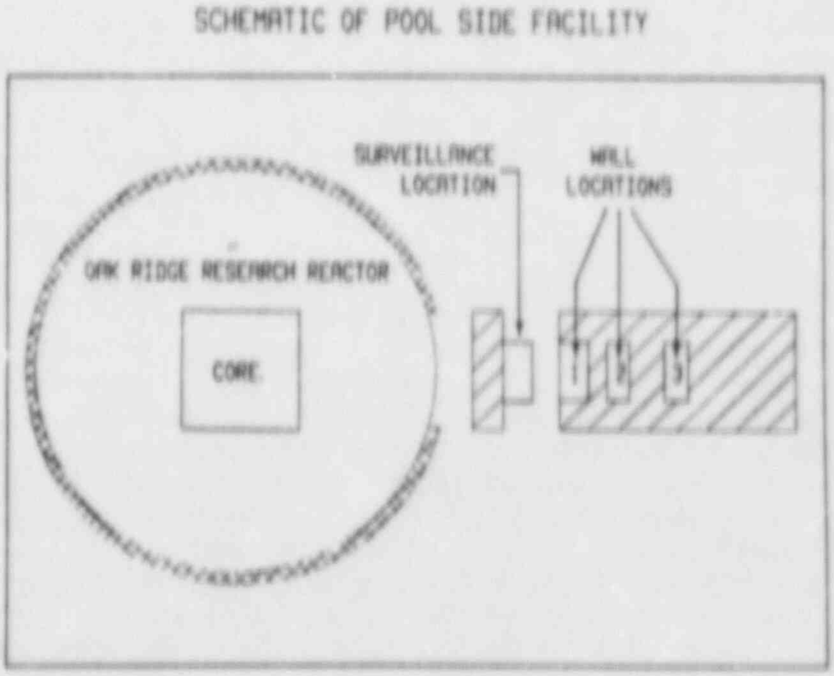

Fig. 2 Schematic illustration of the PSF Facility showing the locations of the specimen capsules in simulated surveillance and through-wall irradiation locations.

tioned at the thermal shield on the side away from the core and that the wall capsules are placed in cavities in the vessel simulator itself. In the present set of experiments, specimen temperatures typically were held within 10°C of the target exposure temperature of 288°C. (For additional details of the PSF pertinent to the specimen irradiations, see Ref. 3.)

To date five capsules have been irradiated (Ref. 6) with the goal of developing physics-dosimetry-metallurgy correlations. Two of the capsules (designated SSC-1 and SSC-2) respectively depict surveillance capsules taken from a pressurized water reactor plant after about 15 years and 30 years of operation, i.e., at plant mid-life and at plant end-of-life. The remaining three capsules (Wall-1, 2 and 3) represent vessel surface (OT), quarter wall thickness (1/4T) and half wall thickness (1/2T) locations. The lead factor, i.e., the ratio of neutron flux levels between the surveillance capsule location and the wall surface location, was about eight for the particular PSF configuration used.

2. MATERIALS

The materials investigated are identified by type, supplier, heat treatment condition and initial yield strength level in Table 1. Table 2 lists the material compositions. The A 302-B plate (Code F23) has seen extensive use in reactor vessel surveillance applications and in test reactor studies (Refs. 4,7). The A 533-B plate (Codes 3PS, 3PT and 3 PU) has been applied as a reference material in the International Atomic Energy Agency's co-ordinated program on the behavior of advanced reactor pressure vessel steels under neutron irradiation (Ref. 8). The respective plates are considered representative of early vessel manufacture and more recent vessel fabrication. The submerged arc weld, Code EC, has been studied extensively by programs at the Naval Research Laboratory (NRL) and at Westinghouse (Nuclear Technology Division) under the sponsorship of the Electric Power Research Institute (EPRI) (Refs. 9, 10). A significant amount of irradiation embrittlement data thus were preexistent for these three materials. Less extensive data were available for the remaining materials at the beginning of the Program.

In Table 2, the materials are seen to differ considerably in their respective contents of copper (an impurity) and nickel (an alloying element). A high copper content in pressure vessel steels is known to be detrimental to radiation embrittlement resistance at 288°C (Ref. 11). For new reactor vessels, a copper content less than 0.10% Cu is now generally specified. Nickel alloying in amounts of 0.4% Ni or more has been found to reinforce or magnify the deleterious effect of a high copper content (Ref. 12). A phosphorus content in amounts of 0.010% or more also has been shown harmful to radiation resistance; the mechanism for its contribution to radiation sensitivity is different from that of copper (Ref. 13). In the present study, the phosphorus contents of the six materials are essentially the same, ranging from 0.007 to 0.011%. Accordingly, phosphorus would not be a factor in materials variability here.

3. SPECIMENS

Standard C_v specimens (ASTM Type A) and 4.52 mm diameter tension specimens were used for making the notch ductility and tensile strength determinations. The respective specimen designs are illustrated in Figs. 3 and 4.

Table 1. Materials

Material	Heat Code	Supplier	Thickness (mm)	Yield[a] Strength (MPa)	Heat Treatment
A 533-B (HSST Plate 03)	3PS, 3PT, 3PU	NRL	305	454	843 to 899°C - 4 h, water quenched 649 to 677°C - 4 h, air cooled 607 to 636°C - 20 h, furnace cooled
A 302-B (ASTM Reference Plate)	F23	NRL	152	482	899°C-6 h, water quenched 649°C-6 h, air cooled
Submerged Arc Weld (Single Vee type, A 533-B Base Plate)	R	Rolls-Royce & Assoc., Ltd.	160	489	920°C ±15°C-6 h, water spray quenched 600°C-6 h, air cooled 600°C-36 h, air cooled 650°C-6 h, air cooled
Submerged Arc Weld (Single Vee type, A 533-B Base Plate)	EC	EPRI	235	456	621°C ±28°C-50 h, furnace cooled
22NiMoCr37 Forging	K	KFA	295	407	Not Reported to MEA or ORNL
A 508-3 Forging	MO	MOL	238	462	900-955°C-12.8 h, air cooled 630-665°C-14 h, furnace cooled 610°C >10°C-24 h, furnace cooled

[a]Ambient temperature strength

Table 2. Chemical Compositions (wt-%)

Material	Code	C	Si	Mn	P	S	Cr	Mo	Ni	Al	Cu	Sn	Ti	V
A 533-B (HSST Plate 03)	3PS, 3PT, 3PU	0.20	0.25	1.26	0.011	0.018	0.10	0.45	0.56	---	0.12	---	---	---
A 302B (ASTM Ref. Plate)	F23	0.24	0.23	1.34	0.011	0.023	0.11	0.51	0.18	0.04	0.20	0.037	0.015	0.001
A 533-B S/A Weld	R	0.05	0.45	1.54	0.009	0.008	0.12	0.34	1.58	0.01	0.23	0.006	0.003	0.01
A 533-B S/A Weld	EC	0.11	0.52	1.57	0.007	0.011	0.02	0.48	0.64	0.008	0.24	[illegible]	<.01	[illegible]
22NiMoCr37 Forging	K	0.18	0.16	0.72	0.009	0.004	0.45	0.63	0.96	0.031	0.12	---	---	---
A 508-3 Forging	MO	0.20	0.28	1.43	0.008	0.008	---	0.53	0.75	0.031	0.05	---	---	<.01

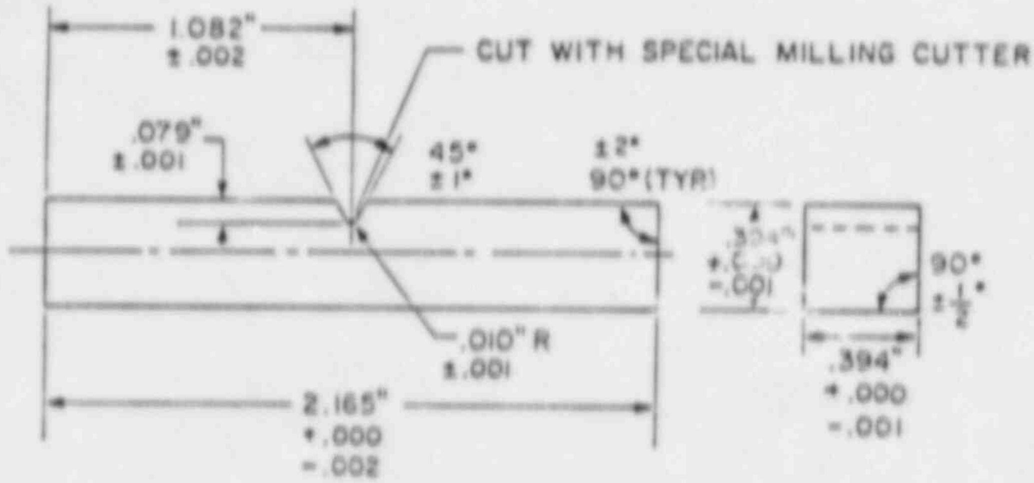

Fig. 3 Charpy V-notch specimen design. (Dimensions in inches, 1" = 2.54 cm.)

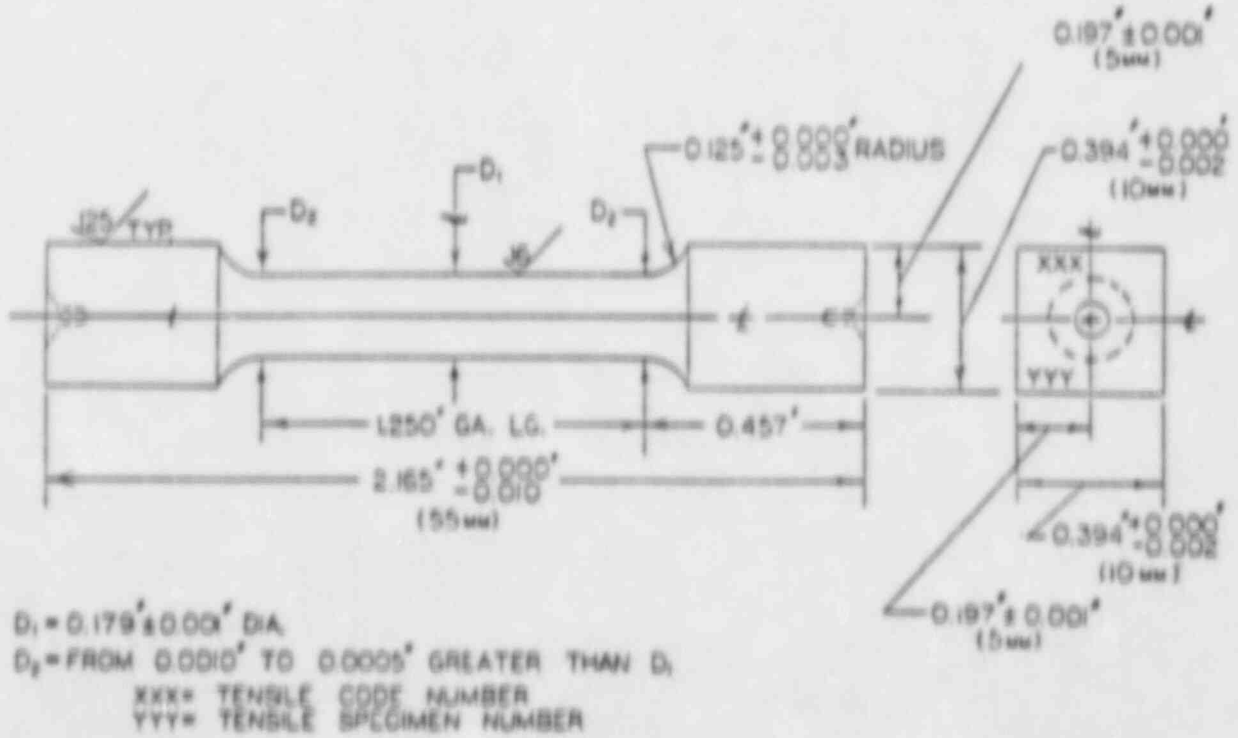

Fig. 4 Tension test specimen design. (Dimensions in inches, 1 in. = 2.54 cm.)

Specimen blanks were removed from the A 302-B plate and the A 508-3 forging in two layers spanning the quarter thickness plane and from the A 533-B plate in four layers spanning this plane. Blanks of the 22NiMoCr37 forging were removed in eight layers between the one-eighth thickness and one-half thickness planes. In the case of the welds, the blanks were taken through the weld deposit thickness except for a 12.7 mm thick exclusion region adjacent to the weldment (outer) surfaces.

The specimens of the A 533-B plate and the 22NiMoCr37 forging were oriented in the transverse (TL, weak) direction; those of the A 302-B plate and the A 508-3 forging were oriented in the longitudinal (LT, strong) orientation. Currently, the TL orientation is that specified for reactor vessel surveillance programs (Ref. 14). The decision to use the LT orientation for the A 302-B material here was to avoid a potential problem in postirradiation analyses stemming from the relatively low, preirradiation C_v upper shelf level (~68J) of the weak orientation. The reason(s) for the supplier's selection of the LT orientation for the A 508-3 forging, on the other hand, is unknown. Unirradiated condition data developed by the supplier indicates a close similarity in properties of LT and TL orientations, however (Ref. 15). Specimens of the welds were removed in a manner placing their long axis perpendicular to the welding direction and parallel to the weldment surface. For C_v specimens, the V-notch was placed in the face perpendicular to the material surface. Before irradiation, close fitting shrouds were placed over the gage section of the tensile specimens to aid heat transfer and to aid the uniformity of neutron flux conditions throughout the irradiation capsule.

4. MATERIAL IRRADIATION

Capsule construction, irradiation and disassembly operations were conducted by the Oak Ridge National Laboratory (ORNL) for the NRC. Primary responsibility for neutron dosimetry and fluence determinations is shared by ORNL and HEDL.

The irradiation histories and target fluence conditions of the five capsules are summarized in Table 3. The exposure time of capsule SSC-1 was adjusted to provide a fluence matching that of the Wall-2 capsule located in the quarter wall thickness position. The exposure time of capsule SSC-2 was similarly adjusted to match its fluence against that of the Wall-1 capsule located at the wall inner surface. The Wall-1, Wall-2 and Wall-3 capsules were irradiated simultaneously and were exposed for the same time period. In turn, the spread in fluences between these capsules should reflect normal flux attenuation conditions through a vessel thickness.

Fluence determinations are not yet available for capsule SSC-2 or for the three in-wall capsules. For capsule SSC-1, preliminary fluence data are available as indicated in a later section. From these results, fluence estimates were made as necessary.

TABLE 3. Capsule Irradiation Conditions

Capsule No.	PSF Location	Irradiation Time (Hours at Power)	MW Hours Exposure	Target Neutron Fluence ($n/cm^2, E > 1$ MeV)
SSC-1	Thermal Shield	1,291	32,000	3×10^{19}
SSC-2	Thermal Shield	2,845	64,700	$\sim 6 \times 10^{19}$
Wall-1	Simulator (Surface, OT)	18,748	430,000*	$\sim 6 \times 10^{19}$
Wall-2	Simulator (Quarter T)	18,748	430,000	$\sim$ [illegible] $\times 10^{19}$
Wall-3	Simulator	18,748	430,000	$\sim 1.5 \times 10^{19}$

* Approximate

The specimen and material contents of the capsules are indicated schematically in Figs. 5 to 9. Each material was assigned a specific code number (see Table 1). For instance, code F23 identifies the A 302-B plate. The code numbers of the A 533-B plate are, in fact, code identifications carried over from the sectioning of the original plate (Ref. 5). In the case of the code K material, the prefix to the specimen consecutive number indicates the particular layer from which the specimen came in the forging, e.g., specimens 65 and 610 were from layer no. 6.

Irradiation temperatures for all specimens are assumed to be 288°C for this report. It should be obvious from the capsule loadings that neutron exposure differences did arise between specimen groups as a normal result of flux gradients across the capsule face and because the C_v and tensile specimens were placed two layers deep within the capsule. Note that, for a given material, the same specimen locations were reserved in all five capsules.

5. CHARPY-V ASSESSMENTS

5.1 Procedure

Tests were performed on two impact test machines verified for accuracy against calibration standards supplied by the Army Materials and Mechanics Research Center (AMMRC). One machine located at the Naval Research Laboratory was used for preirradiation condition (reference) tests and for tests of the capsule SSC-1 specimens. In the case of the weld code R, preirradiation data of the supplier (Ref. 16) were used for pre-postirradiation comparisons. A second tester, located at the Nuclear Science and Technology Facility at the State University of New York (SUNY) at Buffalo was employed

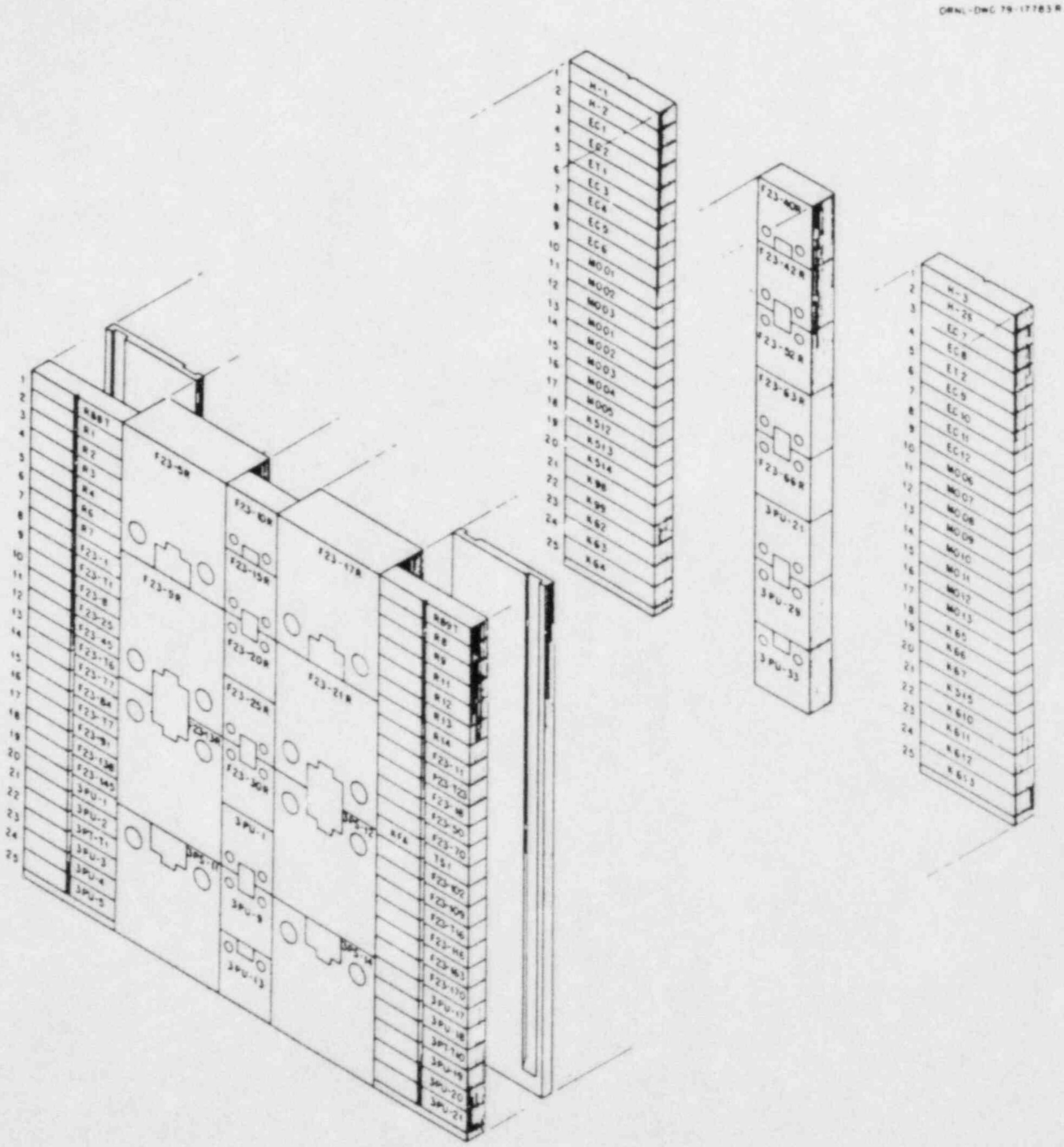

Fig. 5 C_V, CT and tension test specimen locations in the simulated surveillance capsule SSC-1 (courtesy ORNL). Tension test specimens are identified by the letter T in the specimen number.

Fig. 6 C_V, CT and tension test specimen locations in the simulated surveillance capsule SSC-2 (courtesy ORNL).

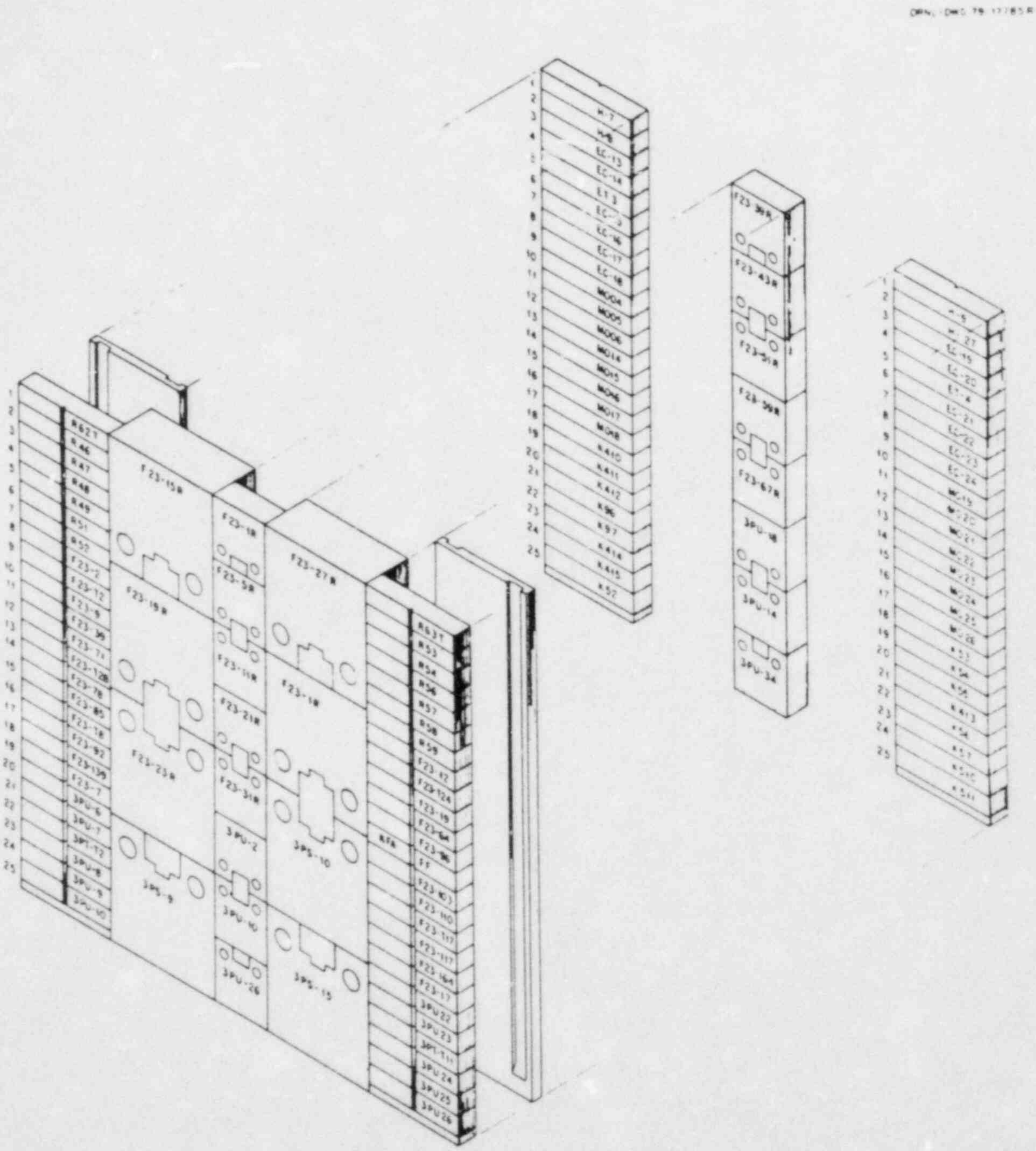

Fig. 7 C_V, CT and tension test specimen locations in the pressure vessel wall capsule W-1 (courtesy ORNL).

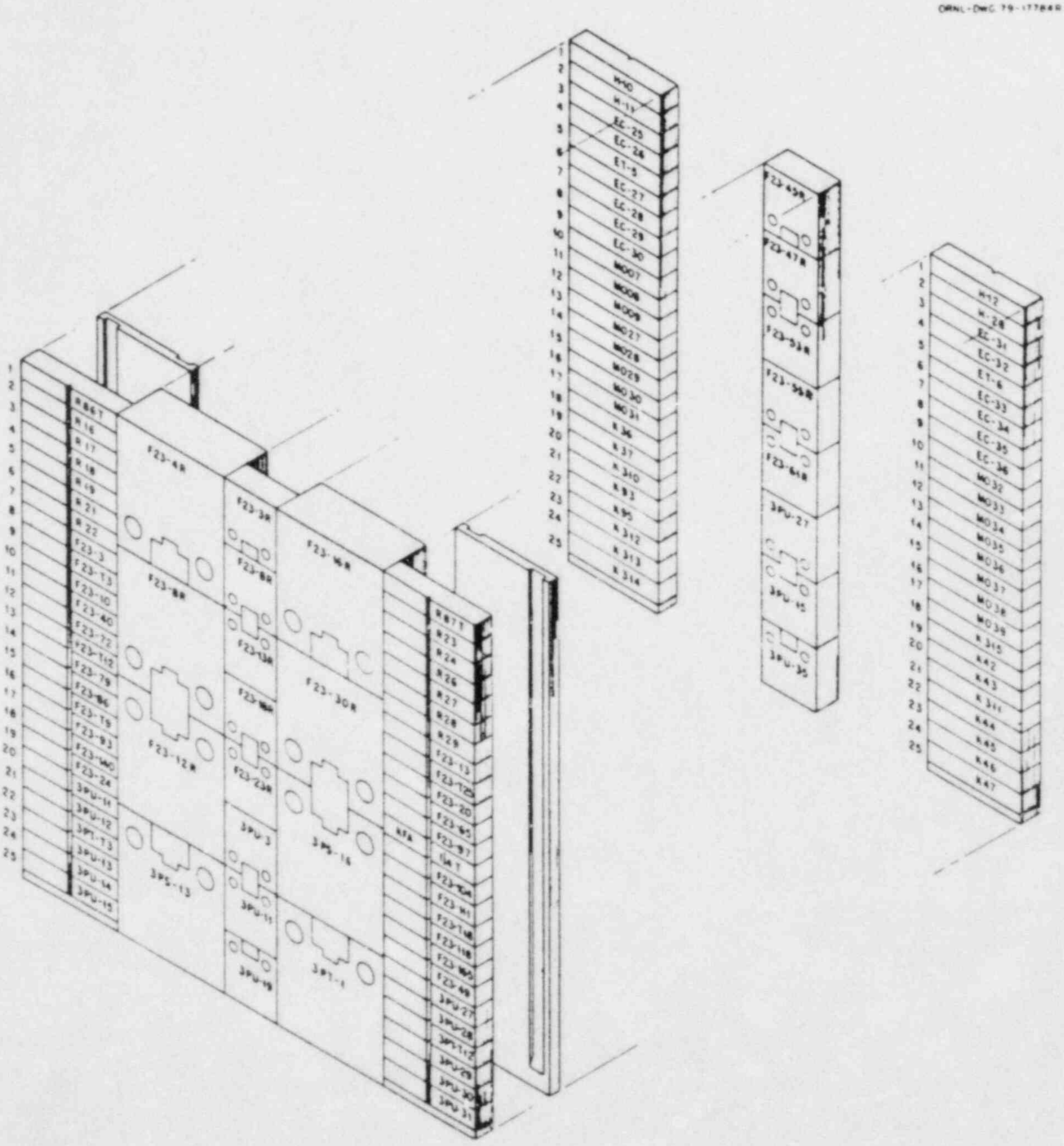

Fig. 8 C_V, CT and tension test specimen locations in the pressure vessel wall capsule W-2 (courtesy ORNL).

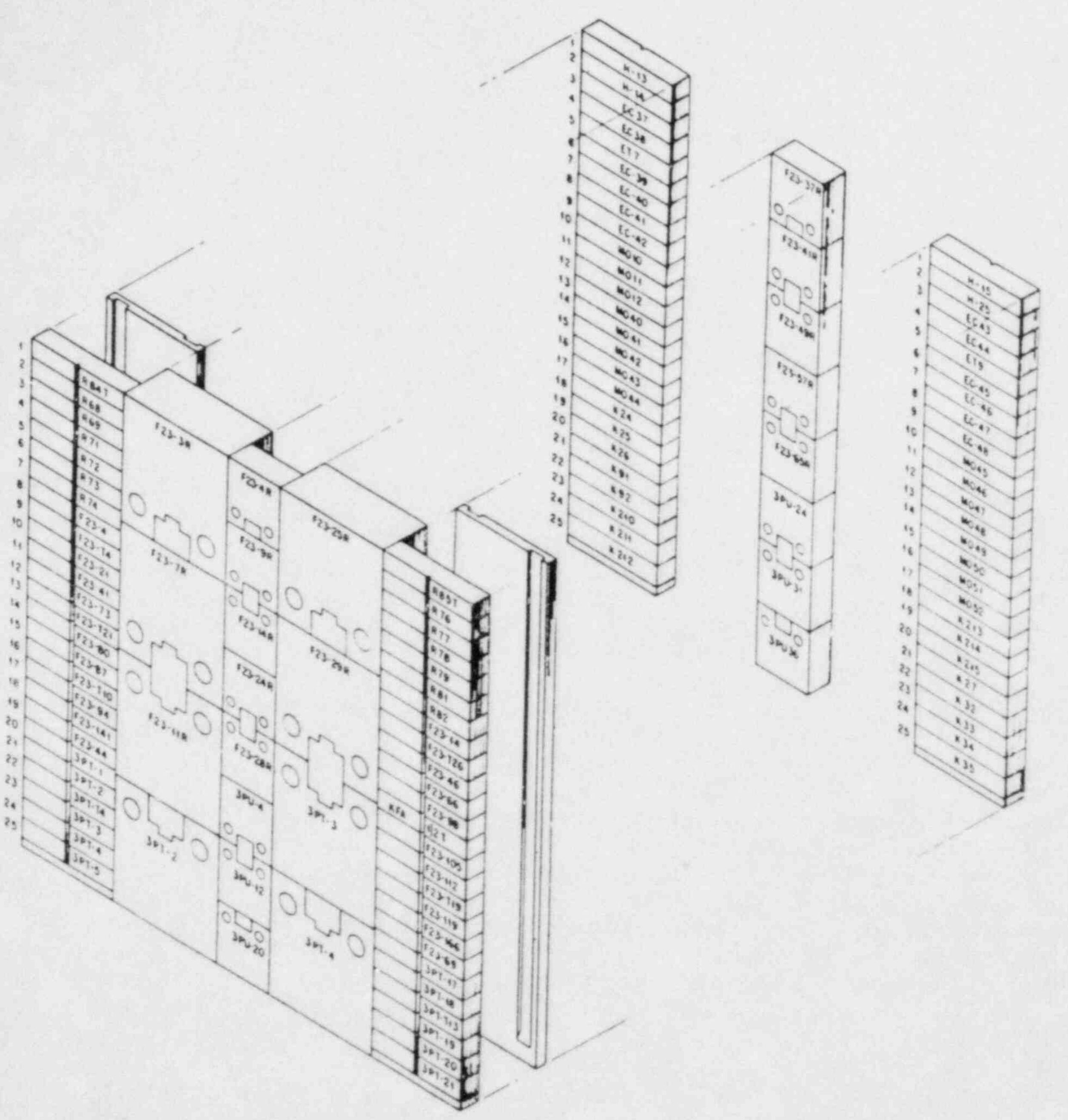

Fig. 9 C_V, CT and tension test specimen locations in the pressure vessel wall capsule W-3 (courtesy ORNL).

for the balance of the C_v specimens. The SSC-2, Wall-1, Wall-2 and Wall-3 specimens were tested concurrently.

Specimen energy absorption and lateral expansion were determined in each test; in addition, applied load vs. time-of-fracture records were made using a Dynatup system for future NRC studies. Data listings for the six materials by capsule number are given in Appendix A. Preirradiation test results (energy absorption, lateral expansion) for the two plates and the 22NiMoCr37 forging are compared in Figs. 10-12. Fig. 13 shows preirradiation data for the A 508-3 forging developed by NRL and by the supplier. Postirradiation energy absorption vs. temperature trends are illustrated in Figs. 14 - 43. Figures showing lateral expansion vs. temperature trends are provided in Appendix B. The C_v 41 J temperature was used as the primary index of the brittle/ductile transition for making radiation effects comparisons. Radiation-induced elevations of the C_v 68 J and C_v 0.89 mm transition temperatures were also determined. Observations for the materials are summarized in Tables 4-9. Portions of the data analysis for the A 302-B and A 533-B reference plates from Reference 3 are repeated here in the interests of consistency and completeness.

5.2 Unirradiated Condition

In Figure 10, good agreement in C_v properties between layer 1 and layer 2 of the A 302-B plate is observed. This will be seen to have special importance to the postirradiation data analyses for this material. The 41 J temperature is -4°C (25°F); the upper shelf energy level taken at 260°C is 108 J (80 ft-lb). Tests of the A 533-B plate (Fig. 11) showed a comparable transition temperature, -1°C (30°F), but a much higher upper shelf energy level, 150 J (111 ft-lb). Good agreement of properties between specimen layers is also found for this material. In the upper graph, the data suggest a slight increase in the lateral expansion value with temperature; however, the dashed line may be more descriptive of actual behavior in view of the "flat" upper shelf energy trend curve (lower graph).

Figure 13 compares notch ductility determinations made by NRL and by the laboratories of C.E.N./S.C.K. for the A 508-3 forging. Good agreement is again observed. Rather large data scatter is typical for forgings of this type and makes the indexing of 41 J and 68 J temperatures difficult. For the irradiated condition average transition behavior was usually estimated at the half width of the data scatter band. In Figure 12, data for the 22NiMoCr37 forging shows less scatter and a lower 41 J transition temperature, compared to the observations of Fig. 13. The 22NiMoCr37 composition is very similar to that of ASTM A 508-2.

The two welds, codes EC and R, differ appreciably in their preirradiation 41 J temperatures and in addition, differ in their upper shelf energy levels (see Figs. 34 and 39.) Here dissimilar weld deposit compositions, welding fluxes, welding parameters, and/ or postweld heat treatments are responsible for the property differences. Note from Table 1 that the weld code R was fully heat treated after welding, not just stress-relief-annealed as was the case with the weld code EC.

(Text resumes on page 52.)

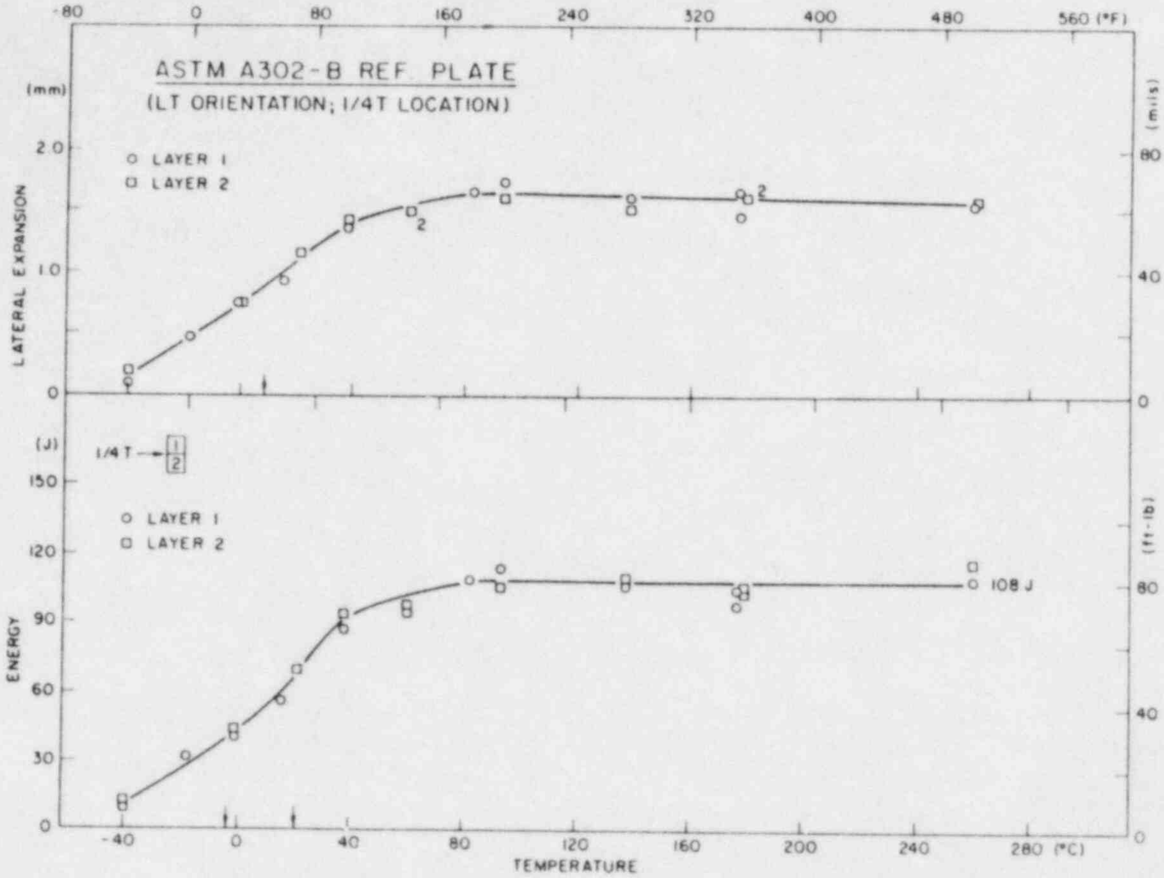

Fig. 10 Charpy-V notch ductility of the A 302-B reference plate before irradiation. Specimens were selected at random from the total specimen complement fabricated for the study. The vertical arrows on the abscissa show the 41 J, 68 J or 0.89 mm transition temperatures.

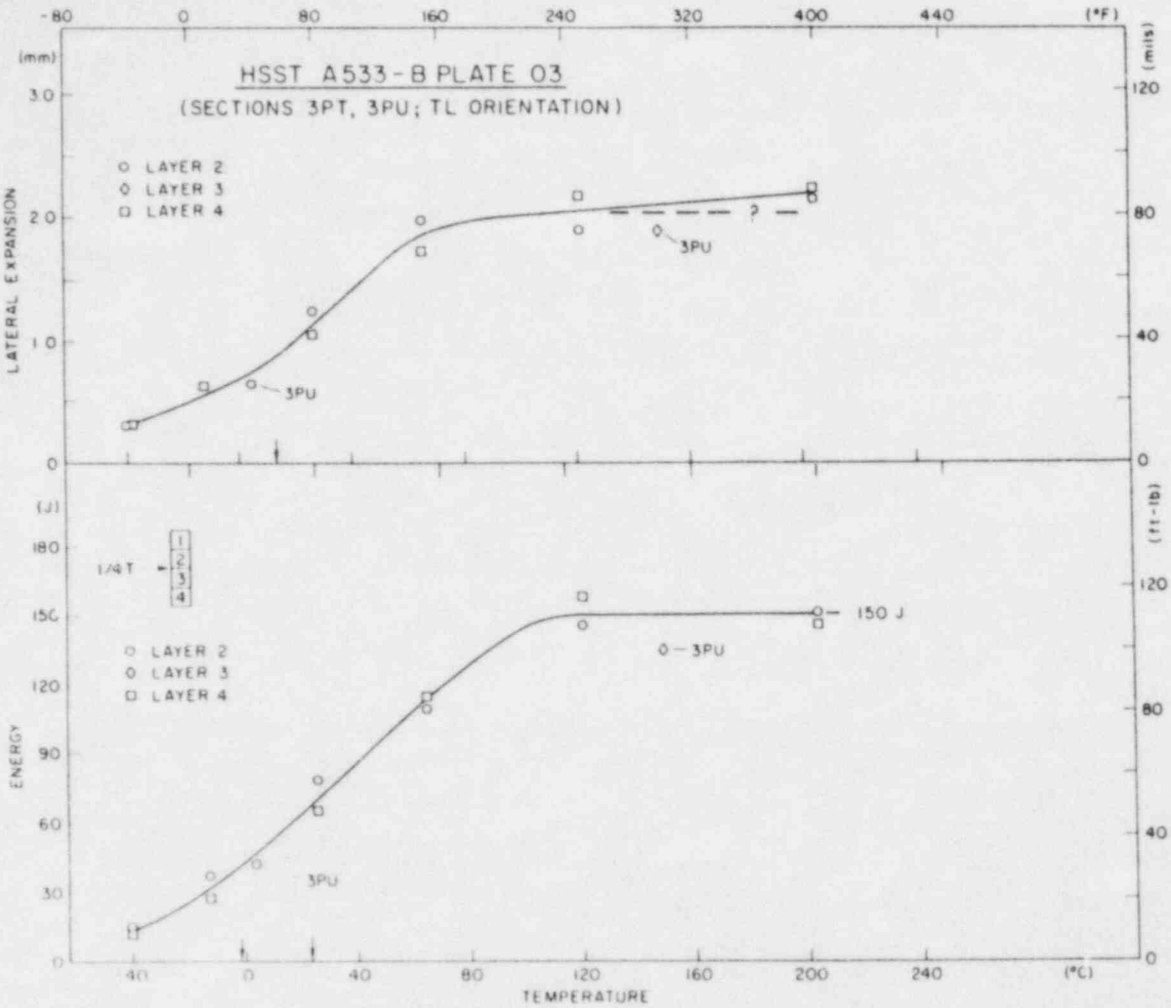

Fig. 11 Charpy-V notch ductility of the A 533-B reference plate (HSST Program Plate 03) before irradiation. Sections 3PT and 3PU were adjoining blocks (152 x 152 mm x full thickness, each) in the main plate.

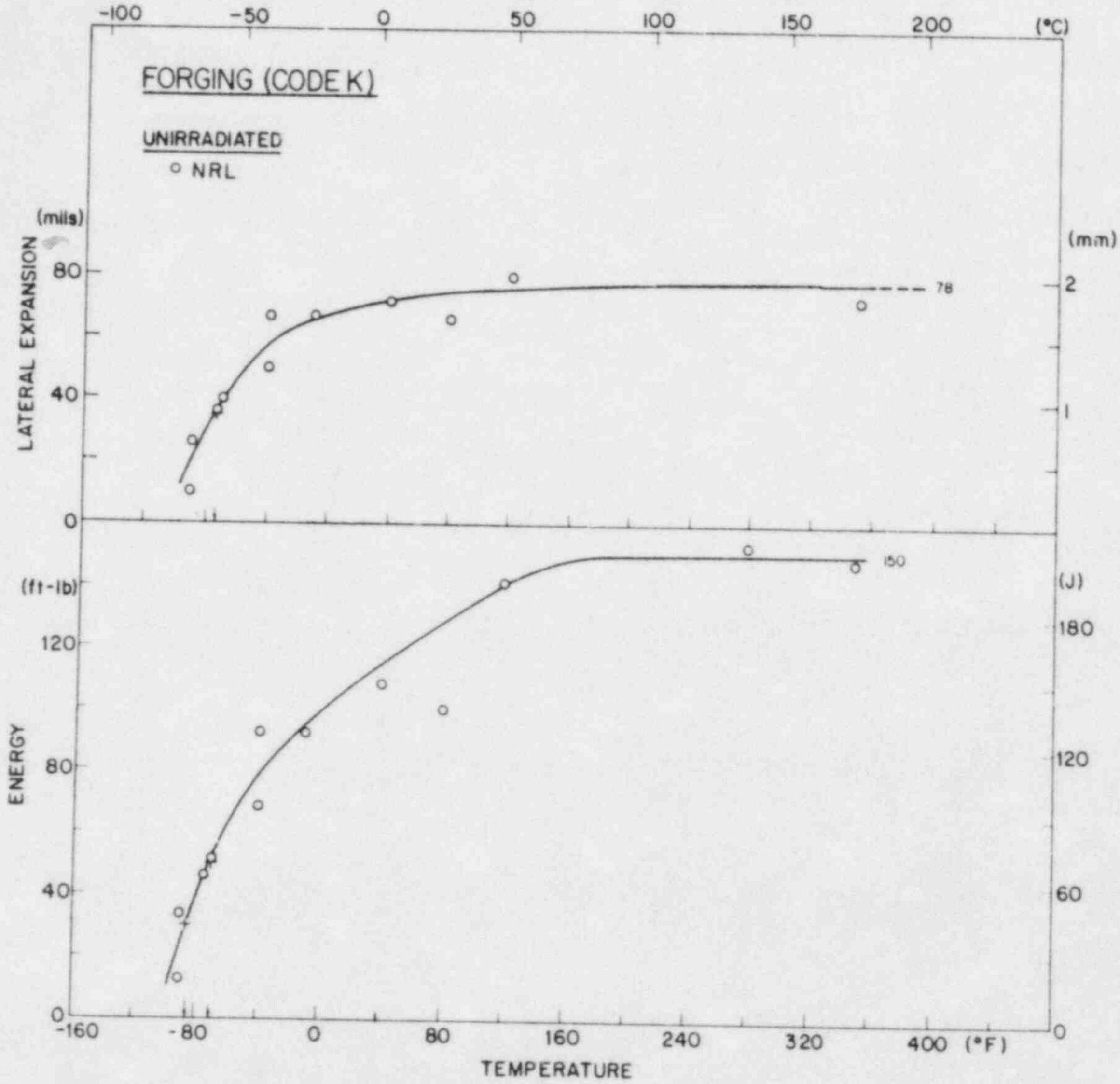

Fig. 12 Charpy-V notch ductility of the 22NiMoCr37 forging before irradiation (KFA, supplier). All specimens for this determination were from layer 8 in the forging (1/2T location).

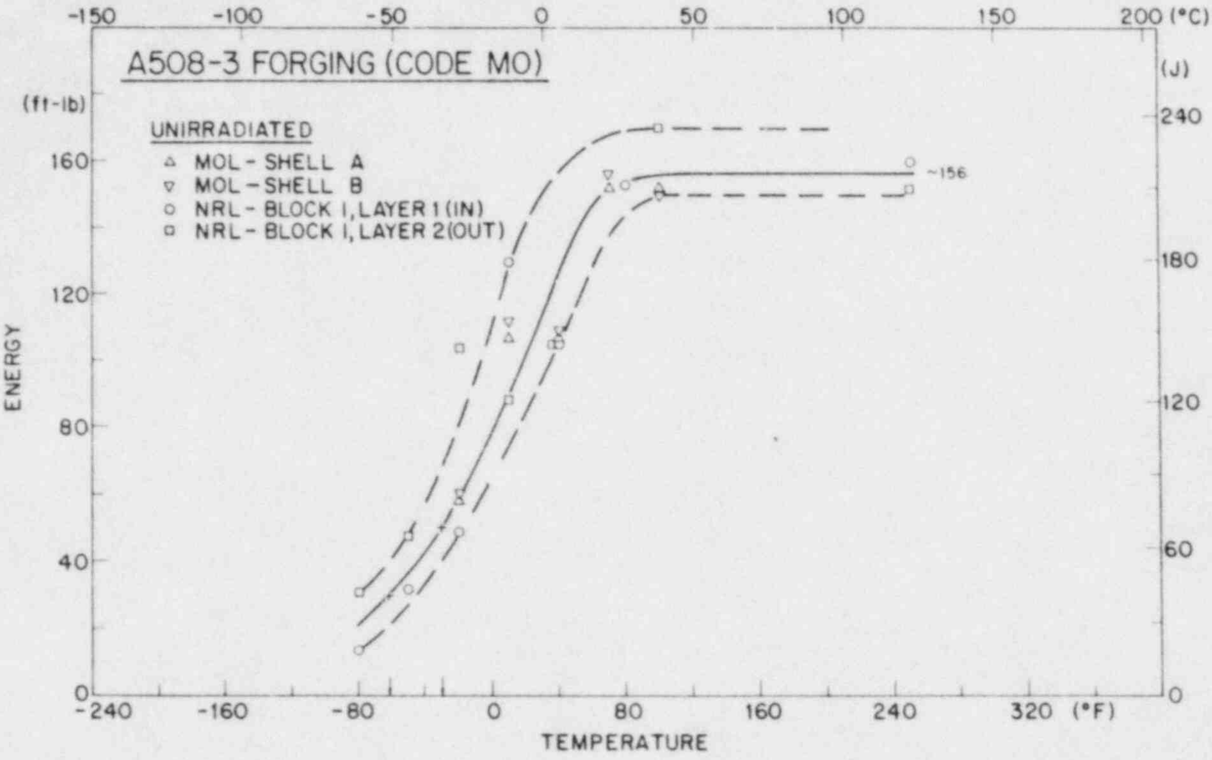

Fig. 13 Charpy-V notch ductility of the A 508-3 forging before irradiation (C.E.N./S.C.K., supplier). Good agreement between test results developed independently by C.E.N. and NRL laboratories is observed.

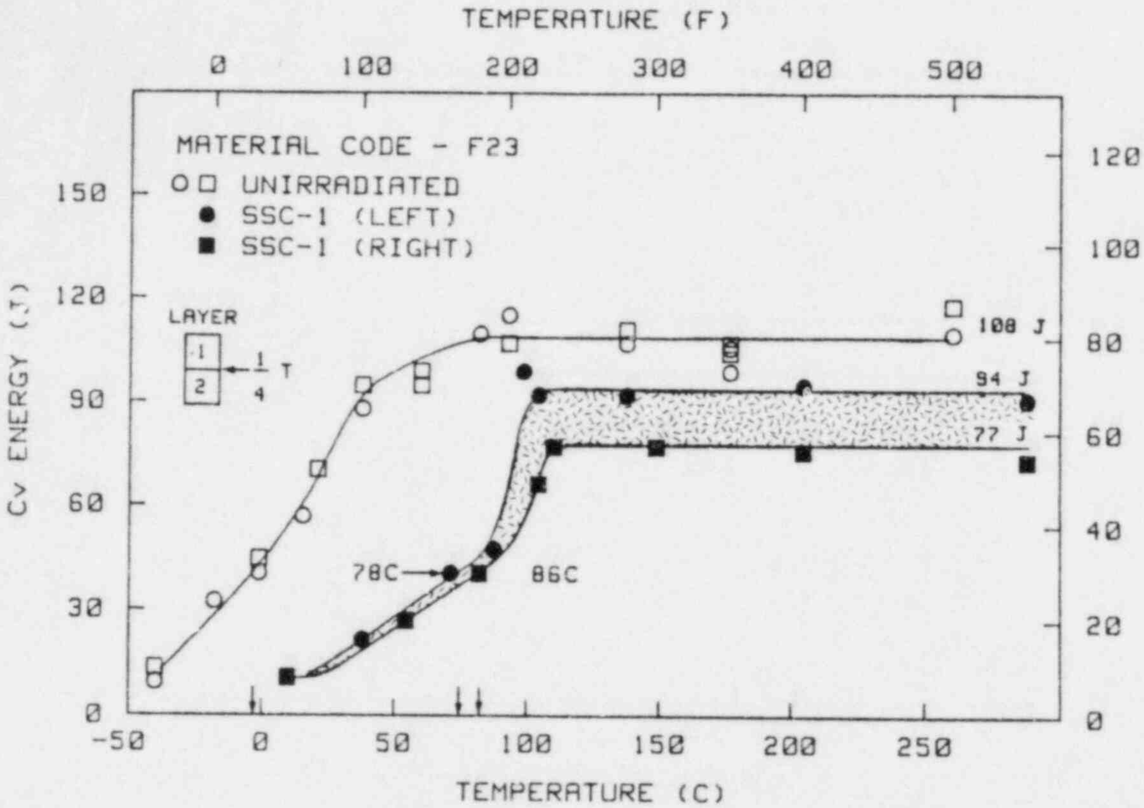

Fig. 14 Charpy-V notch ductility of the A 302-B plate before and after irradiation in capsule SSC-1. The vertical arrows on the abscissa in this and subsequent figures point to 41 J transition temperatures.

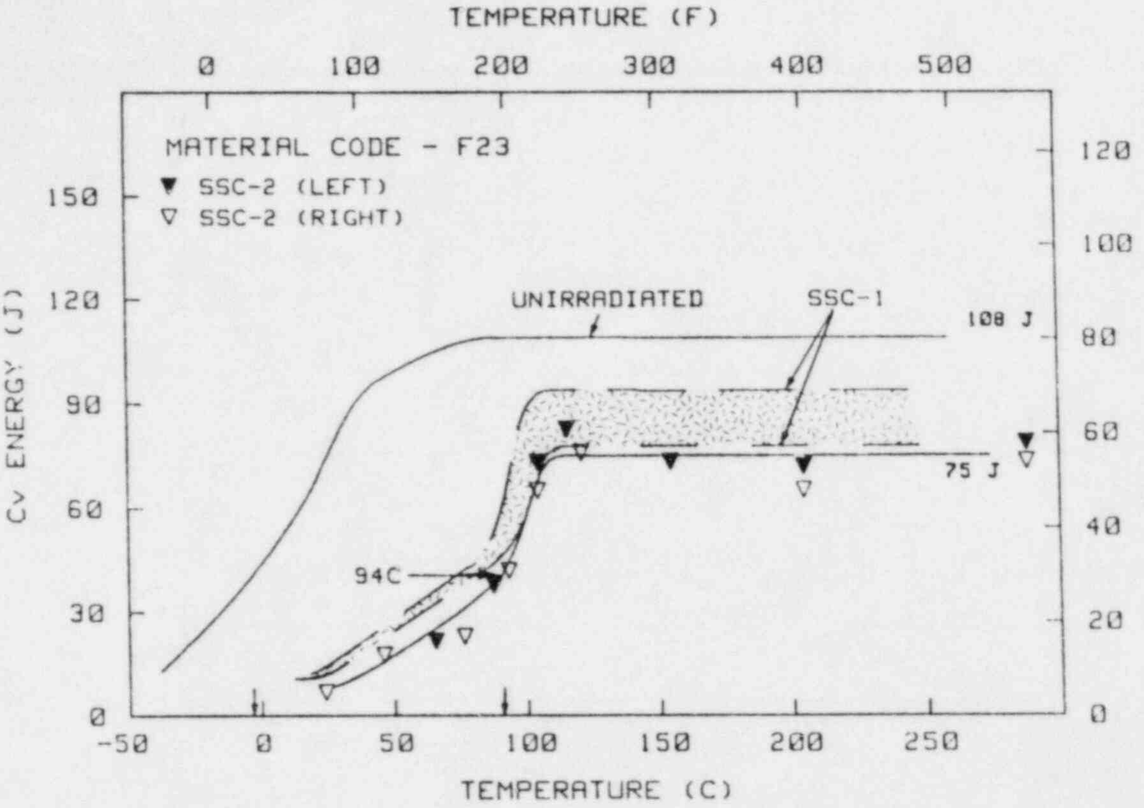

Fig. 15 Charpy-V notch ductility of the A 302-B plate before and after irradiation in capsule SSC-2.

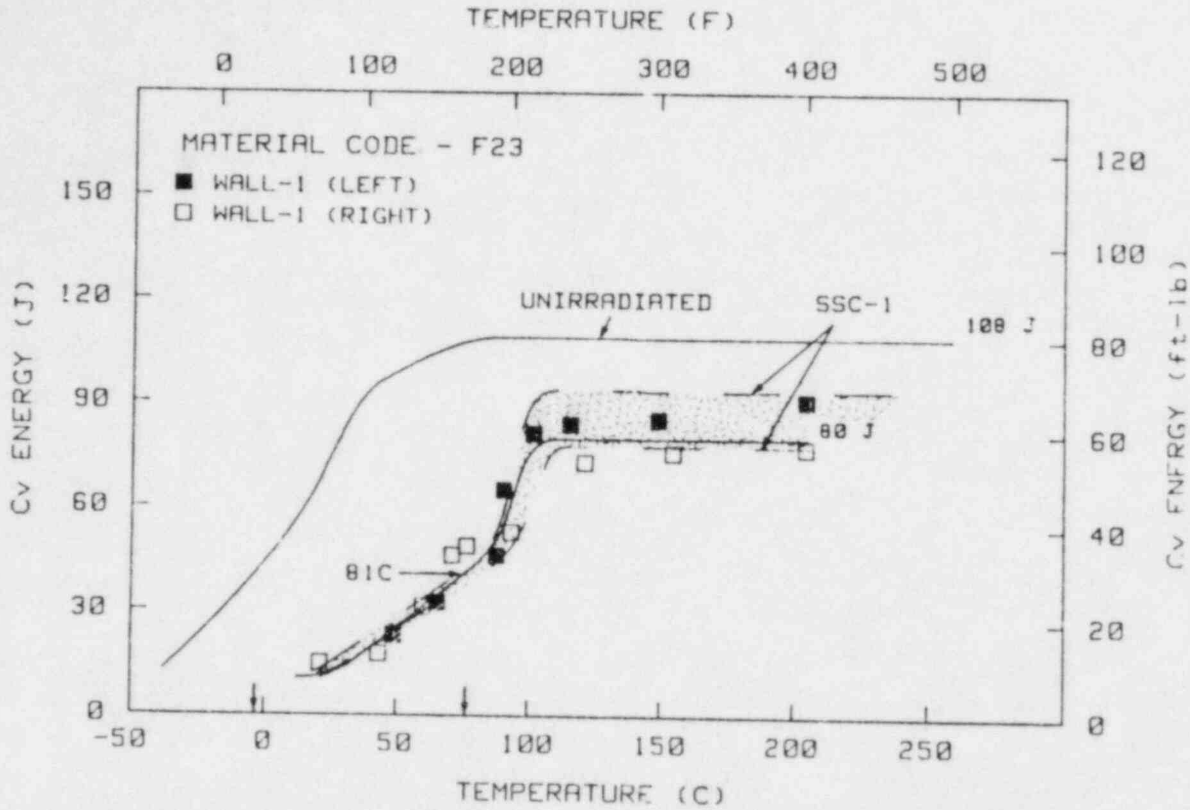

Fig. 16 Charpy-V notch ductility of the A 302-B plate before and after irradiation in capsule Wall-1.

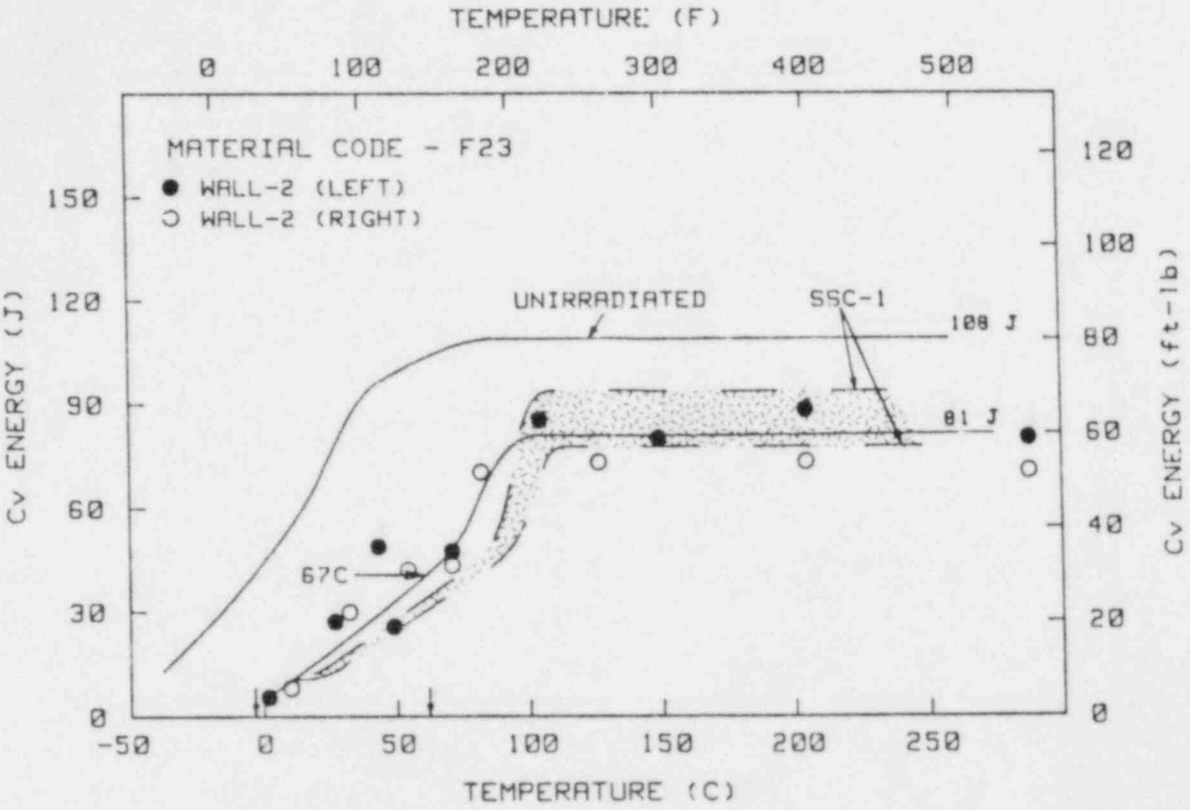

Fig. 17 Charpy-V notch ductility of the A 302-B plate before and after irradiation in capsule Wall-2.

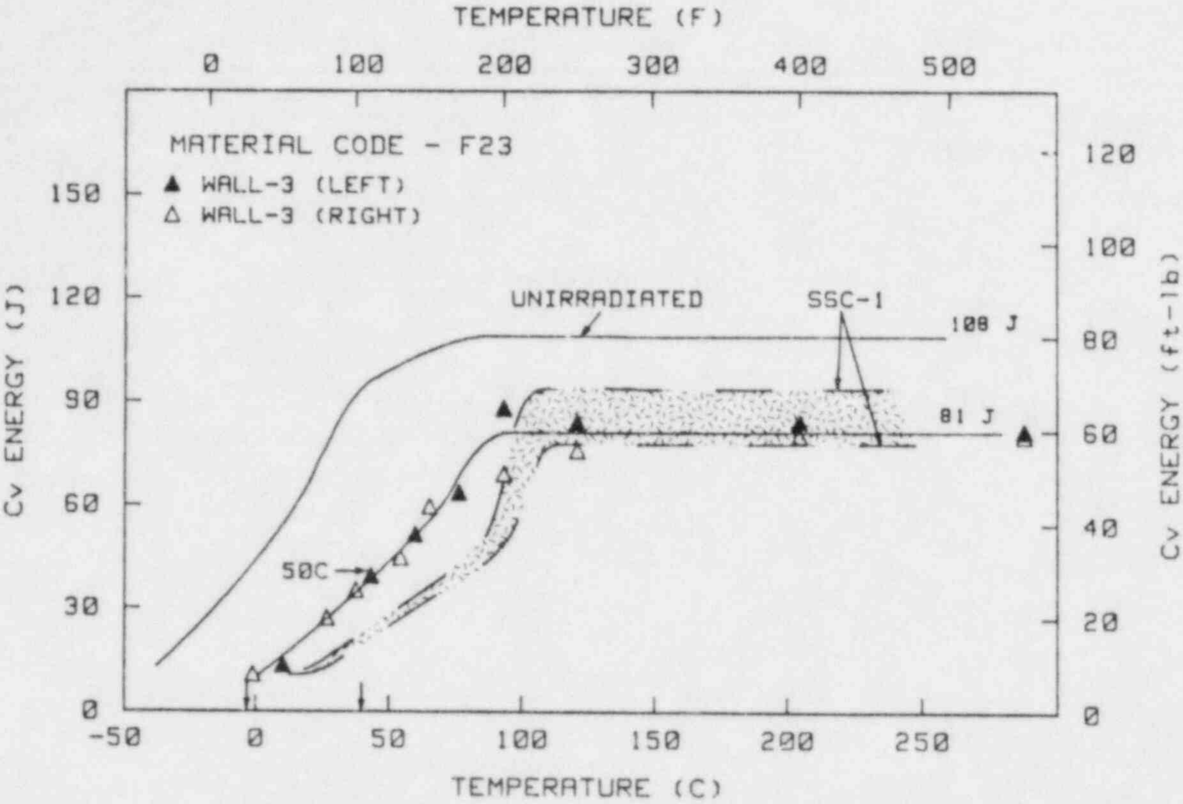

Fig. 18 Charpy-V notch ductility of the A 302-B plate before and after irradiation in capsule Wall-3.

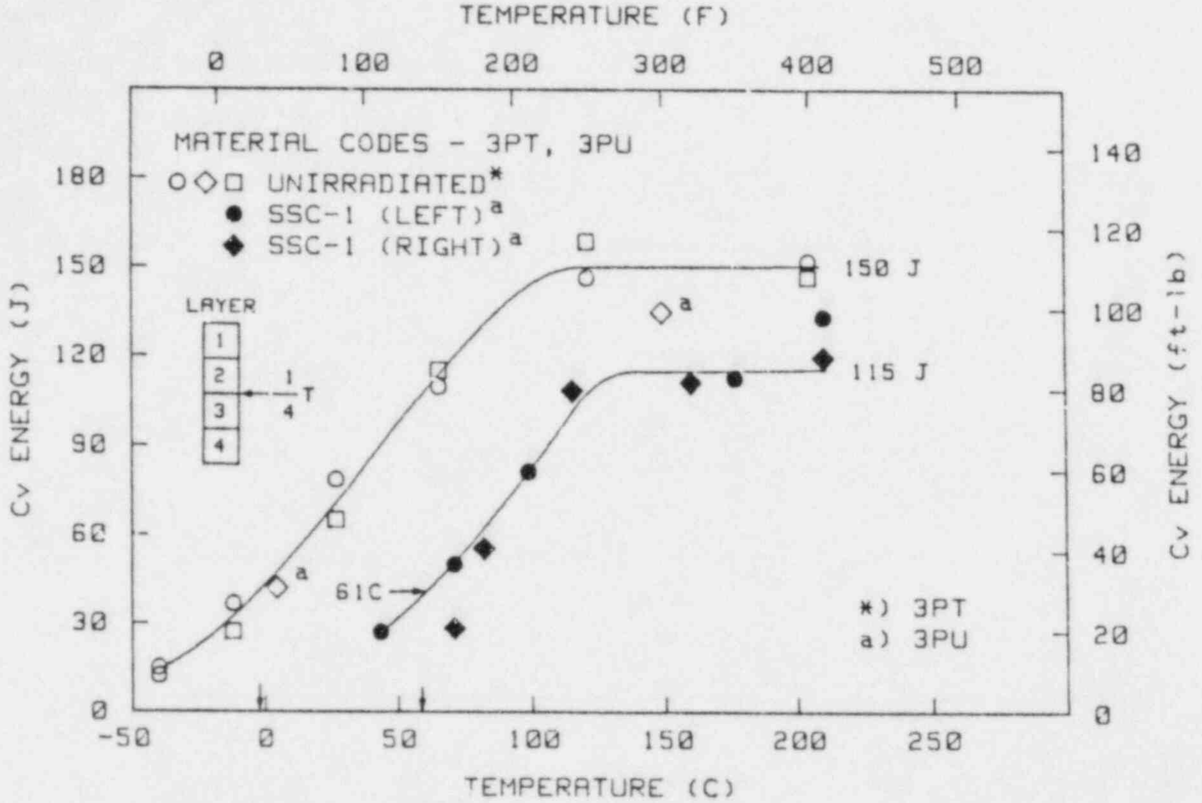

Fig. 19 Charpy-V notch ductility of the A 533-B plate before and after irradiation in capsule SSC-1.

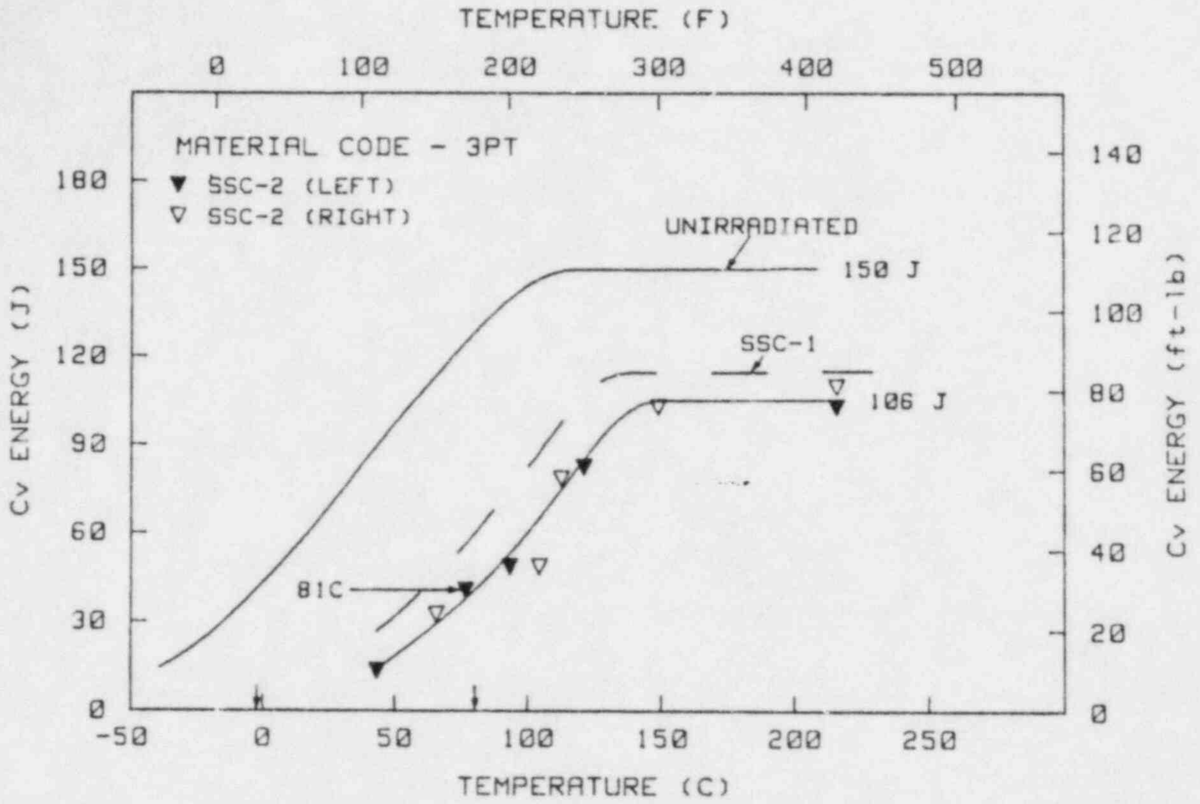

Fig. 20 Charpy-V notch ductility of the A 533-B plate before and after irradiation in capsule SSC-2.

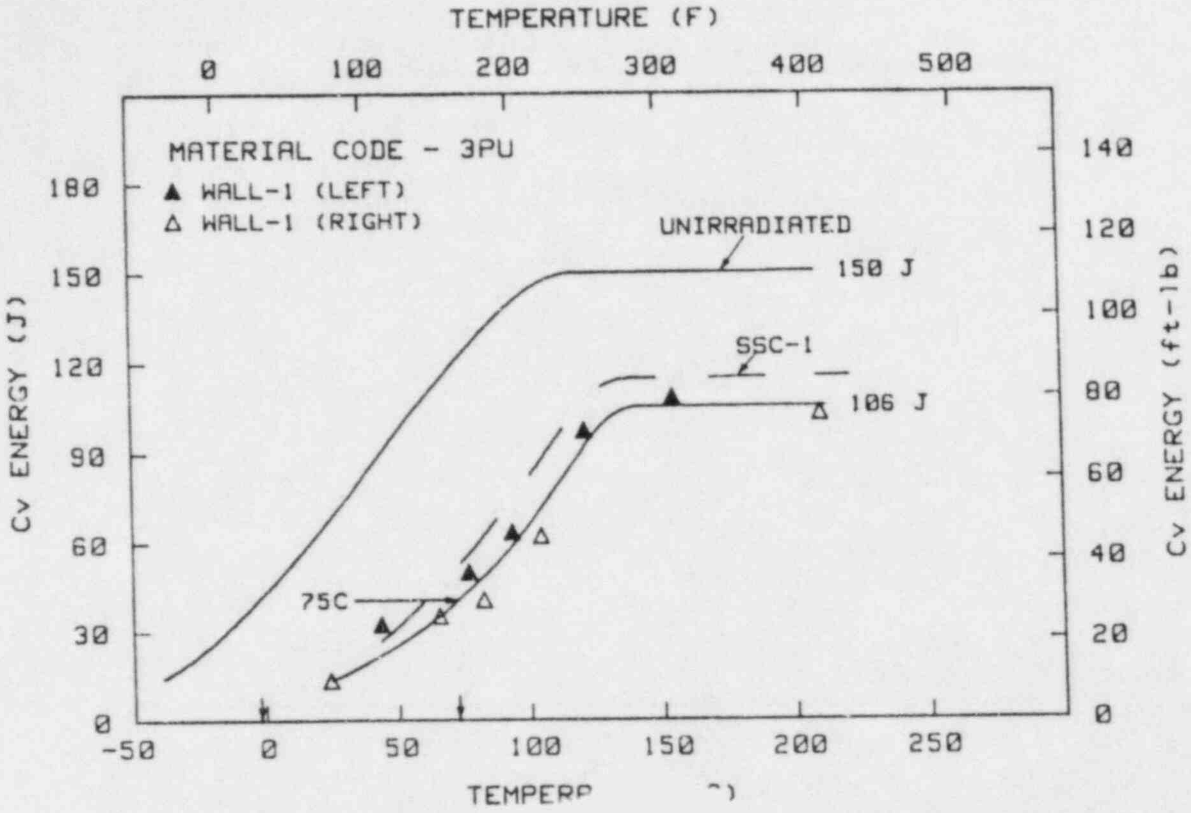

Fig. 21 Charpy-V notch ductility of the ¯33-B plate before and after irradiation in capsule W. -1.

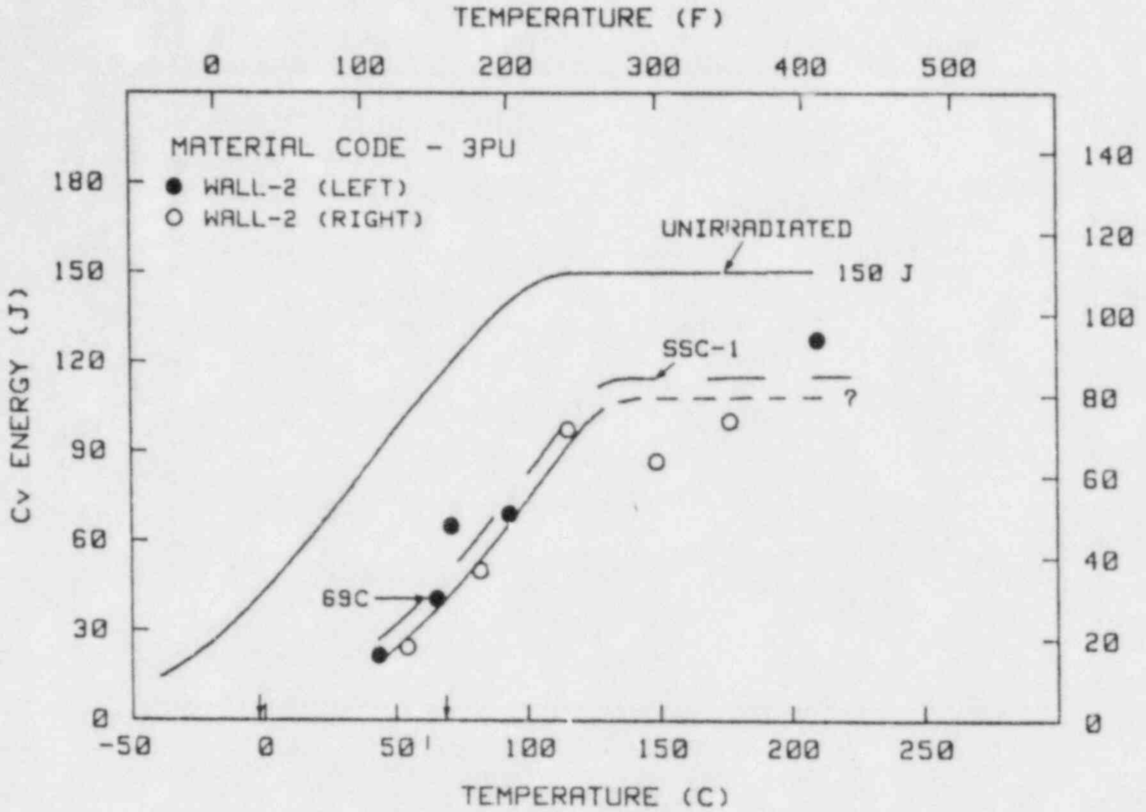

Fig. 22 Charpy-V notch ductility of the A 533-B plate before and after irradiation in capsule Wall-2.

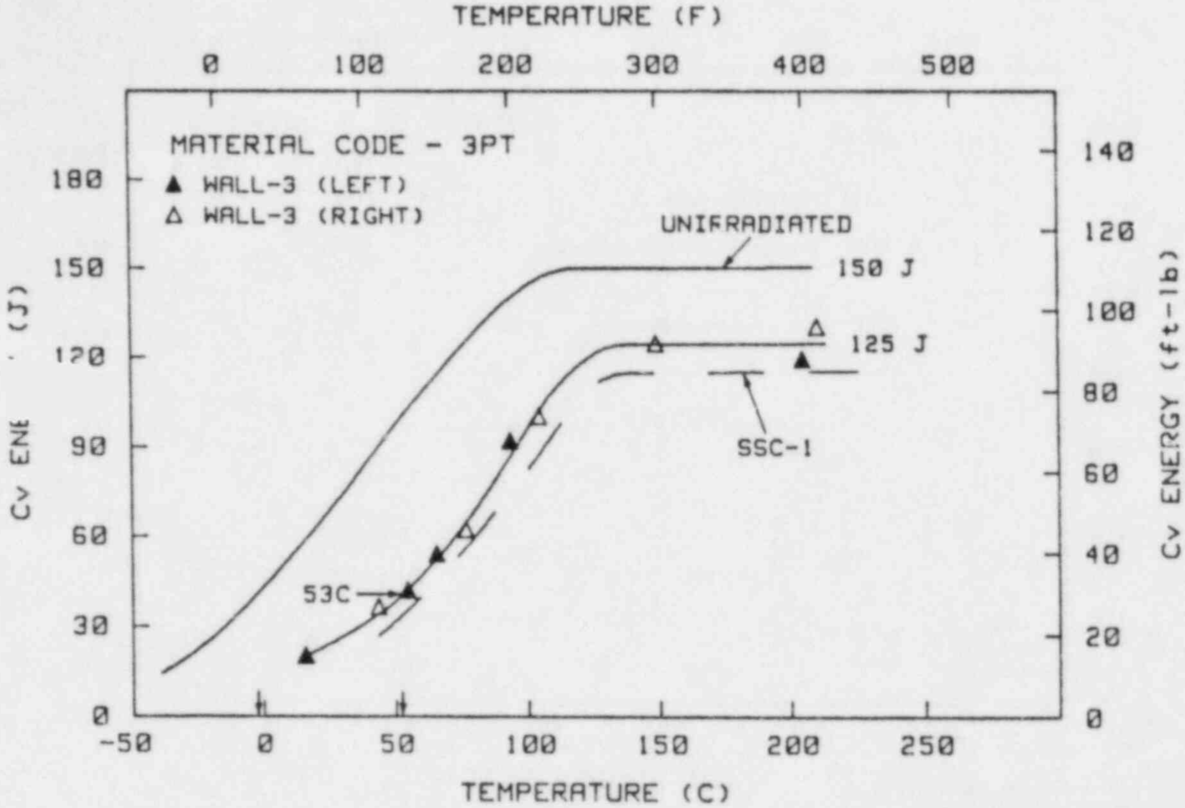

Fig. 23 Charpy-V notch ductility of the A 533-B plate before and after irradiation in capsule Wall-3.

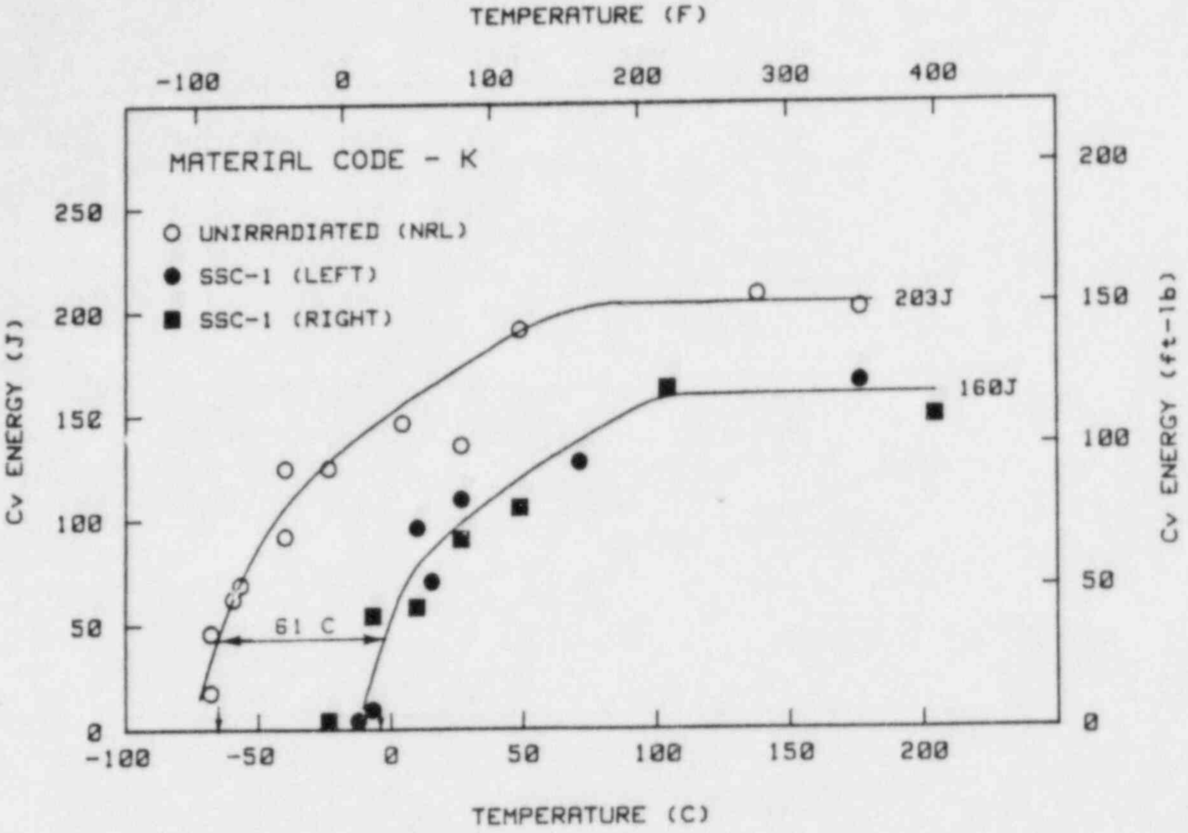

Fig. 24 Charpy-V notch ductility of the 22NiMoCr37 forging before and after irradiation in capsule SSC-1.

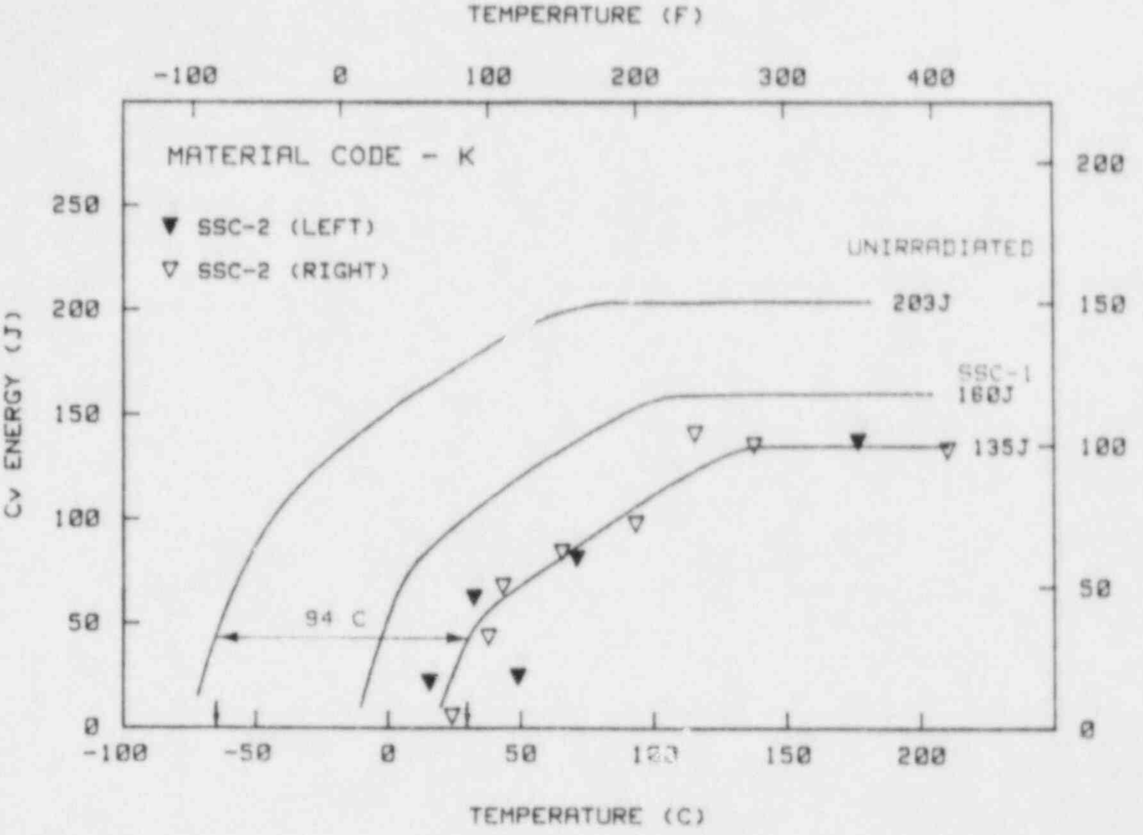

Fig. 25 Charpy-V notch ductility of the 22NiMoCr37 forging before and after irradiation in capsule SSC-2.

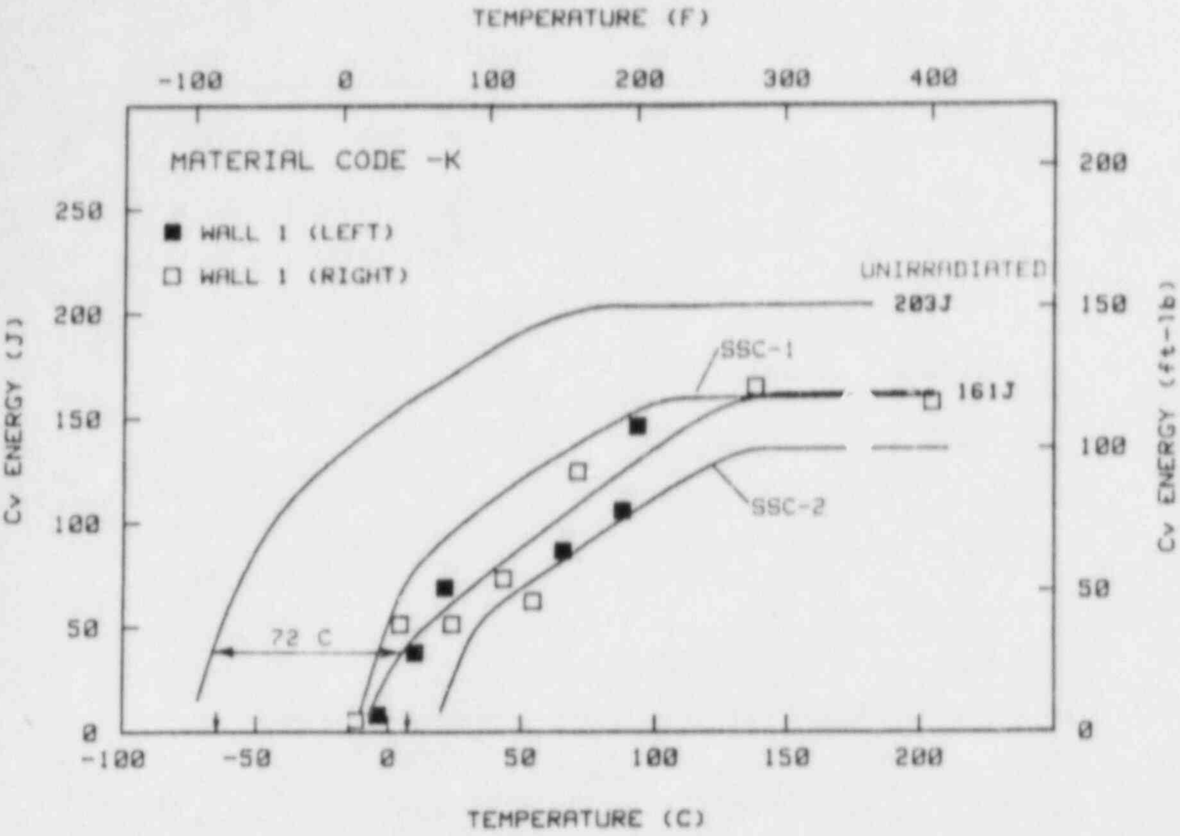

Fig. 26 Charpy-V notch ductility of the 22NiMoCr37 forging before and after irradiation in capsule Wall-1.

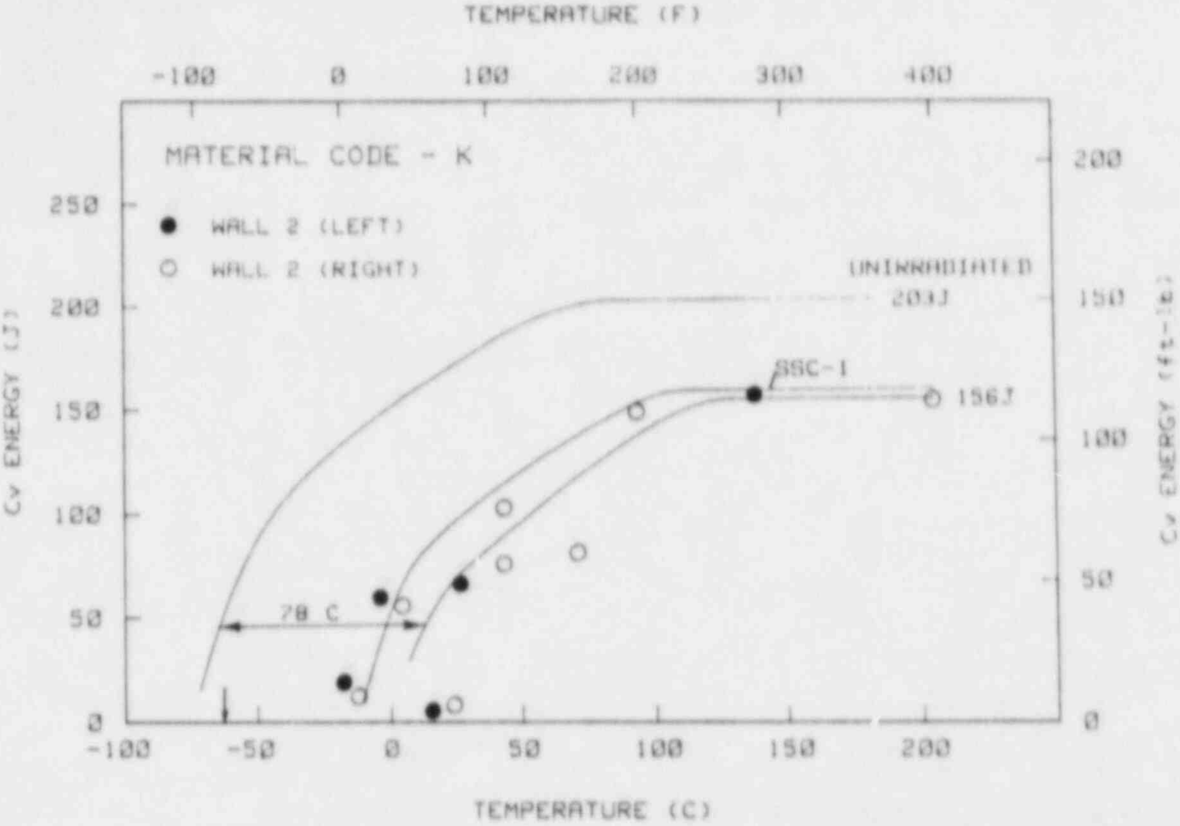

Fig. 27 Charpy-V notch ductility of the 22NiMoCr37 forging before and after irradiation in capsule Wall-2.

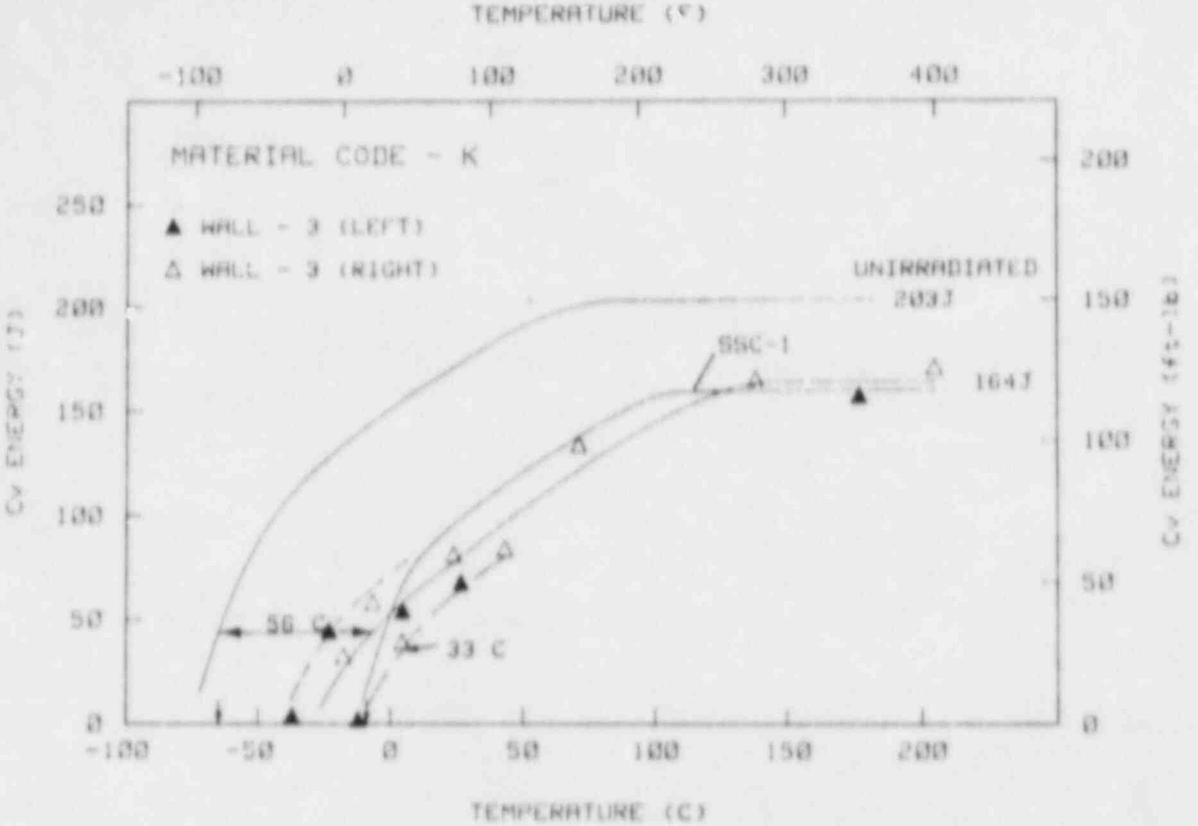

Fig. 28 Charpy-V notch ductility of the 22NiMoCr37 forging before and after irradiation in capsule Wall-3.

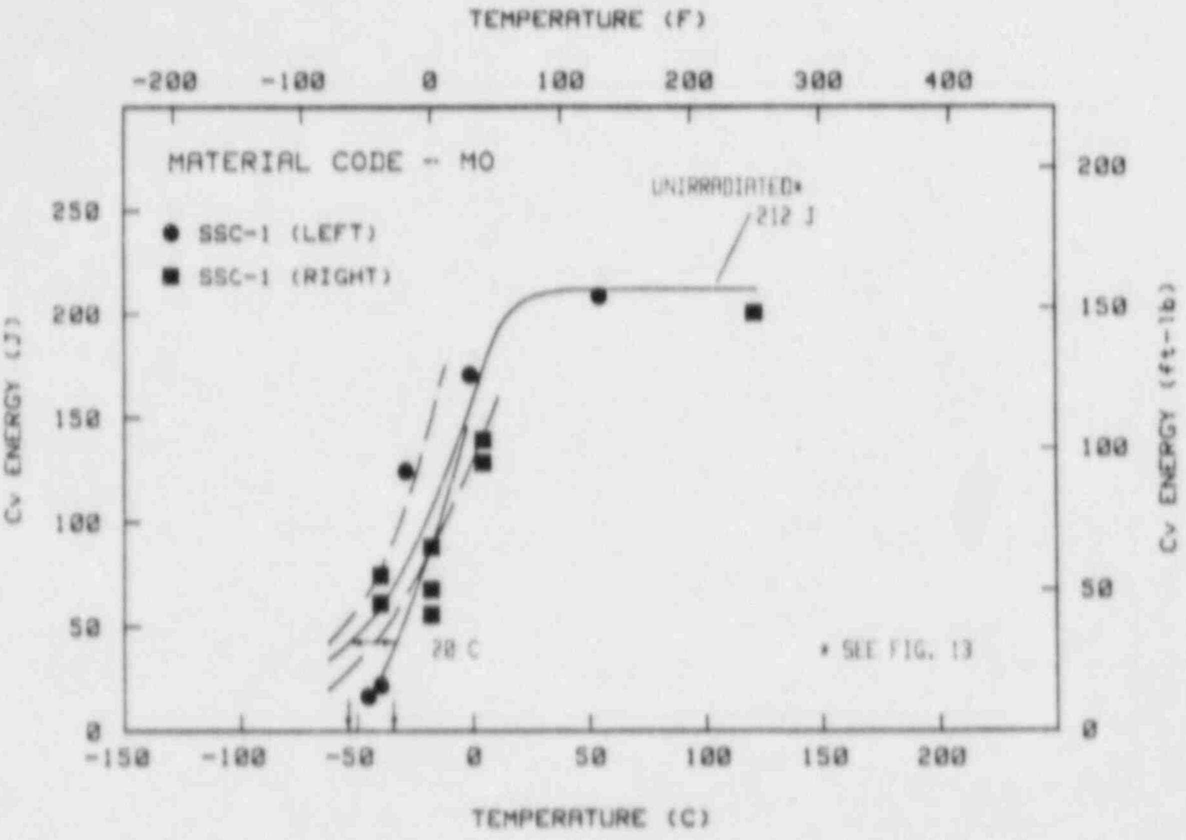

Fig. 29 Charpy-V notch ductility of the A 508-3 forging before and after irradiation in capsule SSC-1.

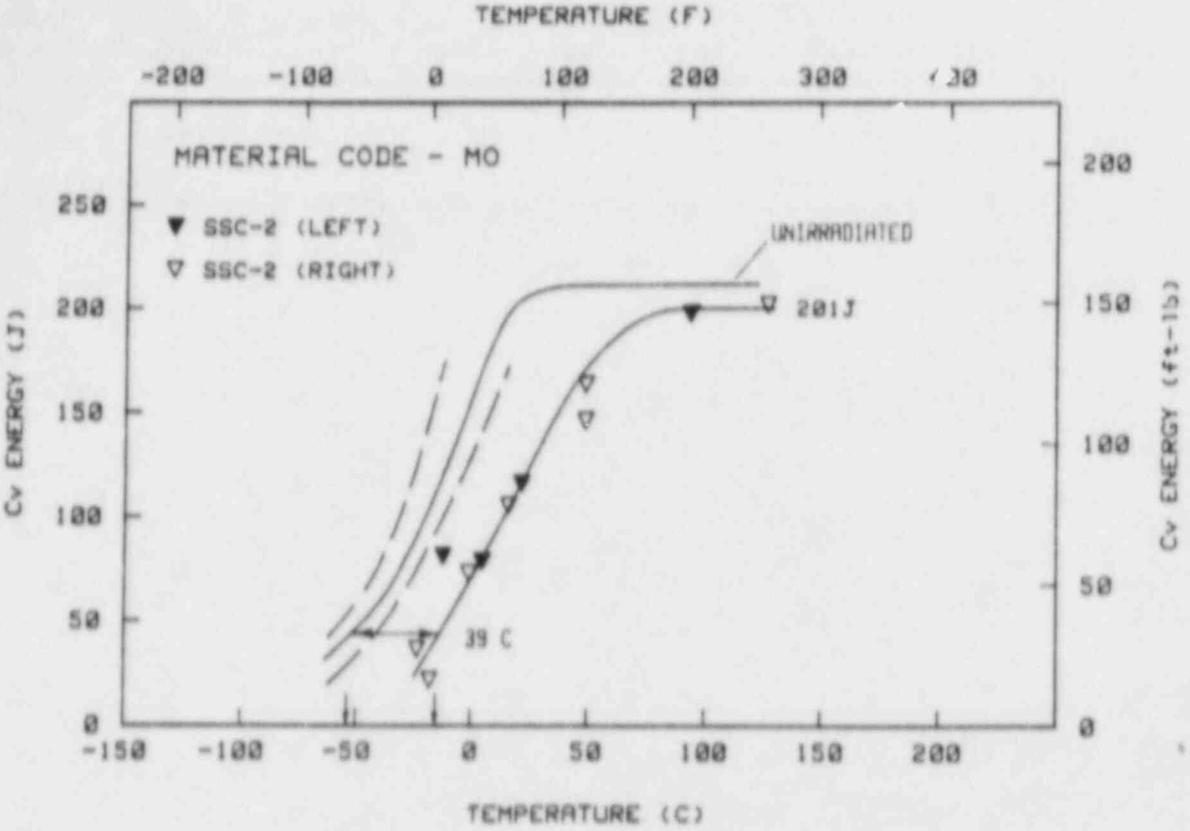

Fig. 30 Charpy-V notch ductility of the A 508-3 forging before and after irradiation in capsule SSC-2.

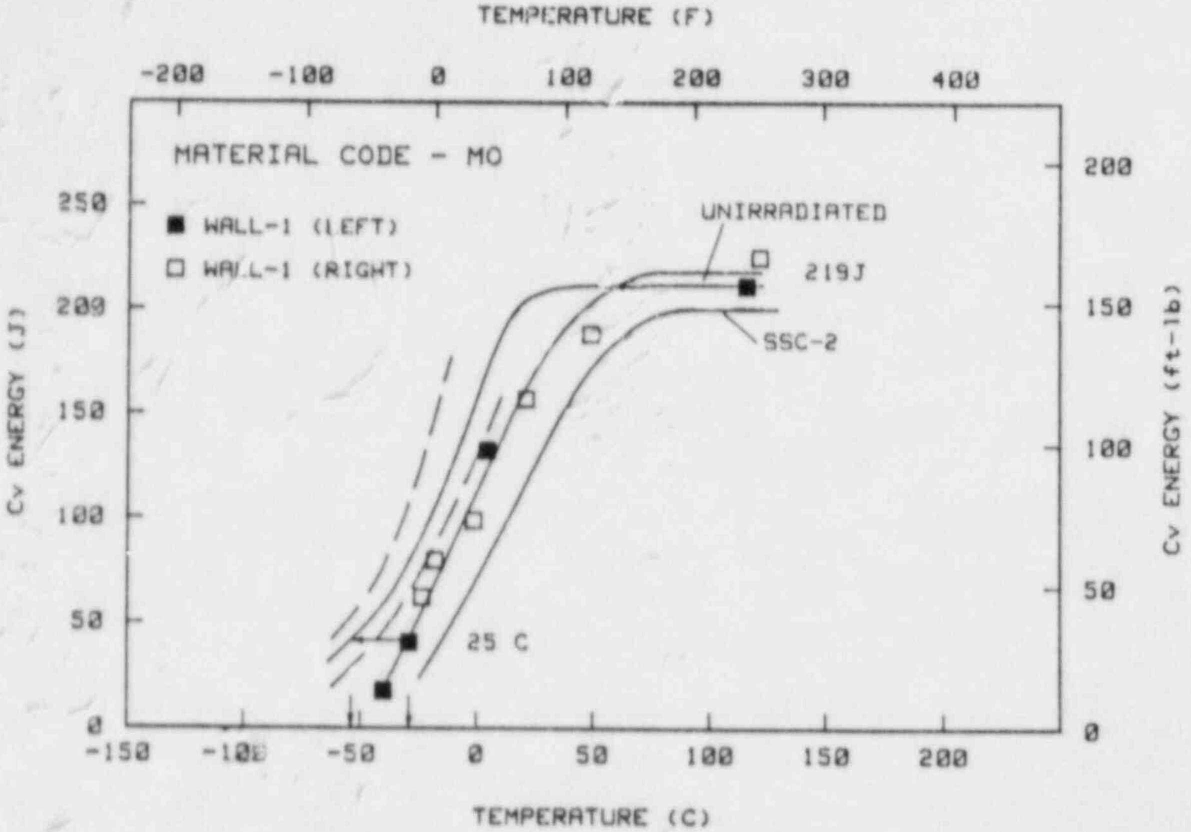

Fig. 31 Charpy-V notch ductility of the A 508-3 forging before and after irradiation in capsule Wall-1.

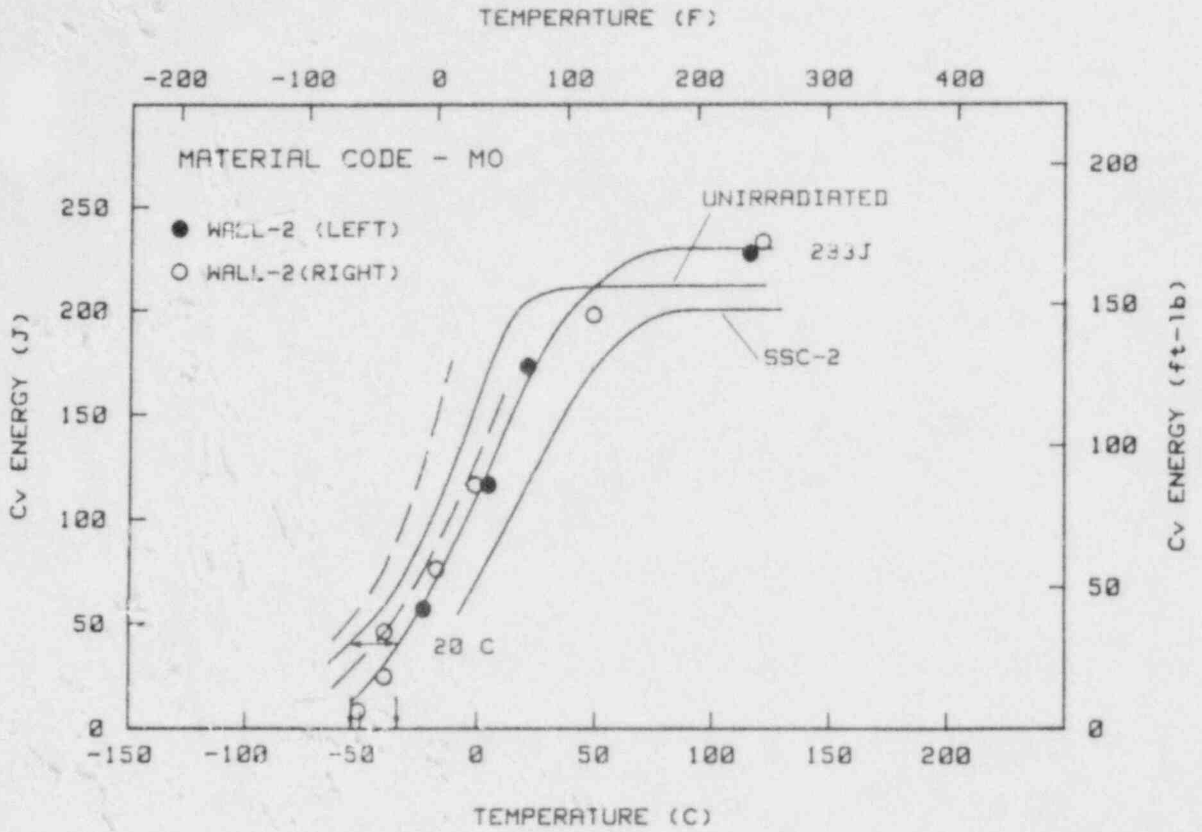

Fig. 13 Charpy-V notch ductility of the A 508-3 forging before and after irradiation in capsule Wall-2.

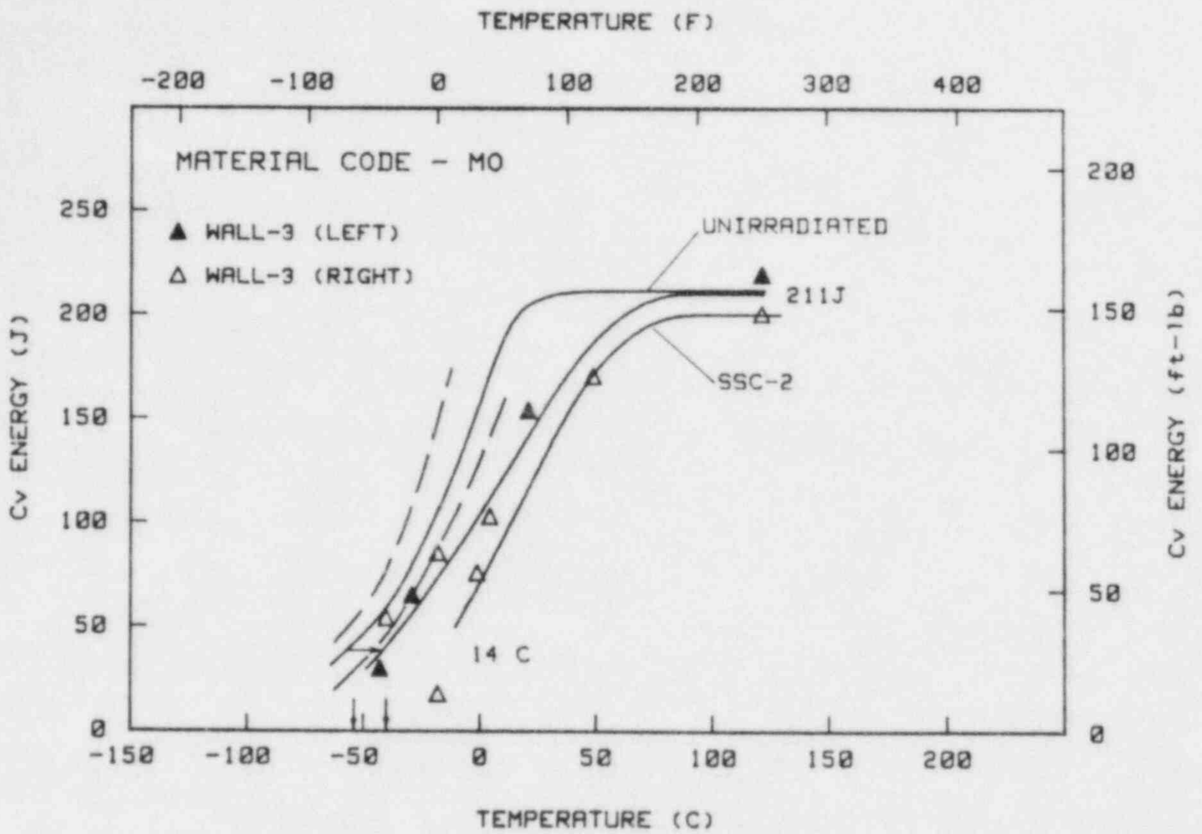

Fig. 33 Charpy-V notch ductility of the A 508-3 forging before and after irradiation in capsule Wall-3.

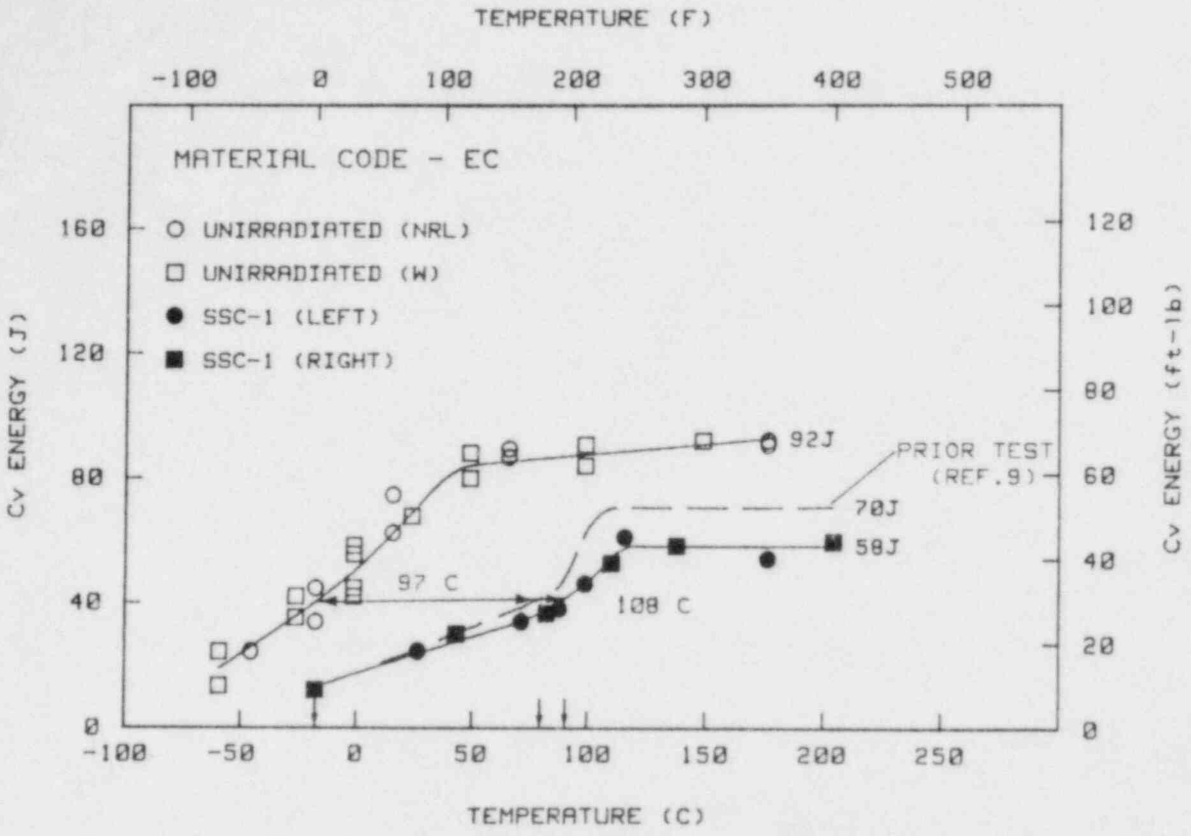

Fig. 34 Charpy-V notch ductility of the submerged arc weld code EC before and after irradiation in capsule SSC-1.

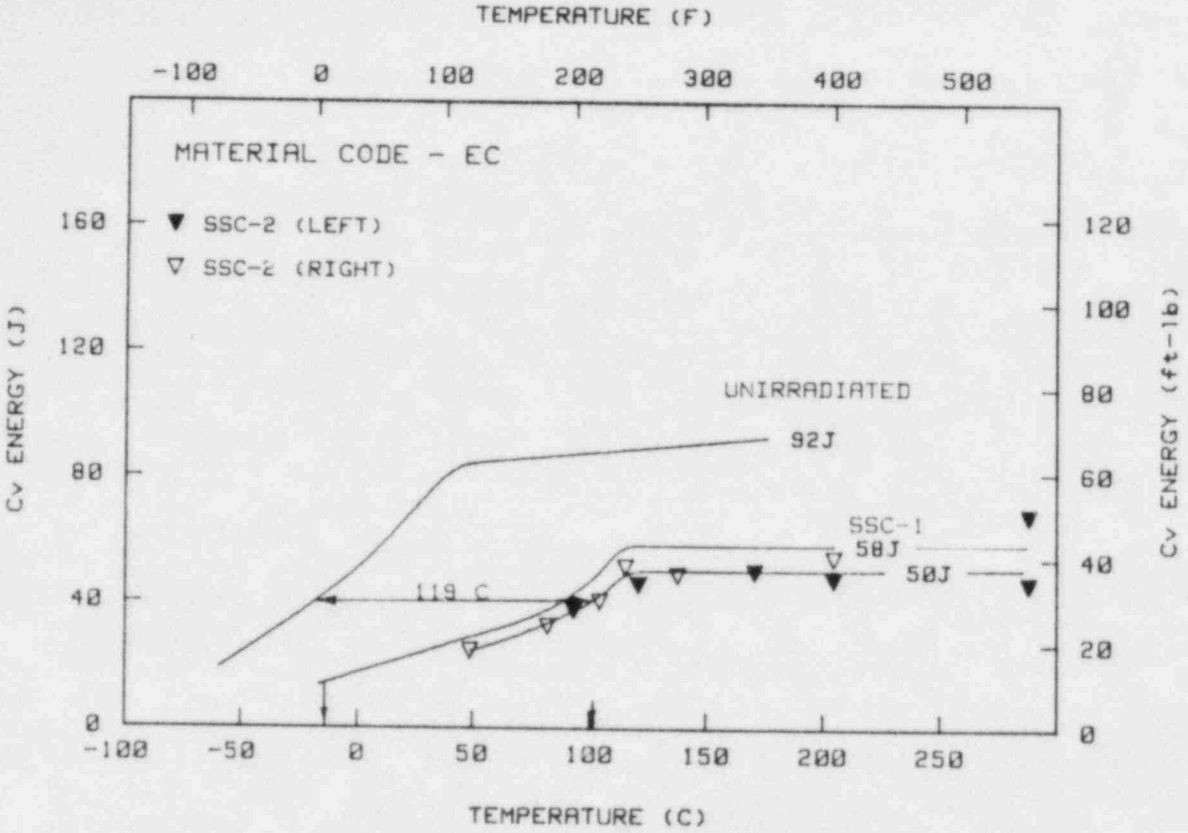

Fig. 35 Charpy-V notch ductility of the submerged arc weld code EC before and after irradiation in capsule SSC-2.

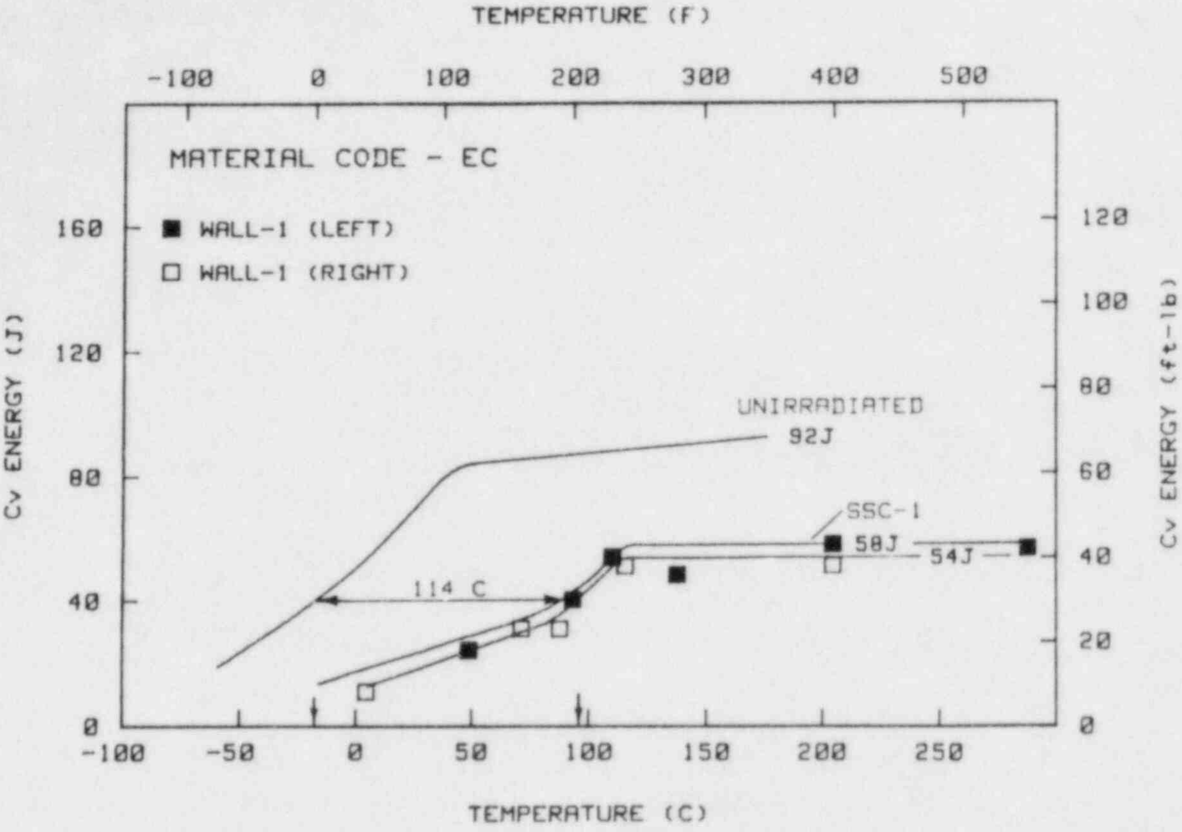

Fig. 36 Charpy-V notch ductility of the submerged arc weld code EC before and after irradiation in capsule Wall-1.

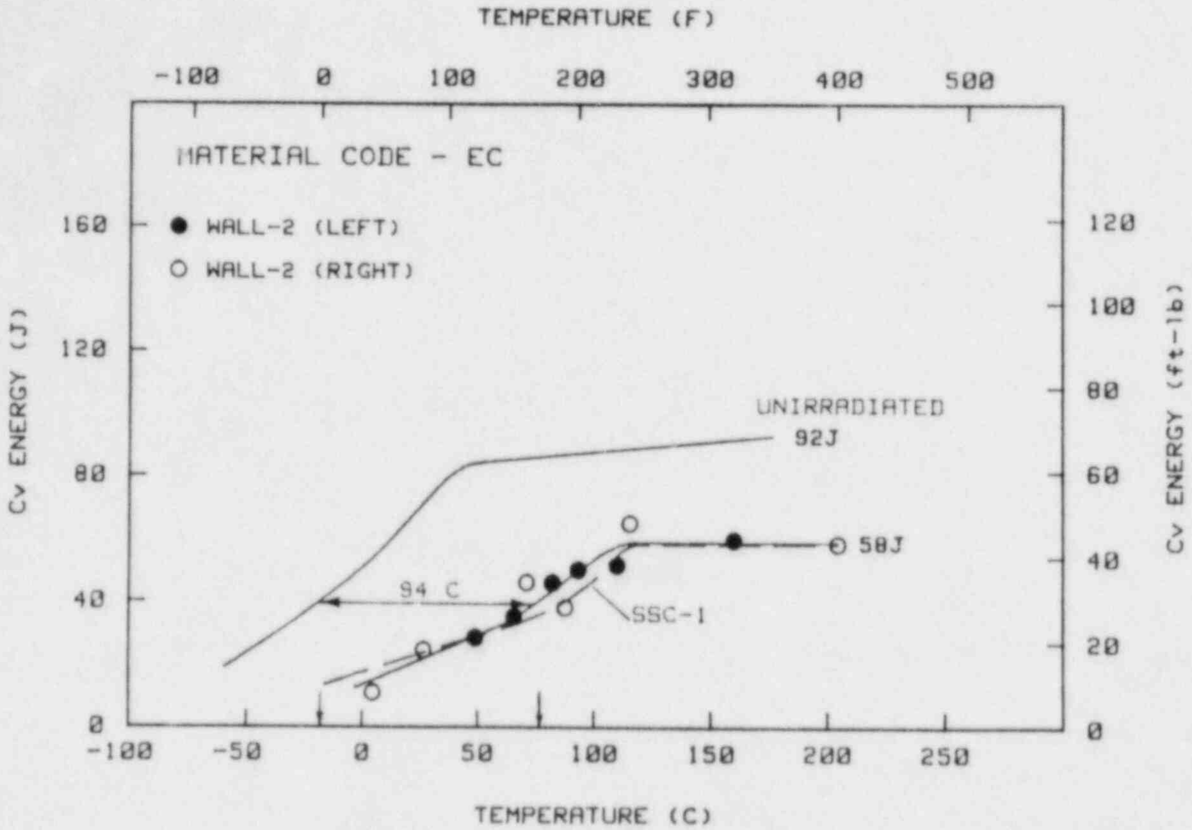

Fig. 37 Charpy-V notch ductility of the submerged arc weld code EC before and after irradiation in capsule Wall-2.

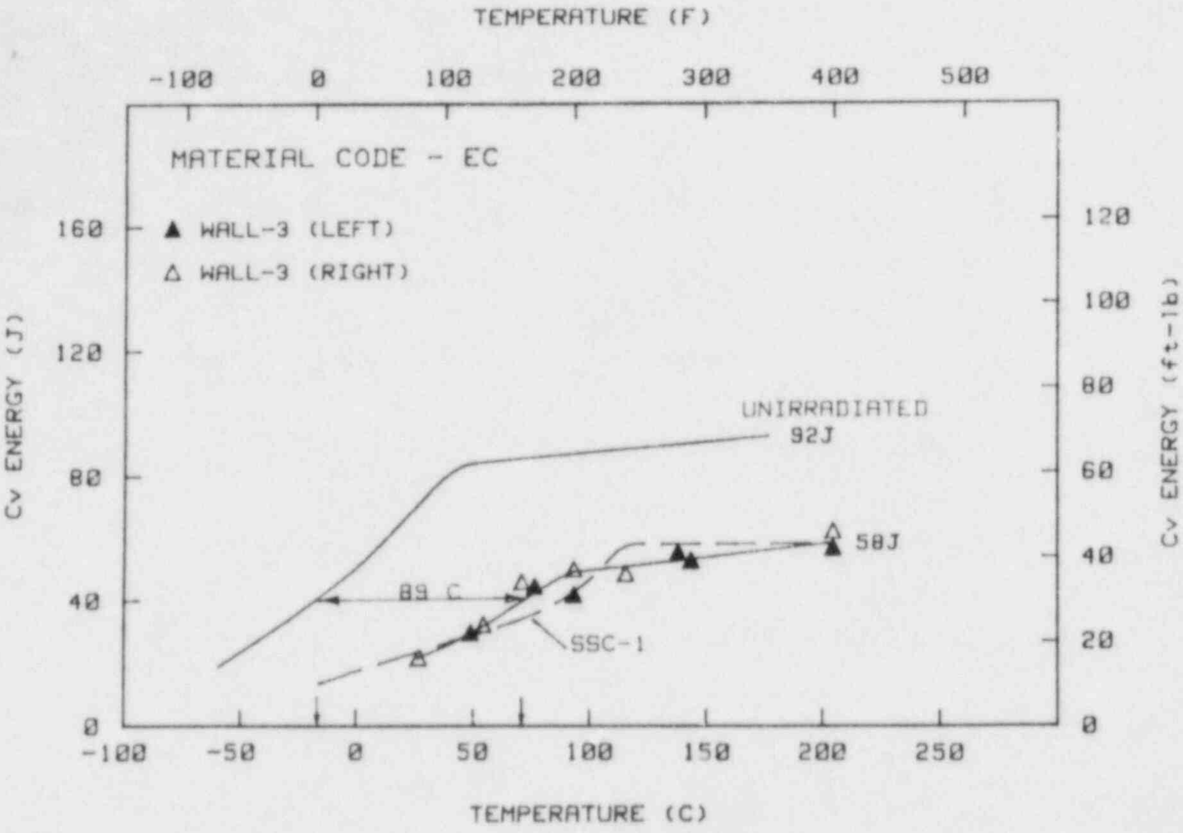

Fig. 38 Charpy-V notch ductility of the submerged arc weld code EC before and after irradiation in capsule Wall-3.

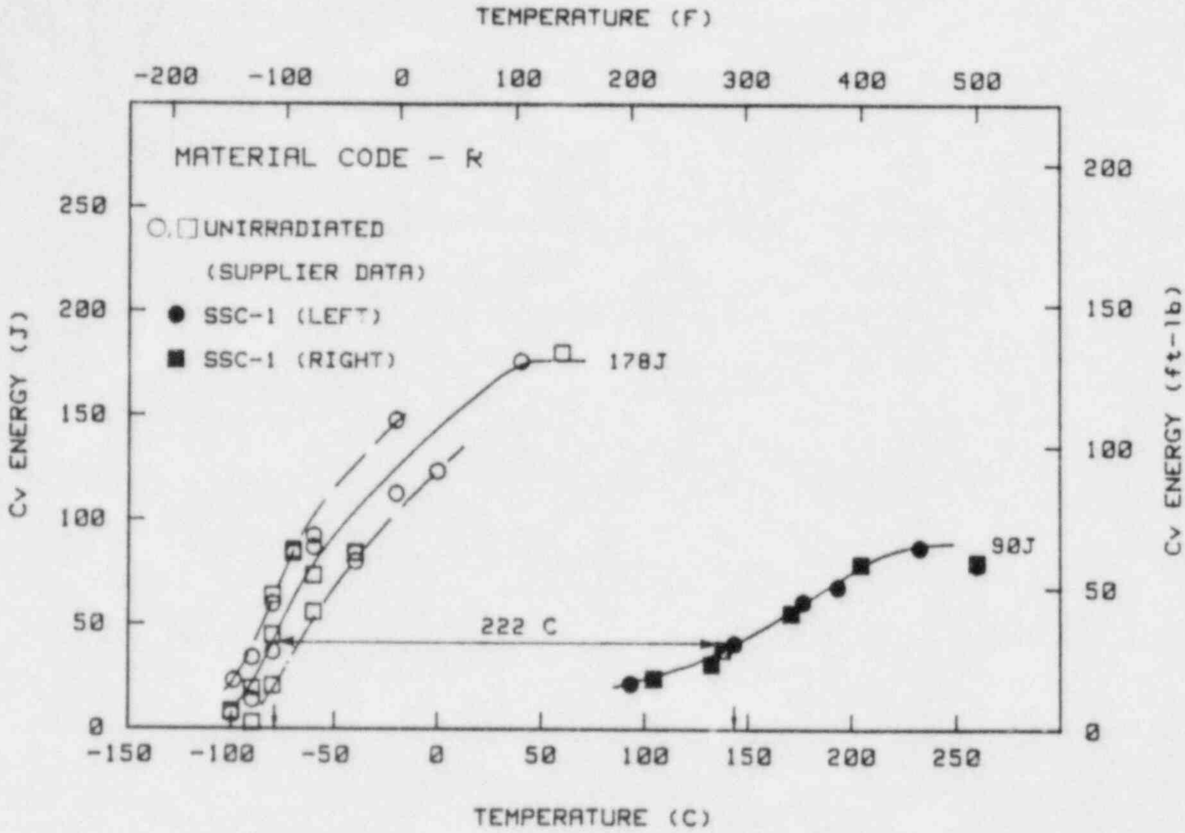

Fig. 39 Charpy-V notch ductility of the submerged arc weld code R before and after irradiation in capsule SSC-1.

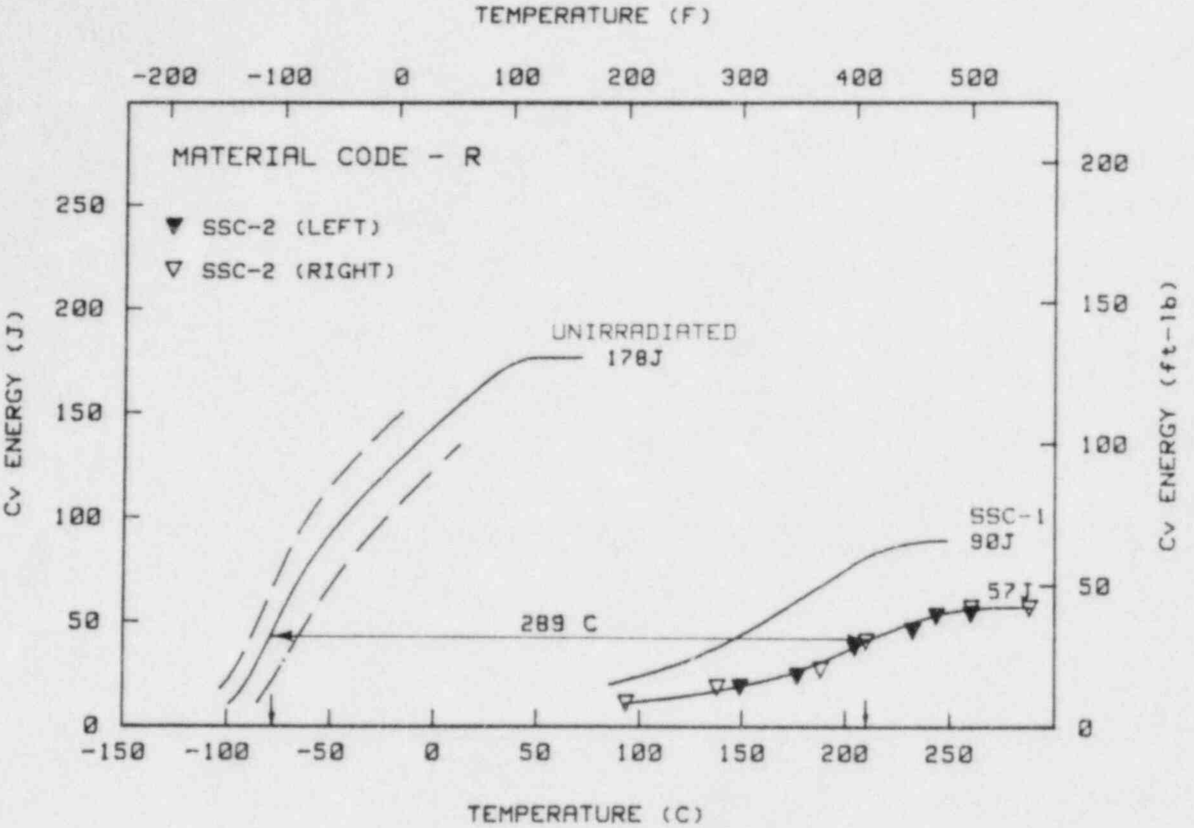

Fig. 40 Charpy-V notch ductility of the submerged arc weld code R before and after irradiation in capsule SSC-2.

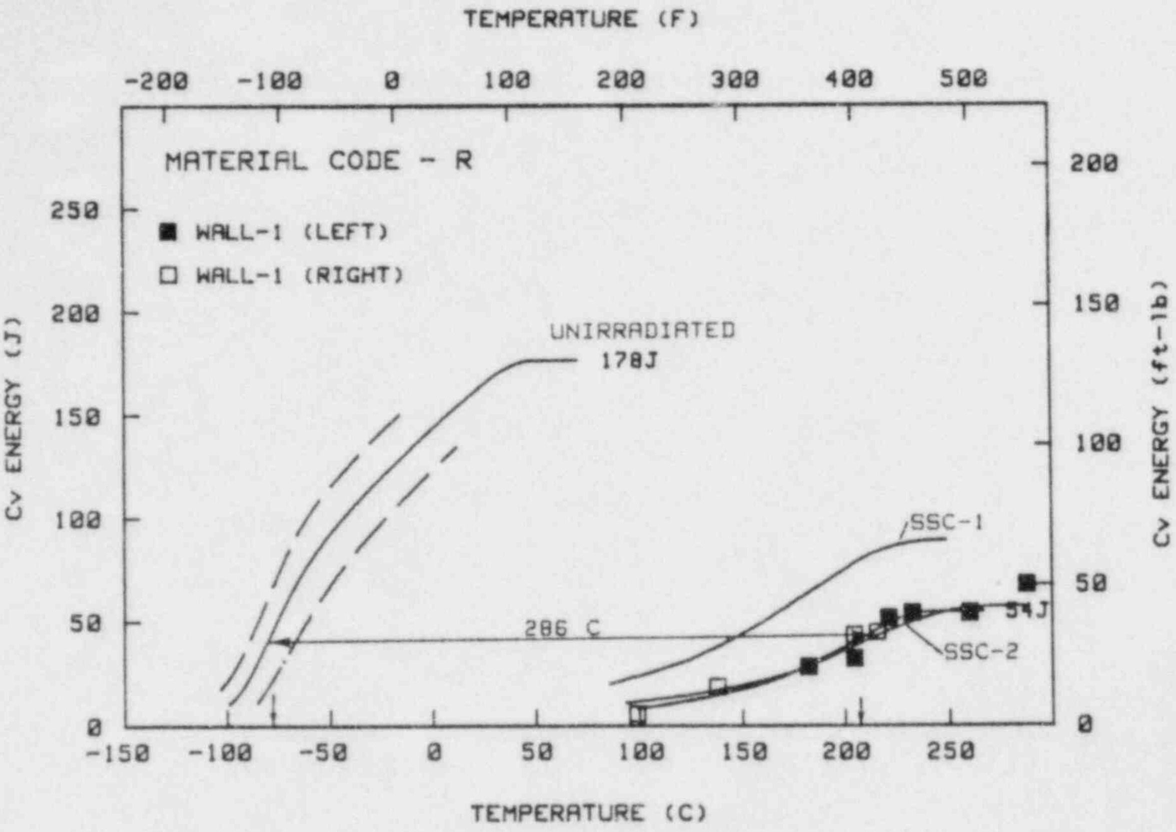

Fig. 41 Charpy-V notch ductility of the submerged arc weld code R before and after irradiation in capsule Wall-1.

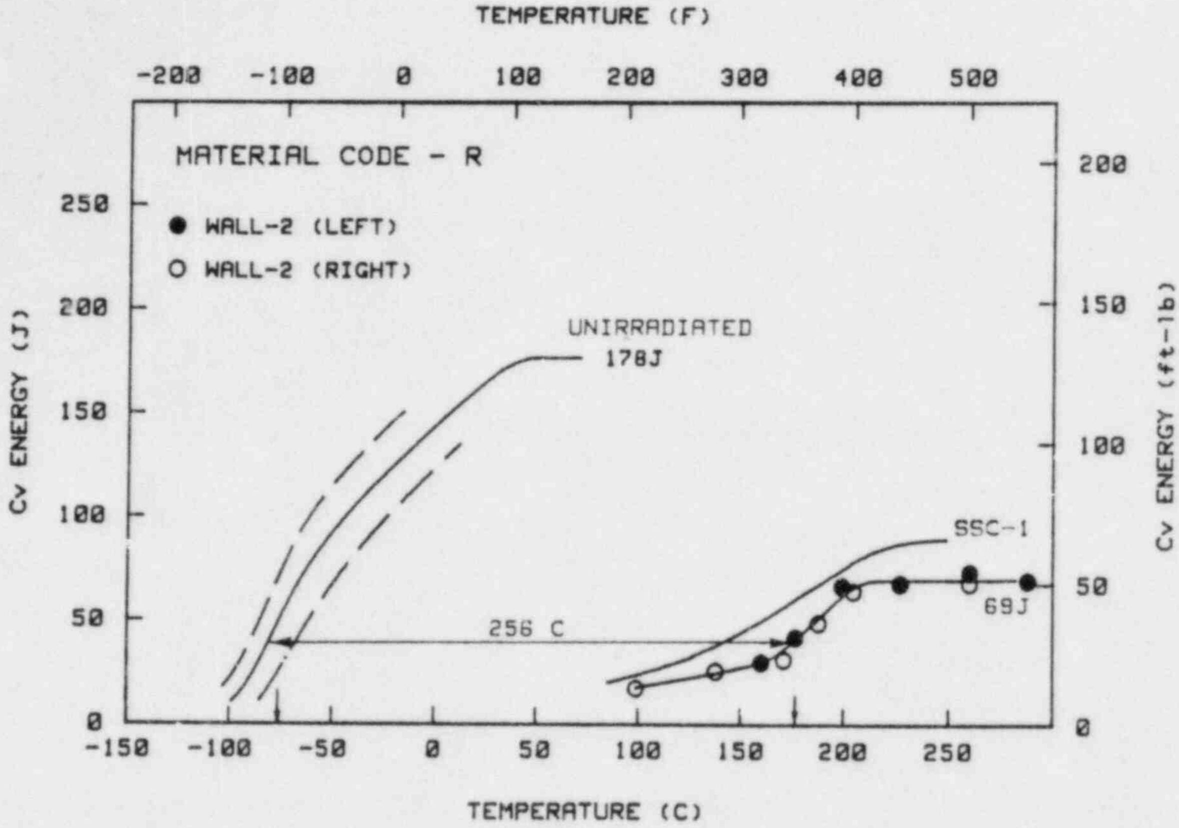

Fig. 42 Charpy-V notch ductility of the submerged arc weld code R before and after irradiation in capsule Wall-2.

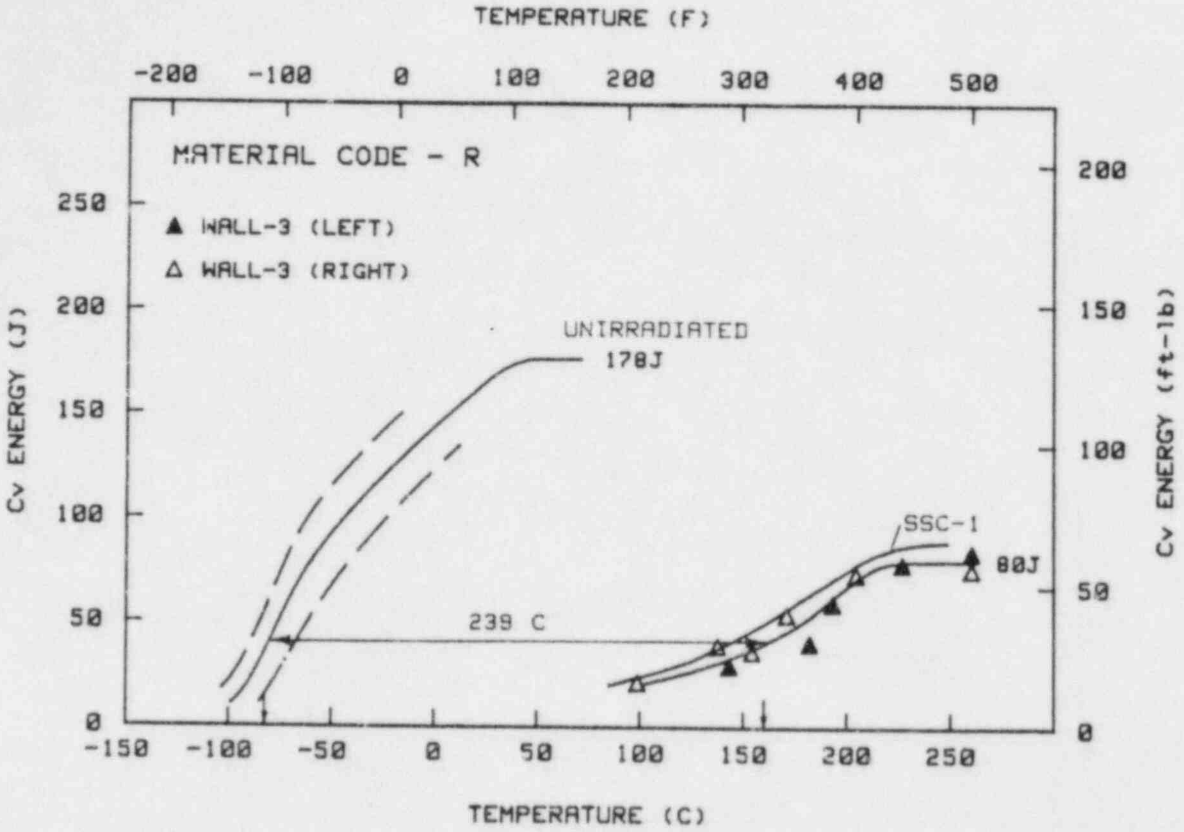

Fig. 43 Charpy-V notch ductility of the submerged arc weld code R before and after irradiation in capsule Wall-3.

Table 4. Summary of Observations on Notch Ductility of A 302-B Plate

Irradiation Capsule	Fluence Estimate[a] ($\times 10^{19} n/cm^2$)	Transition Temp (°C) 41 J	68 J	0.89 mm	Irradiation Increase (Δ°C) 41 J	68 J	0.89 mm	Upper Shelf Level J	mm	Irradiation Decrease ΔJ	Δmm
Unirradiated	–	−4	21	7	—	—	—	108	1.60	—	—
SSC-1 (Left)	–	74	93	91	78	72	83	94	1.37	14	0.23
(Right)	–	82	104	102	86	83	94	77	1.17	31	0.43
(Avg)	2.79	78	99	97	82	78	89	86	1.27	23	0.33
SSC-2	~5.4	90	104	99	94	83	92	75	1.19	33	0.41
Wall-1	~5.4	77	96	90	81	75	83	80	1.30	28	0.30
Wall-2	~2.8	63	85	74	67	64	67	81	1.32	27	0.28
Wall-3	~1.4	46	77	63	50	56	56	81	1.42	27	0.18

Table 5. Summary of Observations on Notch Ductility of A 533-B Plate

Irradiation Capsule	Fluence Estimate[a] ($\times 10^{19} n/cm^2$)	Transition Temp (°C) 41 J	68 J	0.89 mm	Irradiation Increase (Δ°C) 41 J	68 J	0.89 mm	Upper Shelf Level J	mm	Irradiation Decrease ΔJ	Δmm
Unirradiated	–	−1	24	13	—	—	—	150	2.18	—	—
SSC-1	2.55	60	88	82	61	64	69	115	1.68	35	0.50
SSC-2	~5.0	80	107	99	81	83	86	106	1.73	44	0.45
Wall-1	~5.0	74	102	93	75	78	80	106	1.60	44	0.58
Wall-2	~2.5	68	93	85	69	69	72	—[b]	1.68	—[b]	0.50
Wall-3	~1.3	52	79	66	53	55	53	125	1.93	25	0.25

[a] Fluence > 1 MeV   [b] Not established because of data scatter

Table 6. Summary of Observations on Notch Ductility of Forging Code K

Irradiation Capsule	Fluence Estimate[a] ($\times 10^{19}$ n/cm^2)	Transition Temp (°C)			Irradiation Increase (Δ°C)			Upper Shelf Level		Irradiation Decrease	
		41 J	68 J	0.89 mm	41 J	68 J	0.89 mm	J	mm	ΔJ	Δmm
Unirradiated	-	-65	-57	-59	—	—	—	203	1.93	—	—
SSC-1	1.66	-4	4	7	61	61	66	160	1.98	43	(+0.05)
SSC-2	~3.2	29	49	49	94	106	108	135	1.88	68	0.05
Wall-1	~3.2	7	29	24	72	86	83	161	1.93	42	0.00
Wall-2	~1.7	~13	~24	~24	~78	~81	~83	156	1.78	47	0.15
Wall-3	~0.8	~-9	~13	~10	~56	~70	~69	164	1.90	39	0.03

[a] Fluence, E > 1 MeV

Table 7. Summary of Observations on Notch Ductility of Forging Code MD

Irradiation Capsule	Fluence Estimate[a] ($\times 10^{19}$ n/cm^2)	Transition Temp (°C)			Irradiation Increase (Δ°C)			Upper Shelf Level		Irradiation Decrease	
		41 J	68 J	0.89 mm	41 J	68 J	0.89 mm	J	mm	ΔJ	Δmm
Unirradiated	-	-54	-34	-45	—	—	—	~212	2.34	—	—
SSC-1	1.81	-34	-26	-29	~20	8	16	~205	2.23	~7	0.10
SSC-2	~3.5	-15	-1	-6	39	33	39	~201	2.29	~11	0.05
Wall-1	~3.5	-29	-18	-20	25	16	25	219	2.16	(+)7	0.18
Wall-2	~1.8	-34	-20	-26	20	14	19	233	2.18	(+)22	0.16
Wall-3	~0.9	-40	-20	-34	14	14	11	~211	2.26	~0	0.08

[a] Fluence, E > 1 MeV

Table 8. Summary of Observations on Notch Ductility of Weld Code EC

Irradiation Capsule	Fluence Estimate[a] ($x10^{19} n/cm^2$)	Transition Temp (°C) 41 J	68 J	0.89 mm	Irradiation Increase (Δ°C) 41 J	68 J	0.89 mm	Upper Shelf Level J	mm	Irradiation Decrease ΔJ	Δmm
Unirradiated	–	–18	21	–9	—	—	—	92	1.75	—	—
SSC-1	1.77	90	—[b]	110	108	—[b]	119	58	0.94	34	0.81
SSC-2	~3.5	101	—[b]	113	119	—[b]	~122	50	0.96	42	0.79
Wall-1	~3.5	96	—[b]	113	114	—[b]	~122	54	0.96	38	0.79
Wall-2	~1.8	76	—[b]	105	94	—[b]	~114	58	1.04	34	0.71
Wall-3	~0.9	71	—	105	89	—	~114	58	1.09	34	0.66
BSR-12[c]	0.81	79	104	99	97	83	108	70	0.99	22	0.76

[a] Fluence, E > 1 MeV   [b] Not established   [c] NRL-EPRI experiment (Ref. 9)

Table 9. Summary of Observations on Notch Ductility of Weld Code R

Irradiation Capsule	Fluence Estimate[a] ($x10^{19} n/cm^2$)	Transition Temp (°C) 41 J	68 J	0.89 mm	Irradiation Increase (Δ°C) 41 J	68 J	0.89 mm	Upper Shelf Level J	mm	Irradiation Decrease ΔJ	Δmm
Unirradiated	–	–79	–68	–73	—	—	—	178	1.80	—	—
SSC-1	2.68	143	188	185	222	256	258	90	1.22	88	0.58
SSC-2	~5.2	210	—[b]	—[b]	289	—[b]	—[b]	57	0.87	121	0.93
Wall-1	~5.2	207	—[b]	—[b]	286	—[b]	—[b]	54[c]	0.84	124	0.96
Wall-2	~2.7	177	210[d]	205	256	278[d]	278	69	1.09	109	0.71
Wall-3	~1.4	160	199	194	239	267	267	80	1.09	98	0.71

[a] Fluence, E > 1 MeV   [b] Not established   [c] Value at 260°C   [d] Approximate

5.3 Simulated Surveillance Capsules

Data for capsules SSC-1 and SSC-2 are presented in Figs. 14 and 15 (A 302-B plate, code F23), Figs. 19 and 20 (A 533-B plate, codes 3PT, 3PU), Figs. 24 and 25 (forging, code K), Figs. 29 and 30 (forging, code MO), Figs. 34 and 35 (weld, code EC) and Figs. 39 and 40 (weld, code R). Results from specimens contained in the left hand compartment of the capsules are separately identified from results from specimens in the right hand compartment in each figure. The fluence received by the materials in capsule SSC-1 are summarized in Table 10.

Fluences for the same materials from the capsule SSC-2 are estimated to be 1.95 times higher. For the most part, the fluence variation (minimum vs. maximum value) for individual materials in capsule SSC-1 was ≤10%. The fluence variation between two materials however, was higher in many cases. For example, the variation between the forging code K and the A 302-B plate was 40%.

In Fig. 14, specimens of the A 302-B plate contained in the left compartment of capsule SSC-1 (group 1) indicate a different postirradiation notch ductility than specimens contained in the right compartment (group 2). The low data scatter suggests that the difference is real. The occurrence of the two separate data patterns cannot be attributed to neutron fluence dissimilarities but may be some unknown reflection of the specimen locations in the parent plate. Specimens forming group 1 were from plate thickness layer 1 only; specimens forming group 2 were from plate thickness 2 only. In Fig. 10, unirradiated condition tests of these two adjacent thickness layers indicate identical properties making the postirradiation difference in notch ductility anomalous. The anomaly is compounded by the fact that the specimens for individual capsules were intentionally randomized within the total specimen complement to avoid introducing any across-plate bias. Overall, the difference in transition behaviors is small and average behavior was used for capsule-to-capsule comparisons. In the case of upper shelf behavior, the difference was largest for capsule SSC-1, intermediate with capsule Wall-2 and small for capsules SSC-2, Wall-1 and Wall-3. In the discussion of data which follows, average properties are assumed for the A 302-B material unless noted otherwise.

From the aggregate capsule SSC-1 results, very large material-to-material differences in radiation embrittlement sensitivity are apparent. Taking fluence dissimilarities into account, the materials rank by their sensitivity, i.e., 41 J temperature elevation, as follows: weld code R (highest), weld code EC, A 302-B plate, forging code K, A 533-B plate and forging code MO (lowest). The order of ranking is found unchanged in the capsule SSC-2 data; some differences in relative sensitivity were observed as discussed below.

As expected, the A 302-B plate showed a greater embrittlement sensitivity than the A 533-B plate. The greater radiation effect to the former is consistent with its higher copper content (0.21% vs. 0.12% Cu) and its somewhat higher fluence. The low sensitivity of the forging code MO is a manifestation of its low copper content (0.05% Cu), its low phosphorus content (0.008% P) and, in the opinion of the authors, its prior forging (metal working) history. The high and very high radiation embrittlement

Table 10. Fluence Exposures of Materials in Capsule SSC-1

Material	Average Fluence[a] ($\times 10^{19} n/cm^2$)	Fluence Variation[b] (%)	41 J Temperature Increase (Δ°C)	Sensitivity Ranking
A 302-B Plate (Code F23)	2.79	7.0	82	3
A 533-B Plate (Codes 3PT, 3PU)	2.55	10.1	61	5
Forging (Code K)	1.66	14.5	61	4
Forging (Code MD)	1.81	3.9	20	6 (lowest)
Weld (Code EC)	1.77	8.8	108	2
Weld (Code R)	2.68	9.7	222	1 (highest)

[a] Fluence, E > 1 MeV [Ref. 18] [b] (1 - minimum/maximum) x 100

sensitivities of, respectively, the welds code EC and code R are readily attributed to their high copper contents (~0.24% Cu) and nickel alloying (0.64% and 1.58% Ni). Recent experiments confirmed a long-suspect synergism between nickel and copper in radiation sensitivity development wherein the former in amounts of 0.4% or more reinforces the detrimental effect of a high copper content. As discussed later, it is believed that more is involved in the very high radiation sensitivity of the weld code R than just nickel and copper content. The embrittlement sensitivity of the forging code K is ranked higher than that of the A533-B plate. The copper contents of the two materials are comparable. Their difference in fluence (1.66×10^{19} vs. 2.55×10^{19} n/cm^2) must be considered in weighing their irradiation responses (equal 41 J temperature elevations).

On balance, the SSC-1 and SSC-2 postirradiation data provide no surprises in regard to material ranking. The absolute level of sensitivity of the weld code R was somewhat unexpected. A comparably high-radiation sensitivity has been observed before, but in another weld composition; i.e., a filler metal for NiCrMo (Ref. 7).

A second primary observation from the capsule SSC-1 vs. capsule SSC-2 data is that the doubling of the fluence exposure of the materials produced only a small, in many cases negligible, additional 41 J temperature elevation. Weld code R was the exception. The 41 J temperatures of the A 302-B plate and the weld code EC were further increased by only 11 to 12°C; those of the A 533-B plate and the forging code MO were further increased by 19 to 20°C. The doubling of the fluence exposure had a somewhat larger effect (33°C change) on the forging code K but a difference in location of the test specimens in the original forging thickness (layers 5 and 6 vs. layer 7) may be partly responsible. In this case, specimens from layer 8 only were provided to MEA for making preirradiation determinations. Thus, the existance (or absence) of a through-thickness notch ductility gradient (which would have an impact on the "measured" 41 J temperature elevations), could not be shown. For the case of a gradient, layer 7 would normally have a higher transition temperature than layers closer to the surface of the forging. For weld code R, the 41 J temperature elevation for specimens from capsule SSC-2 was 67°C or 30% higher than that for capsule SSC-1. The percentage difference is about the same as that observed for the A 533-B plate (33%). Thus the 67°C increase is not disproportionately large for the doubling of the fluence exposure in this case.

The findings for the two plates and the weld code EC are in general agreement with prior observations for these materials following in-core irradiation at 288°C in a test reactor. Figure 44 shows the SSC-1 and SSC-2 data entered on the data trends found with the in-core experiments. At both fluence levels, the data for the A 302-B plate agrees well with the in-core trend. Additionally, the small difference in irradiation effect found between the SSC-1 and SSC-2 tests is predicted well by the data trend.

Not shown, an in-core, 288°C irradiation test of the A 533-B plate at $\sim 1.5 \times 10^{19}$ n/cm^2 produced a 41 J temperature increase of 56°C (Ref. 6). The SSC-1 result for this plate is consistent with this earlier determination when the respective fluence levels are considered. Likewise, the SSC-1 data for the weld code EC agree reasonably well with a prior in-core test (see Fig. 34).

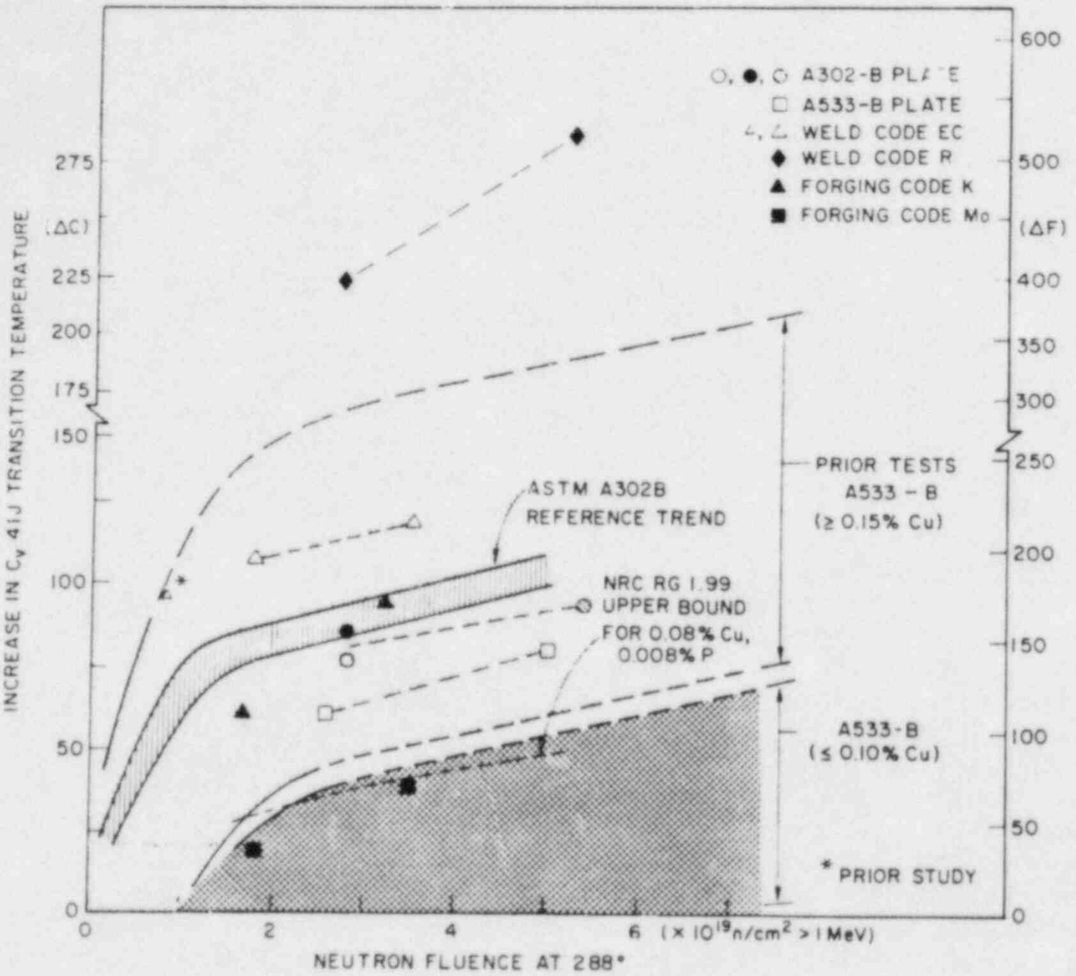

Fig. 44 Data from the capsules SSC-1 and SSC-2 compared against trends of C_V 41 J transition temperature change with irradiation observed with in-core, test reactor experiments. The trend band, marked ASTM A 302-B Reference Trend was established with several independent experiments using code F23 material; good agreement at both fluence levels is indicated. Observations for the remaining five materials show good agreement with projections based on % Cu (and % Ni) content.

Discussions of the relative effects of irradiation on the upper shelf level and on the 68 J and 0.89 mm transition temperatures are presented in later sections (see Intercapsule Comparisons and Embrittlement Assessments by Alternative Indices).

5.4 Wall Capsules

Data for the capsules Wall-1, Wall-2 and Wall-3 are illustrated in Figs. 16-18, Figs. 21-23, Figs. 26-28, Figs. 31-33, Figs. 36-38, and in Fig. 41-43. The data are also summarized in the Tables 4 to 9 and in Fig. 45.

A primary observation for five of the materials is that the increase in fracture resistance with wall depth (surface to the mid-wall) is neither rapid nor dramatic. That is, the 41 J transition temperature elevation for specimens irradiated in capsule Wall-3 is not much lower than that observed for the capsule Wall-1 irradiation. In the case of the A 302-B and A 533-B plates for example (Table 11), the 41 J temperature elevations for capsule Wall-1 are 81°C and 75°C, respectively. Corresponding determinations for capsule Wall-3 (depicting the midwall location) are only 31°C and 22°C lower. The wall surface and mid-wall irradiation locations produced a similar order of differences for the forgings and the weld code EC. The weld code R did not show comparable behavior. Its greater sensitivity to the irradiation location is consistent with its much higher radiation sensitivity level. The data for this weld suggest an embrittlement vs. fluence trend of a much higher slope than found for the remaining five materials. Again, it is cautioned that a 1:1 comparison cannot be made between the weld code R and the other materials because of dissimilar fluence levels. For example, the fluence difference (Wall-1 vs. Wall-3) which produced the 47°C reduction with depth for weld code R was 3.8 x 10^{19} n/cm^2; the fluence difference for weld code EC which produced its 25°C reduction was only 2.6 x 10^{19} n/cm^2. More importantly, the embrittlement trend with fluence in the interval 0.9 x 10^{19} to 1.8 x 10^{19} n/cm^2 is non-linear for many materials (see Fig. 44). This interval encompasses the Wall-2 and Wall-3 exposures of weld code EC, but not of weld code R. Thus, judgements are necessary in making material cross comparisons.

Of additional interest to this investigation, note that the A 302-B and A 533-B plates exhibited about the same transition temperature elevations, i.e., about equal radiation sensitivities, when exposed in the wall capsule locations. This is in clear contrast to the difference in apparent embrittlement sensitivity observed with the simulated surveillance capsule irradiations. Whether or not this change in relative behavior arose from the much longer exposure time of the wall capsules is a key question.

Referring to the test results for the forging code K, the data for capsules Wall-2 and Wall-3 inexplicably show large scatter. For example, the scatter band for the capsule Wall-3 data is approximately 33°C wide. The 41 J temperature elevation based on average behavior, on the other hand, is 56°C. The scatter is of a magnitude making meaningful data comparisons difficult. Accordingly, detailed analyses over those presented above were not attempted for this material.

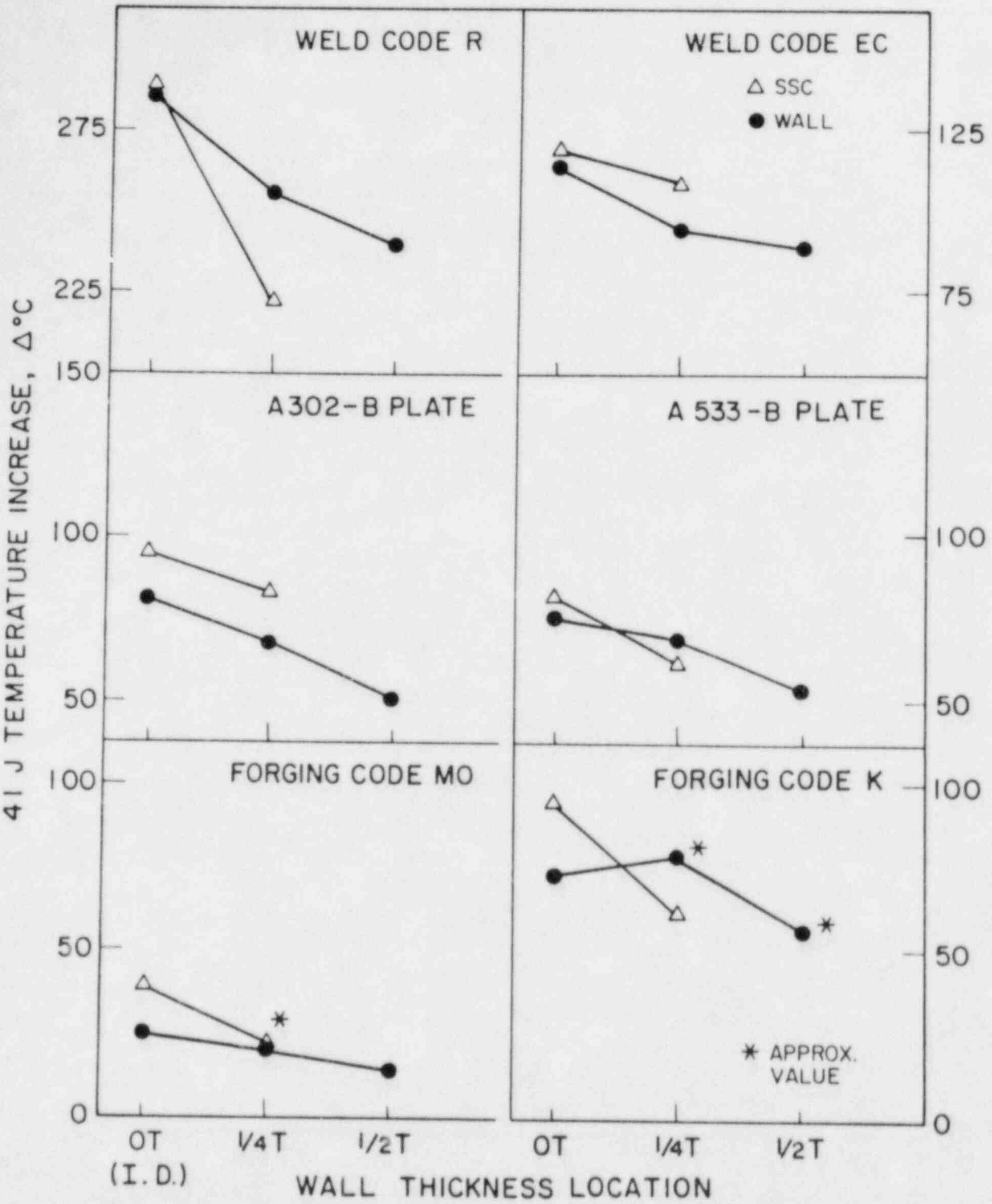

Fig. 45 Comparison of C_v data from simulated surveillance capsules vs. in-wall capsules (open triangle vs. filled circle points). With two exceptions, the surveillance capsule data either predict well or overpredict the transition temperature elevation for the wall location.

Table 11. Observations on 41J Temperature Increase for Capsules Wall-1 and Wall-3

Material	41 J Temperature Increase, Δ°C		
	Capsule Wall-1 (A)	Capsule Wall-3 (B)	Difference, °C (A-B)
A 302-B Plate (Code F23)	81	50	31
A 533-B Plate (Codes 3 PT, 3 PU)	75	53	22
Forging (Code K)	72	~56	~16
Forging (Code MD)	25	14	11
Weld (Code EC)	114	89	25
Weld (Code R)	286	239	47

For the A 302-B plate, essentially the same (reduced) upper shelf level was observed in the Wall-1, Wall-2 and Wall-3 capsule tests. A comparable data pattern is shown for the forging code K and the weld code EC. The upper shelf level of the forging code MD was not reduced significantly by any of the wall capsule exposures. Only the weld code R showed a large change in upper shelf level with wall depth. The upper shelf for the wall surface location was 35 J or 32% lower than the upper shelf at the mid-wall location. From the lateral expansion data for the A 533-B plate, the upper shelf toughness l el of this material would appear to be the same for the Wall-1 and Wall-2 locations but not for the Wall-3 location. Here, the higher upper shelf toughness for the Wall-3 capsule may or may not be a simple manefestation of biased data scatter. The high data scatter found with the Wall-2 upper shelf tests, while not explainable, illustrates well a problem which can be encountered when too few specimens are provided. Many early reactor vessel surveillance programs likewise had only limited specimen numbers.

5.5 Intercapsule Comparisons.

The data from the two sets of capsules (surveillance vs. wall) are in good agreement in showing that the difference in transition temperature elevations between the lowest fluence and the highest fluence condition is not large for typical vessel materials. In turn, the fluence attenuation with wall depth between surface and quarter thickness positions does not translate to a dramatic gradient in fracture toughesss in the general sense. The exception of course is the weld code R but this weld composition has not been used in commercial reactor vessels.

One primary objective of the five capsule series, both from the standpoint of neutron physics calculations and from the standpoint of metallurgical correlations, was to see how well data from capsule SSC-1 predict the irradiation effects to the quarter wall thickness location (capsule Wall-2), and, how well data from capsule SSC-2 predict properties at the wall inner surface (capsule Wall-1). Appropriate comparisons are shown in Table 12. Surveillance vs. the wall capsule data also compared in Fig. 45, open symbols vs. filled symbols, respectively. Differences in transition temperature elevation of 10°C or less are felt to be indicative of 1:1 correspondence.

With few exceptions, the surveillance capsule data either predict well or overpredict the transition temperature elevation for the wall location. For the A 302-B and A 533-B plates and the weld code EC, the amount of overprediction is 20°C or less regardless of the brittle/ductile transition index used (41 J, 68 J or 0.89 mm). Their upper shelf energy changes are also predicted well, i.e., are within about 7 J or 5 ft-lb. Interpretation of the results for the forging code K is difficult. On one hand, we have a case of underprediction (SSC-1 vs. Wall-2) by ~20°C and on the other, a case of overprediction (SSC-2 vs. Wall-1) by approximately the same amount. Possible reasons for the inconsistency were pointed out above. A like situation exists with the weld code R.

Table 12. Comparison of Simulated Surveillance and Wall Capsule Observations (Matching Fluence Conditions)

Capsule	41 J Temp. (Δ°C)	68 J Temp. (Δ°C)	0.89 mm Temp. (Δ°C)	Upper Shelf Energy (Δ J)
		A 302-B Plate (Code F23)		
SSC-1	82	78	89	23
Wall-2	67	64	67	27
Difference[a]	15	14	22	- 4
SSC-2	94	83	92	33
Wall-1	81	75	83	28
Difference	13	8	9	5
		A 533-B Plate (Codes 3PT, 3PU)		
SSC-1	61	64	69	35
Wall-2	69	69	72	35[b]
Difference	- 8	- 5	- 5	0[b]
SSC-2	81	83	86	44
Wall-1	75	78	80	44
Difference	6	5	6	0

[a] SSC Capsule value - Wall Capsule value
[b] Estimate based on lateral expansion data

Table 12. Comparison of Simulated Surveillance and Wall Capsule Observations (Continued)

Capsule	41 J Temp. (Δ°C)	68 J Temp. (Δ°C)	0.89 mm Temp. (Δ°C)	Upper Shelf Energy (Δ J)
		Forging (Code K)		
SSC-1	61	61	66	43
Wall-2	~78	~81	~83	47
Difference	-17	-20	-17	-4
SSC-2	94	106	108	68
Wall-1	72	86	83	42
Difference	22	20	25	26
		Forging (Code MD)		
SSC-1	~20	8	16	~7
Wall-2	20	14	19	22[c]
Difference	0	-6	-3	29
SSC-2	39	33	39	~11
Wall-1	25	16	25	7[c]
Difference	14	17	14	18

[c]Average postirradiation value > average preirradiation value

Table 12. Comparison of Simulated Surveillance and Wall Capsule Observations (Continued)

Capsule	41 J Temp. (Δ°C)	68 J Temp. (Δ°C)	0.89 mm Temp. (Δ°C)	Upper Shelf Energy (Δ J)
		Weld (Code EC)		
SSC-1	108	-	119	34
Wall-2	94	-	114	34
Difference	14	-	5	0
SSC-2	119	-	~122	42
Wall-1	114	-	~122	38
Difference	5	-	0	4
		Weld (Code R)		
SSC-1	222	256	258	88
Wall-2	256	278	278	109
Difference	-34	-22	-20	-21
SSC-2	289	-	-	121
Wall-1	286	-	-	124
Difference	3	-	-	-3

5.6 Embrittlement Assessement by Alternative Indices

Table 13 is a summary comparison of absolute transition temperatures and transition temperature elevations (ΔT's) indexed to the C_V 68 J temperature and the C_V 0.89 mm temperature as alternatives to the C_V 41 J temperature. Typically, the 0.89 mm temperature is higher than the 41 J temperature. On the other hand, this index temperature index is either about equal to or slightly lower than the 68 J temperature, their maximum difference being 14°C for both preirradiation and postirradiation conditions. In turn, the 0.89 mm and 68 J transition temperature elevations are about the same, i.e., within 11°C with an average difference of 6°C. Of greater interest, with the exception of weld code R, the data sets show an agreement of 41 J and 68 J transition temperature elevations to within 14°C. Accordingly, the ranking of the irradiation effect by capsule location is quite independent of the C_V indexing procedure selected (41 J, 68 J or 0.89 mm temperature). Where the 41 J temperature shift was found to be significantly less than the 68 J temperature increase, (see code R), the irradiation produced a marked change (flattening) in the shape of the transition curve. This alteration produced a 34°C difference between transition temperature elevations in the case of the capsule SSC-1 exposure and 22° to 28°C differences in the case of the capsule Wall-1 and Wall-2 exposures.

The close agreement of the 41 J and 68 J transition temperature elevations noted in the present study is consistent with observations made for several other steels earlier (Ref. 9). The prior study however reported a bias toward a greater 0.89 mm transition temperature elevation, compared to the 41 J temperature elevation, on the order of 15°C to 20°C. In the present investigation, only the weld code R showed a consistent bias of this order of magnitude. With the weld code EC and with the forging code K, two out of the five data sets did suggest a moderate or high bias, but factors such as a low postirradiation upper shelf must be considered in judging these data sets.

6. TENSILE PROPERTIES DETERMINATIONS

6.1 Procedure

Tensile properties were established using button head specimens machined from selected C_V specimen blanks (Fig. 4). All tests were conducted at a loading rate less than 690 MPa/min based on the slope of the load-extension curve in the elastic region. Specimen strain was not monitored using an extensometer; instead, elongation of the gage section was monitored from test machine actuator displacement. In Fig. 4, the uniform gage length is shown to be 31.75 mm. For determinations of the 0.2% offset yield strength, however, an effective gage length of 38.1 mm was assumed in order to account fully for the specimen's reduced section and for a portion of the radius blends. All tests were performed on a 55 metric ton MTS servohydraulic test machine. Load cell calibration was performed within in one year of the present tests. A calibration recheck using shunt resistors was made immediately before each test. Likewise, a calibration recheck of actuator deflection was performed before the test series commenced and was verified again after the tests were completed. Specimen load vs. actuator deflection was recorded simultaneously on two X-Y plot-

Table 13. Comparison of Irradiation Effect Assessments by Alternative C_v Indices

Comparison (A) (B)	Weld[a] (Code EC)	Weld[a] (Code R)	Forging (Code MD)	Forging (Code K)	A 302-B Plate (Code F23)	A 533-B Plate (Codes 3PT, 3PU)
ΔT_{41J} vs. ΔT_{68J}	—[b]	A < B (34°C)	A > B (12°C)	A < B (14°C)	A > B (11°C)	A = B (3°C)
ΔT_{41J} vs. $\Delta T_{0.89mm}$	A < B (25°C)	A < B (36°C)	A = B (3°C)	A < B (14°C)	A <> B (7°C)	A < B (8°C)
ΔT_{68J} vs. $\Delta T_{0.89mm}$	—	A < B (2°C)	A ~ B (9°C)	A = B (5°C)	A < B (11°C)	A = B (6°C)
$T_{0.89mm}$ vs. T_{68J}	—	A = B (5°C)	A < B (14°C)	A = B (5°C)	A < B (14°C)	A < B (13°C)
$T_{0.89mm}$ vs. T_{41J}	A < B (34°C)	A > B (42°C)	A > B (9°C)	A > B (20°C)	A > B (19°C)	A > B (22°C)

[a] Where comparisons were possible
[b] Postirradiation upper shelf less than 68 J
[c] Maximum difference between values

ters. One plotter recorded the entire applied load vs. deflection history through to specimen failure. The second plotter provided an expanded load vs. deflection record which was stored digitally via a computer-controlled data acquisition system.

6.2 Observations

Tensile property determinations are listed in Tables 14 to 19 and are illustrated graphically in Figs. 46 and 47. The results represent computer analyses of the stored digital data, and were verified through comparisons with the analog X-Y recorder plots. At this time, percent elongation and percent reduction in area measurements are not available. These measurements will be included in an addendum to be issued by MEA.

Referring to Fig. 47, the data show the expected increase in yield and tensile strengths with increasing fluence. Except for weld code R, the yield strength changes were less than 175 MPa (25 ksi) and yield strength differences between capsules are small (see Table 20). The strength change was least with capsule Wall-3 and greatest with capsule SSC-2.

The changes with capsule Wall-2 were somewhat greater than those of Wall-3 but were less than those observed with capsule Wall-1 or capsule SSC-1. Surveillance capsule results (duplicate test averages) by-in-large gave conservative predictions for material performances in the wall capsules. The reason for the somewhat high degree of scatter found with some of the data sets for the A 302-B and A 533-B plates has not been ascertained but is not due to plate sampling location or testing procedure, i.e., specimens were from one small volume of material and were tested concurrently.

7. DISCUSSION

Further analysis of the data presented here will depend on the availability of "final" fluence values and the confirmation of fluence gradients within the individual capsules. Adjustments to fluences listed in the data tables are not expected to be greater than 10%; accordingly, the conclusions drawn from capsule intercomparisons will remain unchanged.

The very high radiation embrittlement sensitivity observed for the weld code R may be due to more than just the synergism of nickel content with copper content. It is possible that, when the nickel content is high (> 1% Ni), an independent contribution of nickel to radiation sensitivity development occurs. The code R data also could be reflecting some non-nuclear time-at-temperature effect. This suspicion derives from the lower embrittlement observed for the capsule SSC-1 specimens compared to the capsule Wall-2 specimens coupled with their large difference in exposure times, i.e., 1291 hours vs. 18478 hours. Capsule SSC-2 which was exposed for 2845 hours on the other hand, did produce comparable embrittlement to its mating capsule, Wall-1. A larger dissimilarity in yield strength elevation was also recorded for the capsules SSC-1 and Wall-2 (31 MPa) compared to the capsules SSC-2 and Wall-1 (16 MPa). Thermal control data where available are helpful in resolving questions of one vs. two operating mechanisms and can help preclude technical surprises as well.

Table 14. Tensile Properties of A 302-B Plate

Specimen Number	Test Temperature (°C)	0.2% Yield Stress (MPa)	Ultimate Stress (MPa)
Unirradiated			
F23-T22[a]	24	482	660
Capsule SSC-1			
F23-T6[a]	24	581	710
F23-T23[a]	24	611	756
F23-T1	163	507	643
F23-T7	288	499	646
F23-T16	288	538	705
Capsule SSC-2			
F23-T11	26	610	726
F23-T27	26	620	755
F23-T13	163	549	682
F23-T5	288	518	671
F23-T20	288	559	727
Capsule Wall-1			
F23-T2	24	584	711
F23-T17	24	605	762
F23-T28	163	556	703
F23-T8	288	516	675
F23-T24	288	538	712
Capsule Wall-2			
F23-T3	26	571	704
F23-T25	26	588	736
F23-T12	163	519	658
F23-T9	288	506	665
F23-T18	288	527	697
Capsule Wall-3			
F23-T4	27	553	697
F23-T26	27	580	730
F23-T21	163	523	677
F23-T10	288	496	655
F23-T19	288	517	697

[a] Tested at the U.S. Naval Research Laboratory

Table 15. Tensile Properties of A 533-B Plate[a]

Specimen Number	0.2% Yield Stress (MPa)	Ultimate Stress (MPa)
Unirradiated		
3PT-14A	448	641
3PT-14B	459	641
Capsule SSC-1		
3PT-T1[b]	567	715
3PT-T10	573	710
Capsule SSC-2		
3PT-T5	606	744
3PT-T8	595	720
Capsule Wall-1		
3PT-T2	585	734
3PT-T11	577	725
Capsule Wall-2		
3PT-T3	552	707
3PT-T12	565	712
Capsule Wall-3		
3PT-T4	534	687
3PT-T13	543	690

[a] Test temperature 24 to 27°C
[b] Tested at the U.S. Naval Research Laboratory

Table 16. Tensile Properties of 22NiMoCr37 Forging[a]

Specimen Number	0.2% Yield Stress (MPa)	Ultimate Stress (MPa)
Unirradiated		
K-915	409	562
F-920	405	557
Capsule SSC-1		
K-98	514	636
K-99	528	657
Capsule SSC-2		
K-910	575	693
K-911	570	687
Capsule Wall-1		
K-96	540	670
K-97	545	672
Capsule Wall-2		
K-93	515	648
K-95	520	655
Capsule Wall-3		
K-91	516	654
K-92	510	647

[a] Test temperature 24 to 27°C

Table 17. Tensile Properties of A 508-3 Forging[a]

Specimen Number	0.2% Yield Stress (MPa)	Ultimate Stress (MPa)
Unirradiated		
(average)[b]	462	615
Capsule SSC-1		
MO-1	487	614
MO-2[b]	423	590
MO-3	487	613
Capsule SSC-2		
MO-13	508	627
MO-14	510	627
MO-15	512	627
Capsule Wall-1		
MO-4	501	627
MO-5	504	627
MO-6	504	626
Capsule Wall-2		
MO-7	491	616
MO-8	482	615
MO-9[c]	470	615
Capsule Wall-3		
MO-10	475	608
MO-11[b]	407	585
MO-12	480	614

[a] Test temperature 24 to 27°C
[b] 288°C test
[c] Specimen damaged in experiment decanning

Table 18. Tensile Properties of Weld Code EC[a]

Specimen Number	0.2% Yield Stress (MPa)	Ultimate Stress (MPa)
Unirradiated		
(average)[b]	456	583
Capsule SSC-1		
ET-1	602	691
ET-2	598	689
Capsule SSC-2		
ET-10	623	711
ET-11	619	708
Capsule Wall-1		
ET-3	610	703
ET-4	622	709
Capsule Wall-2		
ET-5	599	696
ET-6	609	702
Capsule Wall-3		
ET-7	607	695
ET-9	592	693

[a] Test temperature 24 to 27°C
[b] NRL data

Table 19. Tensile Properties of Weld Code R[a]

Specimen Number	0.2% Yield Stress (MPa)	Ultimate Stress (MPa)
Unirradiated		
Test-1[b]	475	596
Test-2[b]	502	629
Capsule SSC-1		
R88-T	766	820
R89-T	776	840
Capsule SSC-2		
R64-T	830	872
R65-T	815	858
Capsule Wall-1		
R62-T	841	889
R63-T	838	879
Capsule Wall-2		
R86-T	803	854
R87-T	801	853
Capsule Wall-3		
R84-T	777	837
R85-T	773	833

[a] Test temperature 24 to 27°C
[b] Supplier data

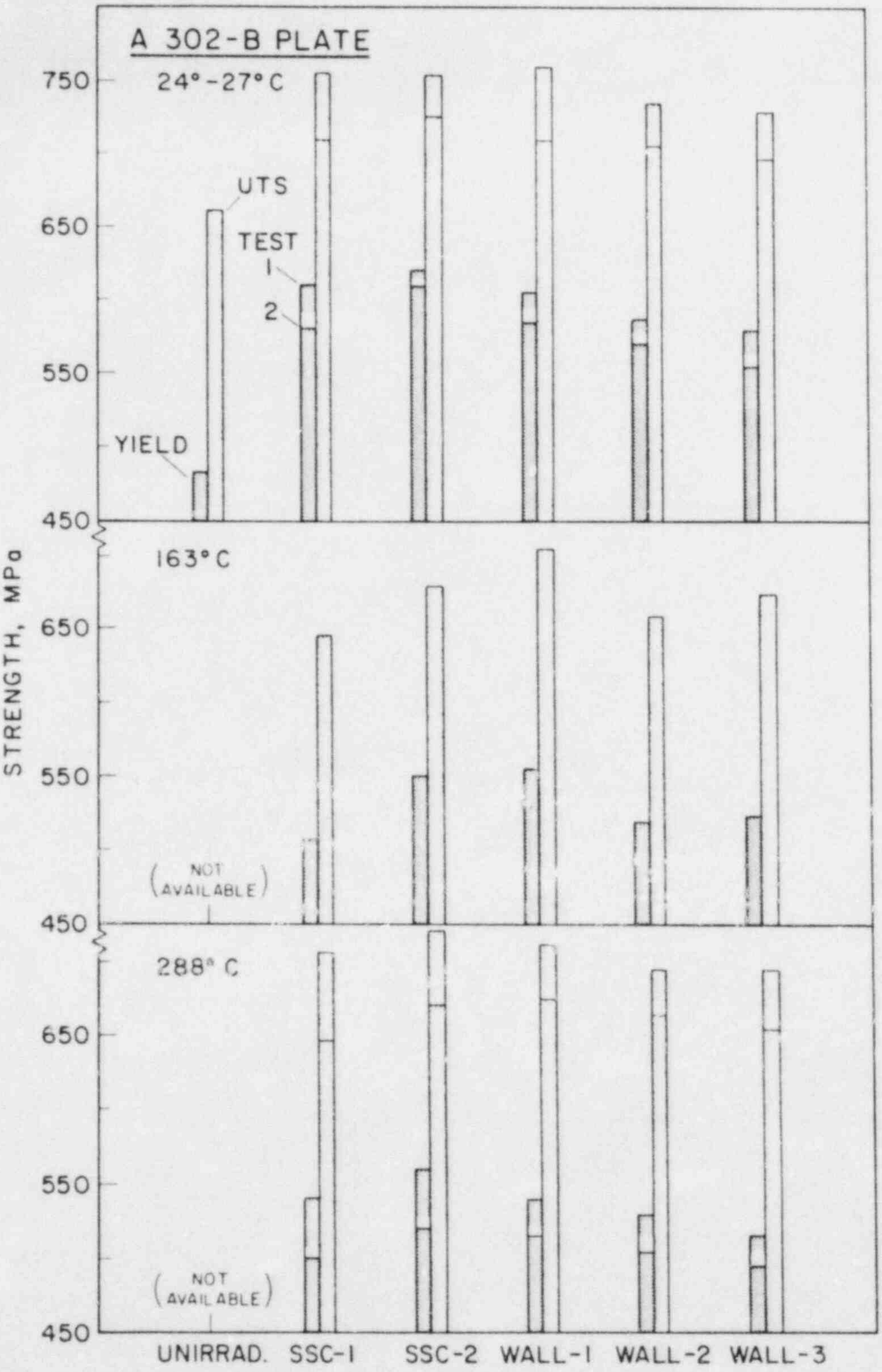

Fig. 46 Variation in tensile properties of the A 302-B plate between irradiation capsules for 24°C (upper graph), 163°C (middle graph) and 288°C (lower graph) test temperatures.

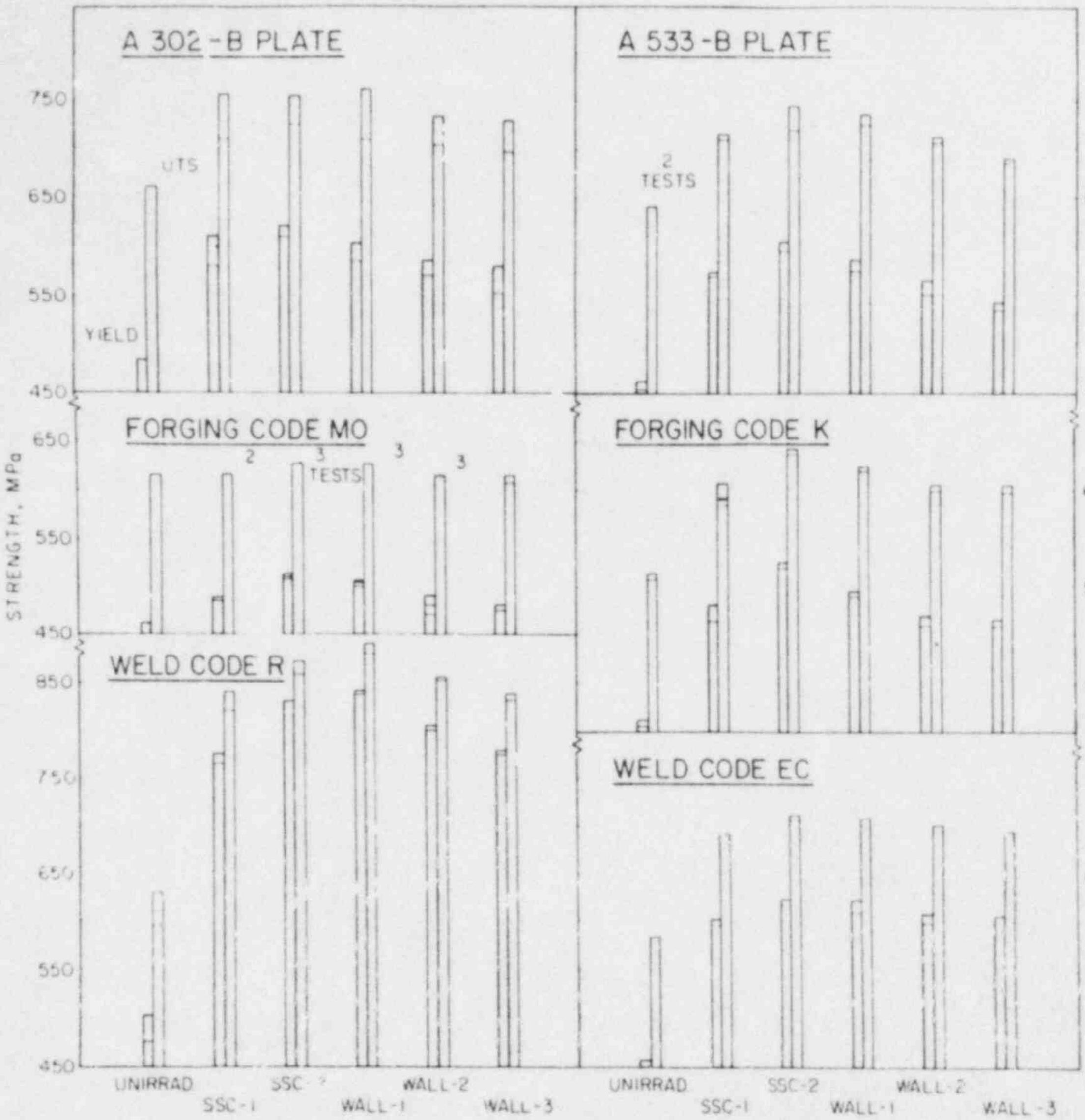

Fig. 47 Variation in tensile properties of the materals between irradiation capsules for ambient temperature tests.

Table 20. Comparison of Strength Changes Produced by Irradiation[a]

Material	Maximum Observed Elevation[b]		Maximum Difference Between Capsules[c]	
	Yield Strength (MPa)	Tensile Strength (MPa)	Yield Strength (MPa)	Tensile Strength (MPa)
A 302-B (Code F23)	133	81	48	27
A 533-B (Codes 3 PT, 3 PU)	147	91	62	43
Forging (Code K)	166	127	60	40
Forging (Code MD)	48	12	32	16
Weld (Code EC)	165	127	22	20
Weld (Code R)	351	272	69	54

[a] Ambient temperature tests; average of test data
[b] Capsule SSC-2 vs. unirradiated condition
[c] Capsule SSC-2 vs. capsule Wall-3 or capsule SSC-1 (code R only)

The relatively small difference in embrittlement level between wall surface and mid-wall positions was expected for the particular fluence ranges examined. The embrittlement (ΔT) trend developed for the A 302-B plate through in-core 288°C irradiation tests (see Fig. 44) shows that the rate of embrittlement accrual is higher for fluences below 1 -1.5×10^{19} n/cm^2 than for fluences above this level. The emphasis of the present PSF study on the higher of the two fluence regimes is consistent with its primary objective of evolving (or refining) physics-dosimetry-metallurgy correlations for near end-of-life (EOL) vessel conditions. EOL fluences on the inner wall in many instances will range from 4 to 6 x 10^{19} n/cm^2. Depending on the direction of the PTS analyses, the performance of a second set of experiments examining in-depth embrittlement for fluences below the knee of the embrittlement trend curve may be in order. The code R, code EC, A 302-B and A 533-B materials would be good candidates for such an investigation. Additionally, a material having a radiation embrittlement sensitivity intermediate to that of welds code R and EC should be included.

Earlier analyses suggested that the benefit of radiation effects attenuation with wall thickness, in terms of the retention of a tough outer wall ligament, would be strongest for the more radiation sensitive materials. Figure 48, taken from an earlier study (Ref. 19) illustrates this difference. The analysis shown was developed on the basis of experimentally defined or projected embrittlement trend curves for medium and high sensitivity cases. Within this framework, high copper content welds would be expected to follow the "high sensitivity" curves. The ASTM A 302-B reference plate illustrating the "medium senstivity case is the code F23 material studied here. As noted, the crack arrest transition (CAT) occurs closer to the wall surface for the "high sensitivity" case than for the "medium sensitivity" case because of the dissimilar gradients in embrittlement. The CAT, by definition, is the fracture transition elastic (FTE) temperature taken to be 33°C (60°F) above the drop weight nil-ductility transition (NDT) temperature.

Among the PSF experiment materials, only the weld code R clearly fits the category of "high sensitivity' in Fig. 48. The weld code EC, although significantly more radiation embrittlement sensitive than the A 302-B plate, showed about the same difference in 41 J temperature increase between capsule Wall-1 and capsule Wall-3 as the A 302-B (25° vs. 31°C). When the data for this weld are superimposed on Fig. 44, an embrittlement trend having a higher slope than that of the A 302-B plate is depicted, but the slope difference is small.

Finally for completeness, it is well to mention here the observation made in postirradiation CT and C_v test comparisons for the A 302-B and A 533-B plates (Ref. 3). On balance, the 41 J temperature elevation had a tendency to be less than the 100 MPa$\sqrt{m}$ temperature elevation. The trend was more apparent for the A 302-B plate where on average, the 41 J temperature increase was about 24°C smaller than the 100 MPa$\sqrt{m}$ temperature increase. However, when the CT fracture toughness data were corrected for constraint by the β_{Ic}-approach postulated by Irwin (Ref. 20), the 100 MPa$\sqrt{m}$ temperature elevations were lower than the 41 J temperature elevations. (The β_{Ic}-correction has been shown by Merkle (Ref. 21) to provide reasonable estimates of the plane strain fracture toughness, K_{Ic}, for cases in which K_{Ic} and some non-plane strain fracture toughness, K_c, are known.) For the referenced CT

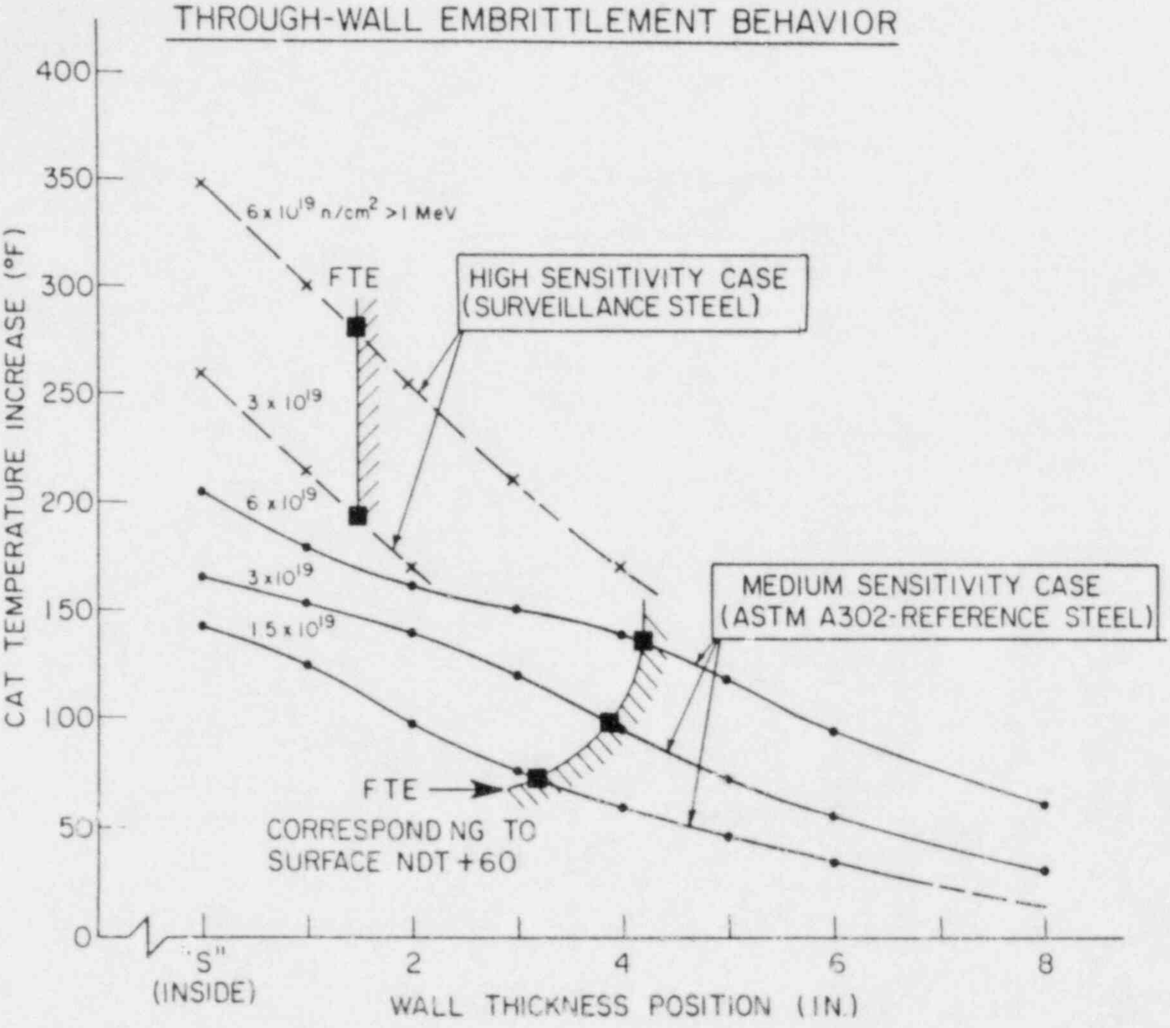

Fig. 48 Projection of through-thickness notch ductility of a 200 mm thick reactor vessel irradiated at 288°C for the case of medium radiation embrittlement sensitive vessel materials (depicted by the ASTM A 302-B reference plate) and for the case of high radiation embrittlement sensitive materials (depicted by the surveillance steel). The loci of the FTE position when the vessel temperature equals the inside surface NDT plus 33°C (60°F) temperature is indicated for each fluence.

data, the K_{Jc} values were taken as K_c values. Before β_{Ic}-corrected data can be applied with full confidence, further experimental confirmation of the approach is required and is a subject of current research.

8. CONCLUSIONS

Primary conclusions and observations drawn from the results for the materials, except for code R, are as follows:

1. The surveillance capsule data indicate reasonably well the irradiation effect to the wall surface and quarter wall thickness locations. With one exception the C_v surveillance results proved conservative where significant (>10°C) differences were observed; predictions of the 41 J transition temperature were within 20°C. The exception pertains to the capsule SSC-1 results for the forging code K which underpredicted the in-wall transition temperature elevation by 17°C.

2. The in-wall toughness gradient produced by irradiation, indexed to the transition temperature, was small. The difference in 41 J temperature between wall surface and midthickness locations ranged between 31°C (A 302-B plate) and 11°C (forging code MO). The average difference for all materials, including the weld code R, was 25°C.

3. In parallel with (2), the doubling of the fluence to the materials produced only a small additional 41 J temperature elevation in the surveillance capsule irradiations (SSC-2 vs. SSC-1).

4. The postirradiation 41 J temperature elevation is in close agreement with the 68 J and 0.89 mm transition temperature elevations (within 14°C in most cases.)

5. Irradiation sensitivity levels of the materials are in accord with initial predictions based on material copper and nickel contents.

6. Tensile test findings support the notch ductility trend determinations.

Additional observations pertaining to the weld code R and the A 302-B plate are:

7. High radiation embrittlement sensitivity was observed for the weld code R which contained 0.23% Cu and 1.58% Ni. The unusually high level of sensitivity suggests contributions by two or more embrittlement mechanisms, in addition to the normal irradiation effect. An independent contribution of Ni to radiation sensitivity development and a time-at-temperature effect are currently suspect.

8. Capsule SSC-1 results for weld code R significantly underpredicted in-wall behavior. A time-at-temperature effect would explain this finding.

9. The postirradiation 41 J temperature elevation for the weld code R underpredicted the 68 J and 0.89 mm transition temperature elevations by as much as 36°C. Differences were due to a pronounced modification of the shape of the brittle/ductile transition curve by irradiation.

10. Postirradiation C_v data for the A 302-B plate show an anomalous difference traceable to specimen thickness location in the original plate. The anomaly is most evident in the upper shelf temperature regime and with data from capsule SSC-1. Good properties uniformity was observed in preirradiation (reference) condition data, however.

Finally, the performance of a second set of experiments to examine in-depth embrittlement for lower fluences, i.e., less than 1 to 1.5 x 10^{19} n/cm^2 on the wall surface, may be warranted depending on future NRC needs for PTS analyses.

REFERENCES

1. C. Z. Serpan, "NRC Light-Water Reactor Pressure Vessel Surveillance Dosimetry Improvement Program," Nuclear Safety, Volume 22, No. 1, July-Aug. 1981.

2. C. Z. Serpan, "USNRC Surveillance Dosimetry Improvement Program," Proceedings of the 6th MPA - Seminar, Safety of the Pressure Boundary of Light Water Reactors, Staatliche Materialprufungsanstalt (MPA), Universitat Stuttgart, 9/10, Oct. 1980.

3. J. R. Hawthorne, B. H. Menke, and A. L. Hiser, "Notch Ductility and Fracture Toughness Degradation of A 302-B and A 533-B Reference Plates from PSF Simulated Surveillance and Through-Wall Irradiation Capsules," USNRC Report NUREG/CR-3295, Vol. 1, MEA-2017, Materials Engineering Associates, April 1984.

4. J. R. Hawthorne, "Radiation Effects Information Generated on the ASTM Reference Correlation-Monitor Steels," ASTM DS 54, American Society For Testing and Materials, July 1974.

5. C. E. Childress, "Manual for ASTM A-533 Grade B Class 1 Steel (HSST Plate 03) Provided to the International Atomic Energy Agency," ORNL-TM-3193, Oak Ridge National Laboratory, March 1971.

6. W. N. McElroy, et. al., "LWR Pressure Vessel Surveillance Dosimetry Improvement Program - 1982 Annual Report," USNRC Report NUREG/CR-2805, Vol. 3; HEDL-TME 82-20, Hanford Engineering Development Laboratory, Jan. 1983.

7. Metal Properties Council, "Prediction of the Shift in the Brittle/Ductile Transition Temperature of LWR Pressure Vessel Materials," ASTM Journal of Testing and Evaluation," July 1983, pp. 237 - 260.

8. "Coordinated Research Program on Analysis of the Behavior of Advanced Reactor Pressure Vessel Steels Under Neutron Irradiation," IWG RRPC-78/81. International Atomic Energy Agency, Vienna, Austria, 17-18 Oct. 1977.

9. J. R. Hawthorne, Ed., "Evaluation and Prediction of Neutron Embrittlement in Reactor Pressure Vessel Materials," EPRI NP-2782, Electric Power Research Institute, Dec. 1982.

10. T. R. Mager, et. al., "Feasibility of and Methodology for Thermal Annealing an Embrittled Reactor Vessel," EPRI NP-2712, Vol. 1, Electric Power Research Institute, Jan. 1983.

11. J. R. Hawthorne, J. J. Koziol, and S. T. Byrne, "Evaluation of Commercial Production A 533-B Steel Plates and Weld Deposits with Extra-Low Copper Content for Radiation Resistance," Effects of Radiation on Structural Materials, ASTM STP 683, American Society for Testing and Materials, Philadelphia, PA, 1979, pp. 278-294.

12. J. R. Hawthorne, "Significance of Nickel and Copper Content to Radiation Sensitivity and Postirradiation Heat Treatment Recovery of Reactor Vessel Steels," USNRC Report NUREG/CR-2948, also MEA-2006, Materials Engineering Associates, Nov. 1982.

13. F. A. Smidt, Jr., and J. A. Sprague, "Property Changes Resulting From Impurity-Defect Interactions in Iron and Pressure Vessel Steel Alloys," Effects of Radiation on Structural Materials, ASTM STP 529, American Society for Testing and Materials, Philadelphia, PA., 1973, pp. 78-91.

14. ASTM E 185-79, "Standard Practice for Conducting Surveillance Tests for Light-Water Cooled Nuclear Power Reactor Vessels," ASTM Book of Standards, Part 45, 1980, p. 865.

15. "Minutes of CEN/SCK/COCKRILL Meeting on Fracture Toughness Characterization of a Belgian LWR Pressure Vessel Steel SA 508 Cl. 3 Forging, June 20, 1978," enclosure (1) to private communication, A. Fabry (C.E.N./S.C.K.) to J. R. Hawthorne (Naval Research Laboratory), Sept. 24, 1980 (Serial No. Reactor Physics AF/eu 380/80-50).

16. "NRC-HEDL RPV Irradiation Surveillance Experiment - Available Data Pertaining to Material Provided by Rolls-Royce & Associates LTD," enclosure (1) to private communication, T. Williams (Rolls-Royce and Associates Ltd.), to J. R. Hawthorne (Naval Research Laboratory), Oct. 16, 1980, (Serial No. TJW M209.9 2/BAB).

17. U. Potapovs and J. R. Hawthorne, "The Effect of Residual Elements on 550°F Irradiation Response of Selected Pressure Vessel Steels and Weldments," Nuclear Applications, Vol. 6, No. 1, Jan. 1969, pp. 27-46.

18. Private communication, J. A. Ulseth (Hanford Engineering Development Laboratory) to J. R. Hawthorne (Naval Research Laboratory), March 3, 1982 (Serial No. 8250808).

19. F. J. Loss, J. R. Hawthorne, C. Z. Serpan, Jr., and P. P. Puzak, "Analysis of Radiation-Induced Embrittlement Gradients on Fracture Characteristics of Thick-Walled Pressure Vessel Steels," ASME Journal of Engineering for Industry, Nov. 1971, pp. 1007-1015.

20. G. R. Irwin, "Fracture Mode Transition for a Crack Transversing a Plate," J. of Basic Eng., ASME, 82 (2), 1960, pp. 417-425.

21. J. G. Merkle, "New Method for Analyzing Small Scale Fracture Specimen Data in the Transition Zone," Tenth Water Reactor Safety Research Information Meeting, USNRC Report NUREG/CR-0041, Washington, D. C., Oct. 1982, pp. 307-315.

APPENDIX A

TABLES OF INDIVIDUAL CHARPY-V TEST RESULTS FROM PSF IRRADIATIONS

APPENDIX A

Table A.1 Charpy-V Test Results for A302-B Plate (ASTM Reference) (Code F23)

Specimen Number	Test Temperature °C	(°F)	Charpy Energy J	(ft-lb)	Lateral Expansion mm	(mils)
			Unirradiated Condition			
Layer 1						
6	-40	(-40)	9	(7)	0.102	(4)
23	-18	(0)	33	(24)	0.483	(19)
43	-1	(30)	41	(30)	0.762	(30)
75	16	(60)	57	(42)	0.940	(37)
82	38	(100)	88	(65)	1.372	(54)
143	82	(180)	110	(81)	1.676	(66)
89	93	(200)	115	(85)	1.753	(69)
90	138	(280)	107	(79)	1.626	(64)
136	177	(350)	99	(73)	1.473	(58)
83	177	(350)	106	(78)	1.676	(66)
137	260	(500)	110	(81)	1.575	(62)
Layer 2						
107	-40	(-40)	14	(10)	0.203	(8)
16	-1	(30)	45	(33)	0.762	(30)
168	21	(70)	71	(52)	1.168	(46)
68	38	(100)	95	(70)	1.448	(57)
114	60	(140)	95	(70)	1.499	(59)
103	60	(140)	99	(73)	1.524	(60)
48	93	(200)	107	(79)	1.626	(64)
161	138	(280)	111	(82)	1.524	(60)
115	177	(350)	104	(77)	1.651	(65)
100	177	(350)	107	(79)	1.626	(64)
162	260	(500)	118	(87)	1.600	(63)
			Capsule SSC-1			
Group 1, Left						
1	138	(280)	92	(68)	1.346	(53)
8	104	(220)	92	(68)	1.448	(57)
25	288	(550)	91	(67)	1.473	(58)
45	38	(100)	22	(16)	0.279	(11)
77	204	(400)	95	(70)	1.397	(55)
84	88	(190)	47	(35)	0.711	(28)
91	71	(160)	41	(30)	0.686	(27)
138	99	(210)	99	(73)	1.346	(53)
Group 2, Right						
11	204	(400)	76	(56)	1.168	(46)
18	82	(180)	41	(30)	0.635	(25)
50	104	(220)	66	(49)	1.041	(41)
70	149	(300)	77	(57)	1.168	(46)
102	110	(230)	77	(57)	1.194	(47)
116	54	(130)	27	(20)	0.381	(15)
163	288	(550)	73	(54)	1.270	(50)
170	10	(50)	11	(8)	0.076	(3)

Table A.1 Continued

Specimen Number	Test Temperature °C	(°F)	Charpy Energy J	(ft-lb)	Lateral Expansion mm	(mils)
Capsule SSC-2						
Group 1, Left						
22	116	(240)	83	(61)	1.295	(51)
42	288	(550)	79	(58)	1.448	(57)
74	104	(220)	73	(54)	1.194	(47)
81	204	(400)	72	(53)	1.194	(47)
88	88	(190)	38	(28)	0.584	(23)
142	66	(150)	22	(16)	0.381	(15)
76	154	(310)	73	(54)	1.219	(48)
Group 2, Right						
15	204	(400)	65	(48)	1.143	(45)
47	93	(200)	42	(31)	0.762	(30)
67	104	(220)	65	(48)	1.168	(46)
99	154	(310)	73	(54)	1.168	(46)
106	77	(170)	23	(17)	0.483	(19)
113	121	(250)	76	(56)	1.092	(43)
120	288	(550)	73	(54)	1.295	(51)
167	24	(75)	7	(5)	0.001	(3)
101	46	(115)	18	(13)	0.254	(10)
Capsule Wall No. 1 (Surface)						
Group 1, Left						
2	149	(300)	85	(63)	1.422	(56)
9	116	(240)	84	(62)	1.295	(51)
39	91	(195)	65	(48)	--	--
71	102	(215)	81	(60)	1.295	(51)
78	204	(400)	91	(67)	1.372	(54)
85	88	(190)	46	(34)	--	--
139	66	(150)	33	(24)	0.483	(19)
7	49	(120)	23	(17)	0.584	(23)
Group 2, Right						
12	204	(400)	77	(57)	1.245	(49)
19	93	(200)	53	(39)	0.838	(33)
64	71	(160)	46	(34)	0.711	(28)
96	154	(310)	76	(56)	1.219	(48)
103	77	(170)	49	(36)	0.838	(33)
110	121	(250)	73	(54)	1.194	(47)
117	60	(140)	31	(23)	0.457	(18)
164	21	(70)	15	(11)	0.178	(7)
17	43	(110)	18	(13)	0.381	(15)

Table A.1 Continued

Specimen Number	Test Temperature °C	(°F)	Charpy Energy J	(ft-lb)	Lateral Expansion mm	(mils)
Capsule Wall No. 2 (Quarter T)						
Group 1, Left						
3	2	(35)	5	(4)	0.000	(0)
10	104	(220)	85	(63)	1.346	(53)
40	288	(550)	80	(59)	1.524	(60)
72	43	(110)	49	(36)	0.711	(28)
79	204	(400)	88	(65)	1.499	(59)
86	49	(120)	26	(19)	0.483	(19)
93	71	(160)	47	(35)	0.813	(32)
140	149	(300)	80	(59)	1.321	(52)
24	27	(80)	27	(20)	0.406	(16)
Group 2, Right						
13	204	(400)	73	(54)	1.245	(49)
20	82	(180)	71	(52)	1.118	(44)
65	32	(90)	30	(22)	0.508	(20)
97	71	(160)	43	(32)	0.737	(29)
104	127	(260)	73	(54)	1.270	(50)
118	54	(130)	42	(31)	0.610	(24)
165	288	(550)	71	(52)	1.245	(49)
49	10	(50)	8	(6)	0.076	(3)
Capsule Wall No. 3 (Half T)						
Group 1, Left						
4	121	(250)	84	(62)	1.499	(59)
21	60	(140)	52	(38)	0.914	(36)
41	288	(550)	81	(60)	1.397	(55)
73	43	(110)	39	(29)	0.559	(22)
80	204	(400)	84	(62)	1.372	(54)
94	77	(170)	64	(47)	1.067	(42)
141	93	(200)	88	(65)	1.372	(54)
44	10	(50)	14	(10)	0.229	(9)
Group 2, Right						
14	93	(200)	69	(51)	1.067	(42)
46	54	(130)	45	(33)	0.762	(30)
66	204	(400)	80	(59)	1.448	(57)
98	121	(250)	76	(56)	1.270	(50)
105	38	(100)	35	(26)	0.533	(21)
112	27	(80)	27	(20)	0.483	(19)
119	66	(150)	60	(44)	0.914	(36)
166	288	(550)	80	(59)	1.422	(56)
69	-1	(30)	11	(8)	0.152	(6)

Table A.2 Charpy V Test Results for A 533-B (HSST 03) Plate (Code 3PT, 3PU)

Specimen Number	Test Temperature °C	(°F)	Charpy Energy J	(ft-lb)	Lateral Expansion mm	(mils)
			Unirradiated Condition			
Layer 2						
3PT-16	-40	(-40)	15	(11)	0.305	(12)
3PT-11	-12	(10)	37	(27)	1.016	(40)
3PT-12	27	(80)	79	(58)	1.245	(49)
3PT-15	66	(150)	110	(81)	1.981	(78)
3PT-13	121	(250)	146	(108)	1.905	(75)
3PT-14	204	(400)	152	(112)	2.159	(85)
3PT-32	-40	(-40)	12	(9)	0.305	(12)
3PU-16	4	(40)	42	(31)	0.635	(25)
Layer 3						
3PU-32	149	(300)	134	(99)	1.905	(75)
Layer 4						
3PT-27	-12	(10)	27	(20)	0.635	(25)
3PT-28	27	(80)	65	(48)	1.067	(42)
3PT-31	66	(150)	115	(85)	1.727	(68)
3PT-29	121	(250)	159	(117)	2.184	(86)
3PT-30	204	(400)	146	(108)	2.235	(88)
			Capsule SSC-1 (Code 3PU)			
Group 1, Left						
1	210	(410)	133	(98)	1.727	(68)
2	43	(110)	27	(20)	0.406	(16)
3	71	(160)	50	(37)	0.737	(29)
4	99	(210)	81	(60)	1.143	(45)
5	177	(350)	113	(83)	1.905	(75)
Group 2, Right						
17	160	(320)	111	(82)	1.600	(63)
18	71	(160)	28	(21)	0.406	(16)
19	116	(240)	108	(80)	1.499	(59)
20	82	(180)	56	(41)	0.838	(33)
21	210	(410)	119	(88)	1.702	(67)

Table A.2 Continued

Specimen Number	Test Temperature °C	(°F)	Charpy Energy J	(ft-lb)	Lateral Expansion mm	(mils)
			Capsule SSC-2 (Code 3PT)			
Group 1, Left						
6	216	(420)	103	(76)	1.778	(70)
7	77	(170)	41	(30)	0.559	(22)
8	93	(200)	49	(36)	0.813	(32)
9	121	(250)	83	(61)	1.397	(55)
10	43	(110)	14	(10)	0.279	(11)
Group 2, Right						
22	113	(235)	79	(58)	1.270	(50)
23	66	(150)	33	(24)	0.508	(20)
24	149	(300)	103	(76)	1.626	(64)
25	104	(220)	49	(36)	0.889	(35)
26	216	(420)	110	(81)	1.803	(71)
			Capsule Wall No. 1 (Surface) (Code 3PU)			
Group 1, Left						
6	154	(310)	108	(80)	1.651	(65)
7	77	(170)	50	(37)	0.737	(29)
8	93	(200)	64	(47)	0.889	(35)
9	121	(250)	98	(72)	1.549	(61)
10	43	(110)	33	(24)	0.483	(19)
Group 2, Right						
22	82	(180)	41	(30)	0.635	(25)
23	66	(150)	35	(26)	0.559	(22)
24	24	(75)	14	(10)	0.102	(4)
25	104	(220)	62	(46)	1.092	(43)
26	210	(410)	103	(76)	1.524	(60)

Table A.2 Continued

Specimen Number	Test Temperature °C	(°F)	Charpy Energy J	(ft-lb)	Lateral Expansion mm	(mils)
Capsule Wall No. 2 (Quarter T) (Code 3PU)						
Group 1, Left						
11	210	(410)	127	(94)	1.753	(69)
12	43	(110)	22	(16)	0.483	(19)
13	71	(160)	65	(48)	1.041	(41)
14	93	(200)	69	(51)	1.143	(45)
15	66	(150)	41	(30)	0.660	(26)
Group 2, Right						
27	149	(300)	87	(64)	1.499	(59)
28	54	(130)	24	(18)	0.406	(16)
29	116	(240)	98	(72)	1.575	(62)
30	82	(180)	50	(37)	0.686	(27)
31	177	(350)	100	(74)	1.676	(66)
Capsule Wall No. 3 (Half T) (Code 3PT)						
Group 1, Left						
1	204	(400)	119	(88)	1.880	(74)
2	16	(60)	20	(15)	0.356	(14)
3	66	(150)	54	(40)	0.838	(33)
4	93	(200)	92	(68)	1.549	(61)
5	54	(130)	42	(31)	0.686	(27)
Group 2, Right						
17	149	(300)	125	(92)	1.880	(74)
18	43	(110)	37	(27)	0.635	(25)
19	104	(220)	100	(74)	1.702	(67)
20	77	(170)	62	(46)	1.118	(44)
21	210	(410)	130	(96)	2.032	(80)

Table A.3 22NiMoCr37 Forging
(Code K)

Specimen Number	Test Temperature °C	(°F)	Charpy Energy J	(ft-lb)	Lateral Expansion mm	(mils)
Unirradiated Condition						
86	-68	(-90)	46	(34)	0.660	(26)
814	-68	(-90)	18	(13)	0.254	(10)
815	-59	(-75)	62	(46)	0.914	(36)
87	-57	(-70)	69	(51)	1.016	(40)
85	-40	(-40)	125	(92)	1.702	(67)
813	-40	(-40)	92	(68)	1.270	(50)
82	-23	(-10)	125	(92)	1.702	(67)
810	4	(40)	146	(108)	1.803	(71)
83	27	(80)	136	(100)	1.676	(66)
811	49	(120)	191	(141)	2.032	(80)
84	138	(280)	207	(153)	1.880	(74)
812	177	(350)	201	(148)	1.854	(73)
Capsule SSC-1						
Group 1, Left						
512	177	(350)	165	(122)	2.007	(79)
513	-7	(20)	9	(7)	0.025	(1)
514	10	(50)	96	(71)	1.270	(50)
99	71	(160)	127	(94)	1.626	(64)
62	16	(60)	71	(52)	0.813	(32)
63	-12	(10)	4	(3)	0.000	(0)
64	27	(80)	110	(81)	1.499	(59)
Group 2, Right						
65	104	(220)	163	(120)	2.007	(79)
67	-7	(20)	54	(40)	0.711	(28)
515	49	(120)	106	(78)	1.372	(54)
610	27	(80)	91	(67)	1.168	(46)
611	-23	(-10)	4	(3)	0.051	(2)
612	204	(400)	149	(110)	1.524	(60)
613	10	(50)	58	(43)	0.711	(28)

Table A.3 Continued

Specimen Number	Test Temperature °C	(°F)	Charpy Energy J	(ft-lb)	Lateral Expansion mm	(mils)
			Capsule SSC-2			
Group 1, Left						
614	177	(350)	137	(101)	1.778	(70)
72	71	(160)	81	(60)	1.016	(40)
74	32	(90)	62	(46)	0.838	(33)
75	49	(120)	24	(18)	0.559	(22)
76	16	(60)	22	(16)	0.279	(11)
Group 2, Right						
77	93	(200)	98	(72)	1.372	(54)
710	43	(110)	68	(50)	0.838	(33)
711	66	(150)	84	(62)	1.143	(45)
73	38	(100)	43	(32)	0.533	(21)
712	116	(240)	141	(104)	1.219	(78)
713	24	(75)	5	(4)	0.000	(0)
714	210	(410)	133	(98)	1.956	(77)
715	138	(280)	136	(100)	1.829	(72)
			Capsule Wall No. 1 (Surface)			
Group 1, Left						
410	88	(190)	106	(78)	1.600	(63)
411	21	(70)	69	(51)	0.965	(38)
412	66	(150)	87	(64)	1.245	(49)
414	10	(50)	38	(28)	0.432	(17)
415	93	(200)	146	(108)	2.057	(81)
52	-4	(25)	8	(6)	0.025	(1)
Group 2, Right						
53	54	(130)	62	(46)	0.864	(34)
54	43	(110)	73	(54)	1.016	(40)
55	71	(160)	125	(92)	1.702	(67)
413	-12	(10)	5	(4)	0.000	(0)
56	4	(40)	52	(38)	0.610	(24)
57	24	(75)	52	(38)	0.737	(29)
510	204	(400)	157	(116)	1.854	(73)
511	138	(280)	165	(122)	1.905	(75)

Table A.3 Continued

Specimen Number	Test Temperature °C	(°F)	Charpy Energy J	(ft-lb)	Lateral Expansion mm	(mils)
			Capsule Wall No. 2 (Quarter T)			
Group 1, Left						
36	138	(280)	157	(116)	1.753	(69)
37	-4	(25)	60	(44)	0.838	(33)
312	-18	(0)	19	(14)	0.203	(8)
313	16	(60)	5	(4)	0.000	(0)
314	27	(80)	66	(49)	0.940	(37)
Group 2, Right						
315	93	(200)	149	(110)	1.753	(69)
42	71	(160)	81	(60)	1.168	(46)
43	-12	(10)	12	(9)	0.076	(3)
311	43	(110)	103	(76)	1.524	(60)
44	24	(75)	8	(6)	0.025	(1)
45	43	(110)	76	(56)	1.118	(44)
46	204	(400)	155	(114)	1.829	(72)
47	4	(40)	56	(41)	0.787	(31)
			Capsule Wall No. 3 (Half T)			
Group 1, Left						
24	177	(350)	157	(116)	1.829	(72)
25	-12	(10)	3	(2)	0.000	(0)
26	4	(40)	54	(40)	0.711	(28)
210	-23	(-10)	45	(33)	0.584	(23)
211	-37	(-35)	4	(3)	0.000	(0)
212	27	(80)	68	(50)	0.965	(38)
Group 2, Right						
213	138	(280)	165	(122)	2.007	(79)
214	71	(160)	134	(99)	1.702	(67)
215	-7	(20)	58	(43)	0.787	(31)
27	43	(110)	84	(62)	1.143	(45)
32	24	(75)	81	(60)	1.270	(50)
33	-18	(0)	33	(24)	0.406	(16)
34	204	(400)	171	(126)	1.549	(61)
35	4	(40)	39	(29)	0.533	(21)

Table A.4 A 508-3 Forging
(Code MO)

Specimen Number		Test Temperature °C	(°F)	Charpy Energy J	(ft-lb)	Lateral Expansion mm	(mils)
			Unirradiated Condition				
Block e, Inside layer							
66		121	(250)	217	(160)	2.311	(91)
67		27	(80)	207	(153)	2.362	(93)
68		4	(40)	142	(105)	1.854	(73)
69		-12	(10)	176	(130)	2.032	(80)
70		-29	(-20)	83	(61)	1.245	(49)
71		-46	(-50)	57	(42)	0.813	(32)
72		-62	(-80)	19	(14)	0.305	(12)
Block e, Outside layer							
73		-62	(-80)	42	(31)	0.635	(25)
74		4	(40)	142	(105)	1.778	(70)
75		121	(250)	206	(152)	2.311	(91)
76		-12	(10)	119	(88)	1.600	(63)
77		-29	(-20)	127	(94)	1.702	(67)
78		-46	(-50)	65	(48)	0.914	(36)
79		-18	(0)	102	(75)	1.499	(59)
80		38	(100)	231	(170)	2.337	(92)
Block e, Inside layer							
81		-18	(0)	113	(83)	1.626	(64)
82		288	(550)	244	(180)	2.083	(82)
84		288	(550)	283	(209)	1.803	(71)
			Capsule SSC-1				
Group 1, Left							
01	O[a]	-1	(30)	171	(126)	2.007	(79)
02	O	-29	(-20)	125	(92)	1.651	(65)
03	O	-46	(-50)	16	(12)	0.203	(8)
04	O	-40	(-40)	22	(16)	0.254	(10)
05	O	54	(130)	209	(154)	2.286	(90)
Group 2, Right							
06	O	-40	(-40)	61	(45)	0.787	(31)
07	O	-18	(0)	56	(41)	0.813	(32)
08	O	-18	(0)	68	(50)	0.965	(38)
09	I[b]	-40	(-40)	75	(55)	1.041	(41)
10	I	4	(40)	140	(103)	1.753	(69)
11	I	4	(40)	129	(95)	1.702	(67)
12	I	-18	(0)	88	(65)	1.245	(49)
13	I	121	(250)	201	(148)	2.210	(87)

[a] Forging Layer: outside
[b] Forging Layer: inside

Table A.4 Continued

Specimen Number		Test Temperature °C	(°F)	Charpy Energy J	(ft-lb)	Lateral Expansion mm	(mils)
			Capsule SSC-2[c]				
Group 1, Left							
53	O	4	(40)	79	(58)	1.219	(48)
54	O	-12	(10)	81	(60)	1.295	(51)
55	O	93	(200)	198	(146)	2.235	(88)
57	I	21	(70)	117	(86)	1.803	(71)
Group 2, Right							
58	I	49	(120)	146	(108)	1.981	(78)
59	I	-18	(0)	22	(16)	0.305	(12)
60	I	16	(60)	106	(78)	1.600	(63)
62	I	49	(120)	164	(121)	2.286	(90)
63	I	127	(260)	202	(149)	2.311	(91)
64	I	-1	(30)	73	(54)	1.118	(44)
65	I	-23	(-10)	37	(27)	0.508	(20)
			Capsule Wall No. 1 (Surface)				
Group 1, Left							
14	I	-29	(-20)	41	(30)	0.559	(22)
16	I	116	(240)	212	(156)	2.057	(81)
17	O	4	(40)	133	(98)	1.803	(71)
18	O	-40	(-40)	18	(13)	0.254	(10)
Group 2, Right							
19	O	121	(250)	225	(166)	2.134	(84)
20	O	-18	(0)	80	(59)	1.245	(49)
21	O	-40	(-40)	18	(13)	0.356	(14)
22	O	21	(70)	157	(116)	2.108	(83)
23	O	49	(120)	188	(139)	2.337	(92)
25	I	-1	(30)	99	(73)	1.397	(55)
26	I	-23	(10)	62	(46)	0.940	(37)

[c] All specimens from block g except specimen no. 65 which is from block e

Table A.4 Continued

Specimen Number		Test Temperature °C	(°F)	Charpy Energy J	(ft-lb)	Lateral Expansion mm	(mils)
		Capsule Wall No. 2 (Quarter T)					
Group 1, Left							
28	I	-23	(-10)	57	(42)	0.889	(35)
29	I	4	(40)	117	(86)	1.702	(67)
30	I	21	(70)	174	(128)	1.803	(71)
31	I	116	(240)	228	(168)	2.032	(80)
Group 2, Right							
32	I	-40	(-40)	24	(18)	0.406	(16)
33	O	-18	(0)	76	(56)	1.143	(45)
34	O	49	(120)	198	(146)	2.286	(90)
35	O	-40	(-40)	46	(34)	0.635	(25)
36	O	-1	(30)	117	(86)	1.778	(70)
37	O	-51	(-60)	8	(6)	0.102	(4)
39	O	121	(250)	233	(172)	2.210	(87)
		Capsule Wall No. 3 (Half T)					
Group 1, Left							
40	O	-43	(-45)	30	(22)	0.660	(26)
41	I	-29	(-20)	65	(48)	1.194	(47)
43	I	121	(250)	220	(162)	2.007	(79)
44	I	21	(70)	155	(114)	2.108	(83)
Group 2, Right							
45	I	4	(40)	103	(76)	1.600	(63)
46	I	-18	(0)	18	(13)	0.330	(13)
47	I	49	(120)	171	(126)	2.310	(91)
48	I	-40	(-40)	54	(40)	0.838	(33)
49	O	-1	(30)	76	(56)	1.245	(49)
51	O	-18	(0)	85	(63)	1.321	(52)
52	O	121	(250)	201	(148)	2.311	(91)

Table A.5 Submerged Arc Weld (Code EC)

Specimen Number	Test Temperature °C	(°F)	Charpy Energy J	(ft-lb)	Lateral Expansion mm	(mils)
			Unirradiated Condition			
NRL Tests	-46	(-50)	24	(18)	0.330	(13)
	-18	(0)	45	(33)	0.889	(35)
	-18	(0)	34	(25)	0.660	(26)
	16	(60)	75	(55)	1.372	(54)
	16	(60)	62	(46)	1.194	(47)
	66	(150)	87	(64)	1.600	(63)
	66	(150)	89	(66)	1.778	(70)
	177	(350)	92	(68)	1.727	(68)
	177	(350)	91	(67)	1.753	(69)
Westinghouse Tests	-59	(-75)	14	(10)		
	-59	(-75)	24	(18)		
	-26	(-15)	35	(26)		
	-26	(-15)	42	(31)		
	-1	(30)	42	(31)		
	-1	(30)	45	(33)		
	-1	(30)	56	(41)		
	-1	(30)	58	(43)		
	24	(75)	68	(50)		
	49	(120)	80	(59)		
	49	(120)	88	(65)		
	99	(210)	84	(62)		
	99	(210)	91	(67)		
	149	(300)	92	(68)		
	149	(300)	92	(68)		
			Capsule SSC-1			
Group 1, Left						
EC-1	27	(80)	24	(18)	0.305	(12)
EC-2	116	(240)	61	(45)	0.889	(35)
EC-3	71	(160)	34	(25)	0.508	(20)
EC-4	99	(210)	46	(34)	0.737	(29)
EC-5	88	(190)	38	(28)	0.584	(23)
EC-6	177	(350)	54	(40)	0.914	(36)
Group 2, Right						
EC-7	43	(110)	30	(22)	0.457	(18)
EC-8	138	(280)	58	(43)	0.965	(38)
EC-9	82	(180)	37	(27)	0.610	(24)
EC-10	204	(400)	60	(44)	1.016	(40)
EC-11	110	(230)	53	(39)	0.940	(37)
EC-12	-18	(0)	12	(9)	0.102	(4)

Table A.5 Continued

Specimen Number	Test Temperature °C	(°F)	Charpy Energy J	(ft-lb)	Lateral Expansion mm	(mils)
			Capsule SSC-2			
Group 1, Left						
49	204	(400)	47	(35)	1.016	(40)
50	288	(550)	68	(50)	1.067	(42)
51	121	(250)	46	(34)	0.813	(32)
52	93	(200)	38	(28)	0.483	(19)
53	171	(340)	50	(37)	0.914	(36)
54	288	(550)	46	(34)	0.965	(38)
Group 2, Right						
55	49	(120)	24	(18)	0.381	(15)
56	138	(280)	49	(36)	0.889	(35)
57	82	(180)	33	(24)	0.559	(22)
58	204	(400)	54	(40)	0.991	(39)
59	104	(220)	41	(30)	0.737	(29)
60	116	(240)	52	(38)	0.965	(38)
			Capsule Wall No. 1 (Surface)			
Group 1, Left						
13	204	(400)	58	(43)	1.041	(41)
14	288	(550)	57	(42)	1.041	(41)
15	138	(280)	49	(36)	0.914	(36)
16	93	(200)	41	(30)	0.635	(25)
17	49	(120)	24	(18)	0.330	(13)
18	110	(230)	54	(40)	0.889	(35)
Group 2, Right						
19	4	(40)	11	(8)	0.203	(8)
20	110	(230)	54	(40)	0.965	(38)
21	71	(160)	31	(23)	0.483	(19)
22	204	(400)	52	(38)	0.991	(39)
23	116	(240)	52	(38)	0.864	(34)
24	88	(190)	31	(23)	0.508	(20)

Table A.5 Continued

Specimen Number	Test Temperature °C	(°F)	Charpy Energy J	(ft-lb)	Lateral Expansion mm	(mils)
			Capsule Wall No. 2 (Quarter T)			
Group 1, Left						
25	49	(120)	28	(21)	0.406	(16)
26	110	(230)	52	(38)	0.914	(36)
27	66	(150)	35	(26)	0.610	(24)
28	93	(200)	50	(37)	0.762	(30)
29	82	(180)	46	(34)	0.762	(30)
30	160	(320)	60	(44)	1.092	(43)
Group 2, Right						
31	4	(40)	11	(8)	0.127	(5)
32	27	(80)	24	(18)	0.356	(14)
33	88	(190)	38	(28)	0.610	(24)
34	71	(160)	46	(34)	0.711	(28)
35	204	(400)	58	(43)	1.041	(41)
36	116	(240)	65	(48)	1.016	(40)
			Capsule Wall No. 3 (Half T)			
Group 1, Left						
37	49	(120)	30	(22)	0.457	(18)
38	143	(290)	53	(39)	0.965	(38)
39	77	(170)	45	(33)	0.711	(28)
40	93	(200)	42	(31)	0.737	(29)
41	138	(280)	56	(41)	1.041	(41)
42	204	(400)	57	(42)	1.143	(45)
Group 2, Right						
43	27	(80)	22	(16)	0.381	(15)
44	93	(200)	50	(37)	0.864	(34)
45	71	(160)	46	(34)	0.508	(20)
46	204	(400)	62	(46)	1.092	(43)
47	116	(240)	49	(36)	0.889	(35)
48	54	(130)	33	(24)	0.508	(20)

Table A.6 Submerged Arc Weld (Code R)

Specimen Number	Test Temperature °C	(°F)	Charpy Energy J	(ft-lb)	Lateral Expansion mm	(mils)
Unirradiated Condition						
3/4T	-100	(-148)	7	(5)	0.076	(3)
	-99	(-146)	23	(17)	0.406	(16)
	-90	(-130)	14	(10)	0.152	(6)
	-90	(-130)	34	(25)	0.584	(23)
	-80	(-112)	60	(44)	0.635	(25)
	-80	(-112)	37	(27)	0.508	(20)
	-70	(-94)	84	(62)	1.422	(56)
	-60	(-76)	92	(68)	1.549	(61)
	-60	(-76)	87	(64)	1.372	(54)
	-40	(-40)	80	(59)	1.346	(53)
	-40	(-40)	84	(62)	1.397	(55)
	-20	(-4)	113	(83)	1.854	(73)
	-20	(-4)	148	(109)	2.235	(88)
	0	(32)	123	(91)	1.727	(68)
	40	(104)	176	(130)	1.880	(74)
1/2T	-100	(-148)	8	(6)	0.127	(5)
	-90	(-130)	19	(14)		
	-80	(-112)	45	(33)	0.737	(29)
	-80	(-112)	20	(15)		
	-80	(-112)	64	(47)		
	-90	(-130)	3	(2)	0.457	(18)
	-70	(-94)	84	(62)		
	-70	(-94)	85	(63)		
	-60	(-76)	73	(54)		
	-60	(-76)	56	(41)	0.914	(36)
	-40	(-40)	84	(62)	1.422	(56)
	60	(140)	180	(133)	1.727	(68)
Capsule SSC-1						
Group 1, Left						
1	143	(290)	41	(30)	0.483	(19)
2	193	(380)	68	(50)	0.889	(35)
3	93	(200)	22	(16)	0.229	(9)
4	232	(450)	87	(64)	1.245	(49)
6	260	(500)	79	(58)	1.168	(46)
7	177	(350)	61	(45)	0.914	(36)
Group 2, Right						
8	204	(400)	79	(58)	1.041	(41)
9	138	(280)	38	(28)	0.457	(18)
11	171	(340)	56	(41)	0.737	(29)
12	260	(500)	80	(59)	1.194	(47)
13	104	(220)	24	(18)	0.305	(12)
14	132	(270)	31	(23)	0.330	(13)

Table A.6 Continued

Specimen Number	Test Temperature °C	(°F)	Charpy Energy J	(ft-lb)	Lateral Expansion mm	(mils)
Capsule SSC-2						
Group 1, Left						
31	243	(470)	53	(39)	0.711	(28)
32	149	(300)	19	(14)	0.279	(11)
33	204	(400)	38	(28)	-----[a]	(--)
34	232	(450)	46	(34)	0.711	(28)
36	260	(500)	54	(40)	0.762	(30)
37	177	(350)	24	(18)	0.279	(11)
Group 2, Right						
38	93	(200)	11	(8)	0.127	(5)
39	188	(370)	27	(20)	0.559	(22)
41	210	(410)	41	(30)	0.610	(24)
42	260	(500)	57	(42)	0.864	(34)
43	138	(280)	19	(14)	0.203	(8)
44	288	(550)	57	(42)	0.914	(36)
Capsule Wall No. 1 (Surface)						
Group 1, Left						
46	221	(430)	52	(38)	0.559	(22)
47	288	(550)	68	(50)	0.813	(32)
48	204	(400)	33	(24)	0.483	(19)
49	232	(450)	54	(40)	0.610	(24)
51	260	(500)	54	(40)	0.813	(32)
52	182	(360)	28	(21)	0.279	(11)
Group 2, Right						
53	99	(210)	5	(4)	0.000	(0)
54	204	(400)	43	(32)	0.513	(21)
56	216	(420)	45	(33)	0.508	(20)
57	260	(500)	54	(40)	0.559	(22)
58	138	(280)	19	(14)	0.203	(3)
59	288	(550)	68	(50)	0.864	(34)

[a]Not determined

Table A.6 Continued

Specimen Number	Test Temperature °C	(°F)	Charpy Energy J	(ft-lb)	Lateral Expansion mm	(mils)
			Capsule Wall No. 2 (Quarter T)			
Group 1, Left						
16	160	(320)	30	(22)	0.432	(17)
17	199	(390)	66	(49)	0.940	(37)
18	288	(550)	69	(51)	1.118	(44)
19	227	(440)	68	(50)	0.940	(37)
21	260	(500)	73	(54)	1.041	(41)
22	177	(350)	42	(31)	0.610	(24)
Group 2, Right						
23	204	(400)	64	(47)	0.838	(33)
24	138	(280)	26	(19)	0.279	(11)
26	171	(340)	31	(23)	0.406	(16)
27	260	(500)	68	(50)	1.118	(44)
28	99	(210)	18	(13)	0.229	(9)
29	188	(370)	49	(36)	0.635	(25)
			Capsule Wall No. 3 (Half T)			
Group 1, Left						
68	260	(500)	84	(62)	1.143	(45)
69	193	(380)	60	(44)	0.914	(36)
71	143	(290)	30	(22)	0.406	(16)
72	227	(440)	79	(58)	1.016	(40)
74	182	(360)	41	(30)	0.610	(24)
Group 2, Right						
76	204	(400)	73	(54)	1.041	(41)
77	138	(280)	39	(29)	0.457	(18)
78	171	(340)	54	(40)	0.711	(28)
79	260	(500)	76	(56)	1.346	(53)
81	154	(310)	37	(27)	0.457	(18)
82	99	(210)	22	(16)	-----[a]	(--)

[a]Not determined

APPENDIX B

ILLUSTRATIONS OF CHARPY-V LATERAL EXPANSION TEST RESULTS FROM PSF IRRADIATIONS

Figure		Page

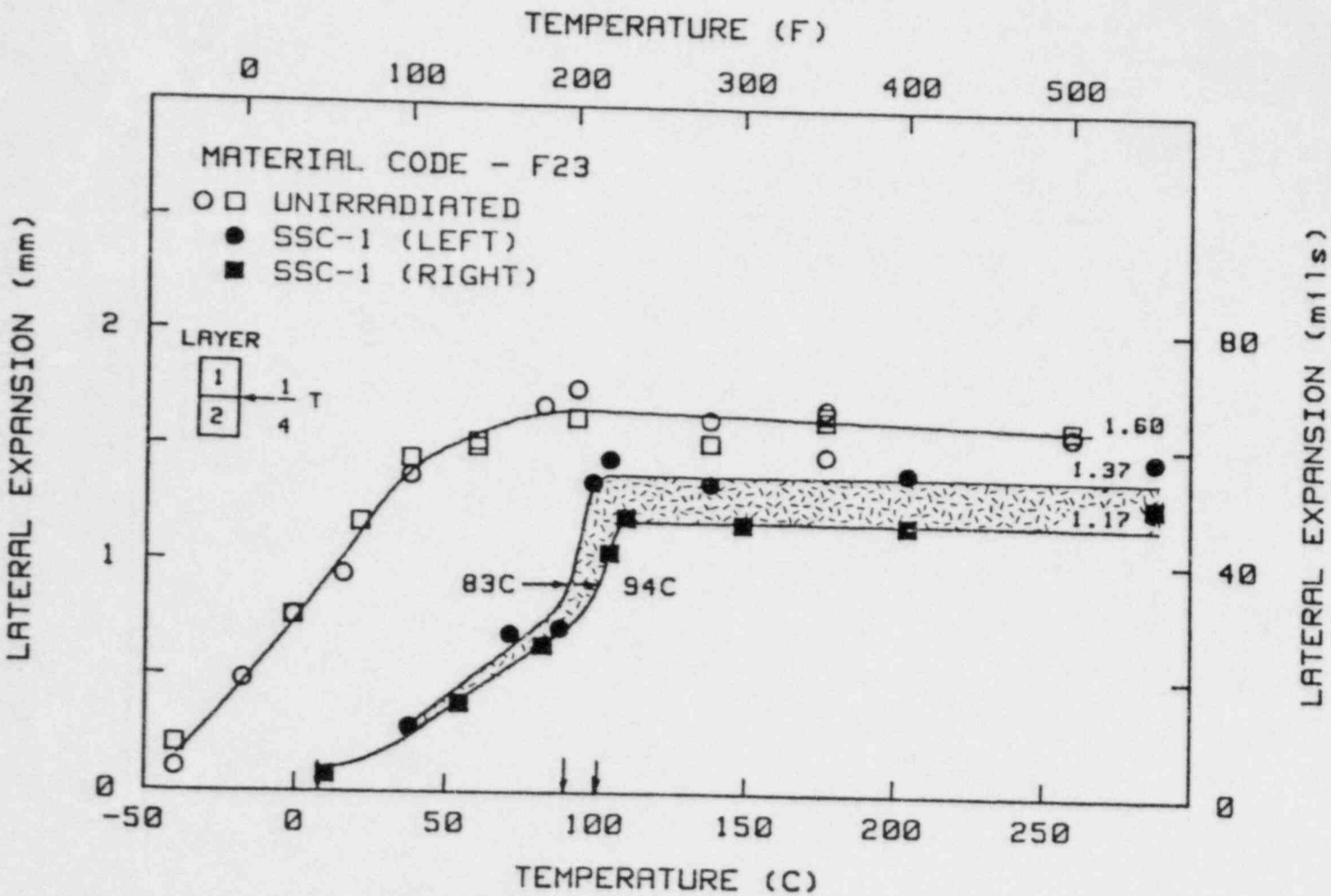

B.1 Charpy-V lateral expansion measurements for the A302-B reference plate before and after irradiation in Capsule SSC-1

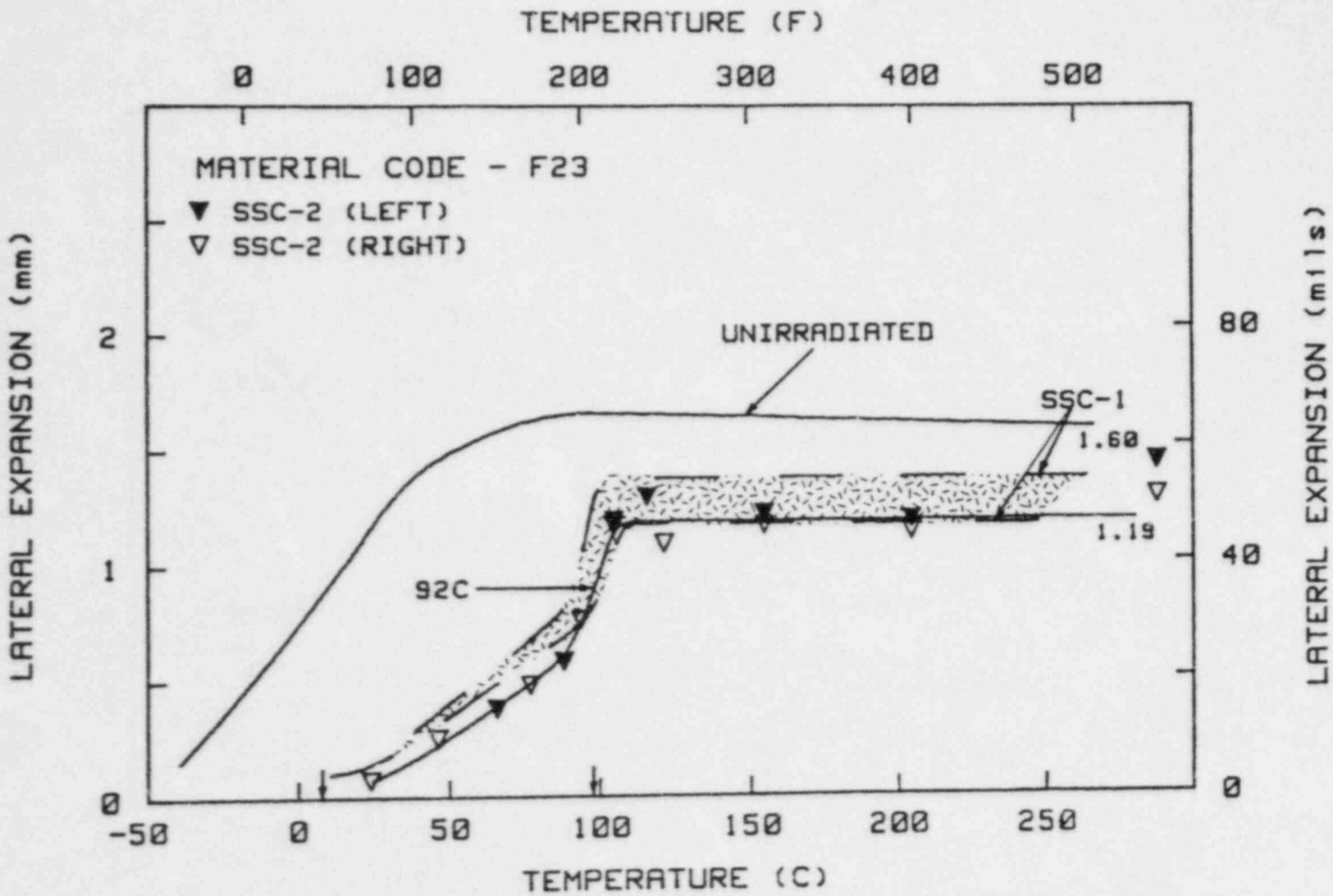

B.2 Charpy-V lateral expansion measurements for the A302-B reference plate before and after irradiation in Capsule SSC-2

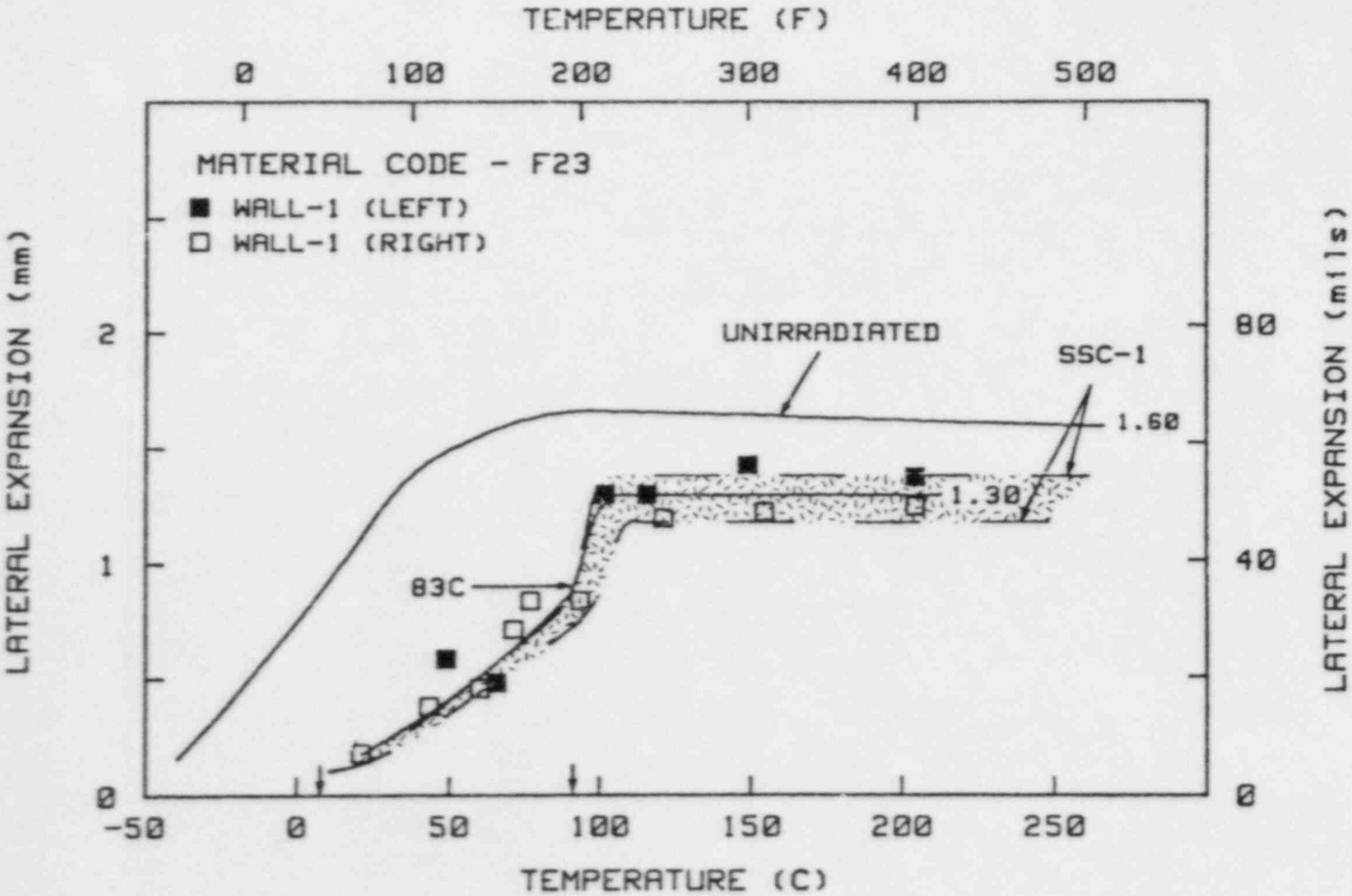

B.3 Charpy-V lateral expansion measurements for the A302-B reference plate before and after irradiation in Capsule Wall-1

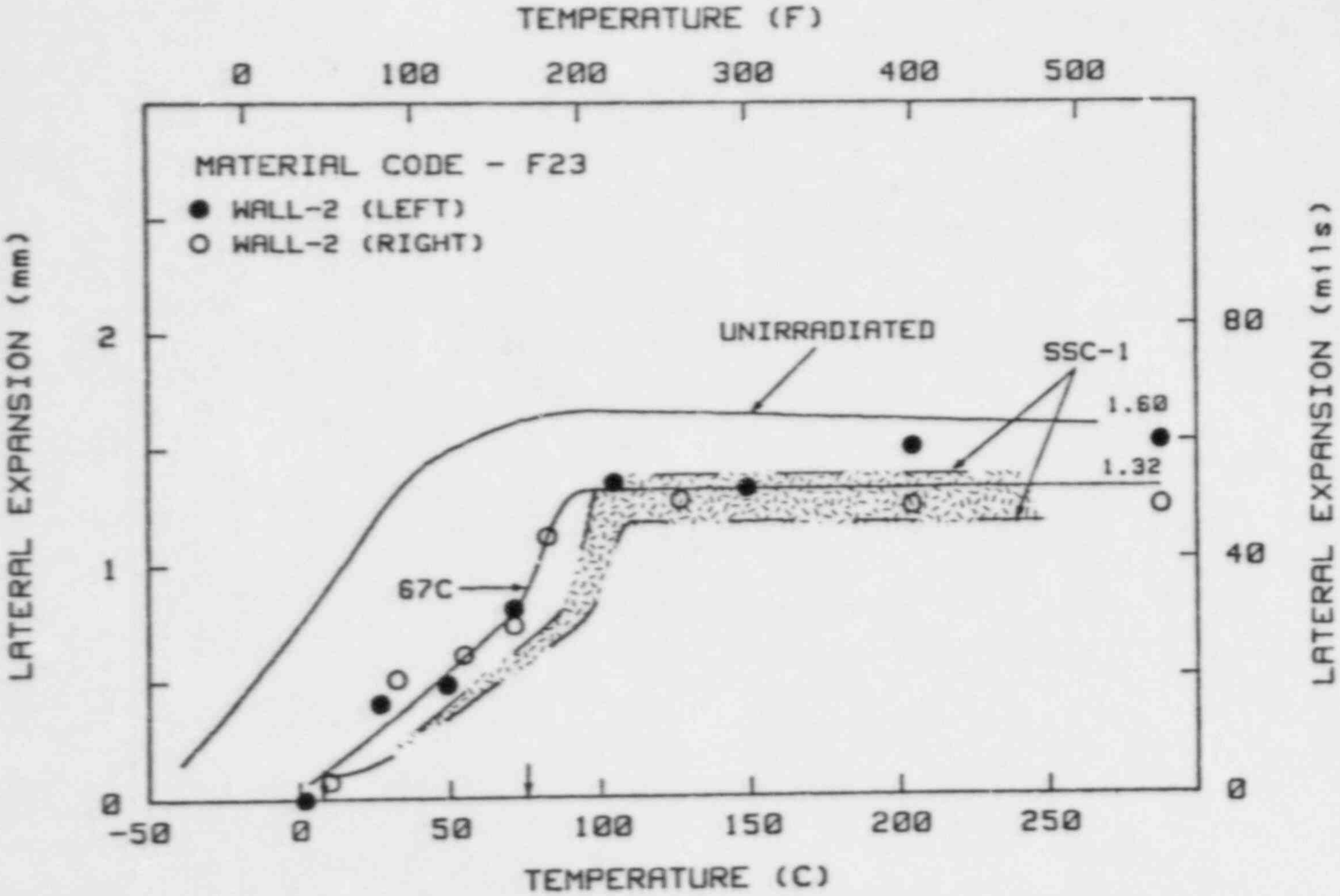

B.4 Charpy-V lateral expansion measurements for the A302-B reference plate before and after irradiation in Capsule Wall-2

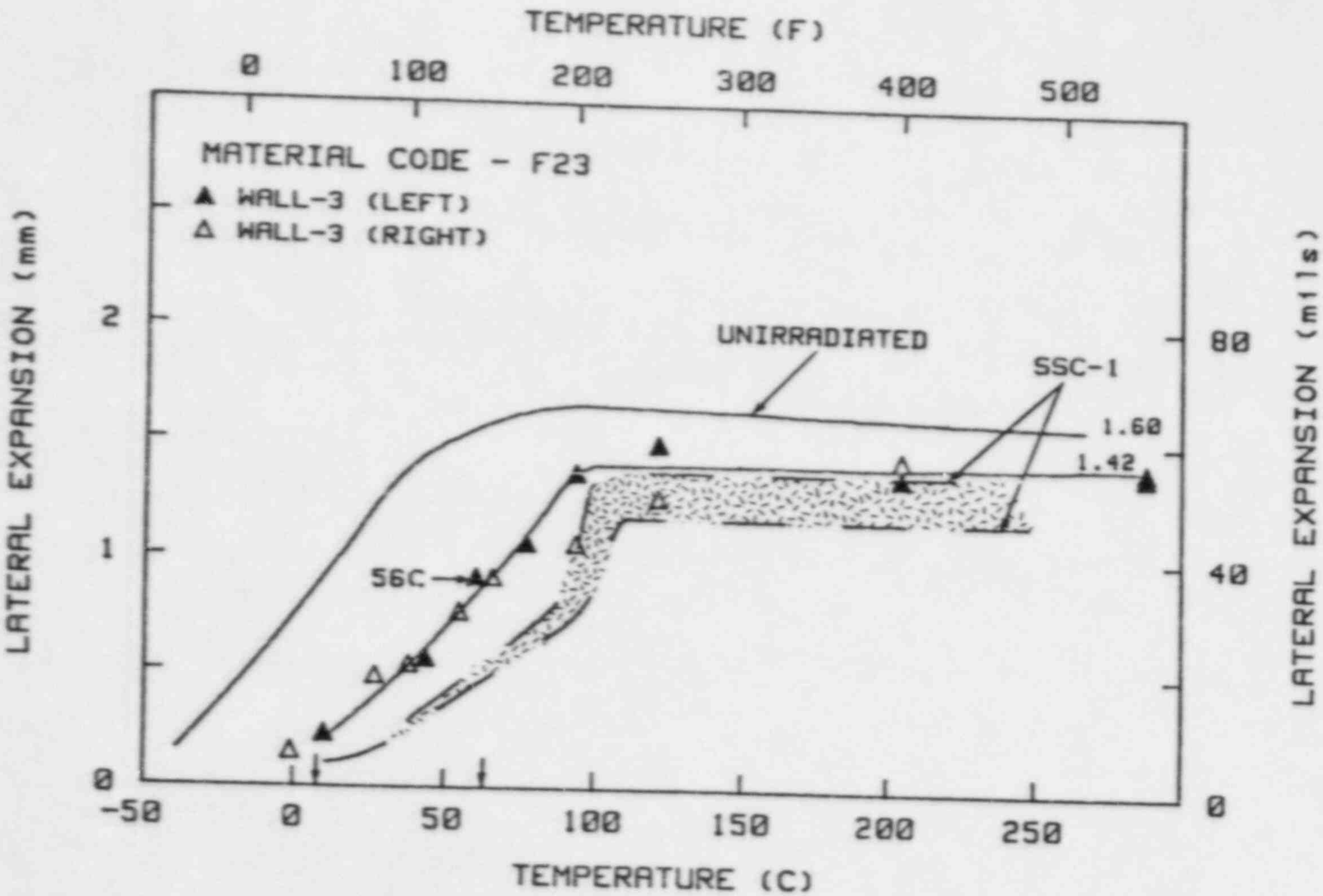

B.5 Charpy-V lateral expansion measurements for the A302-B reference plate before and after irradiation in Capsule Wall-3

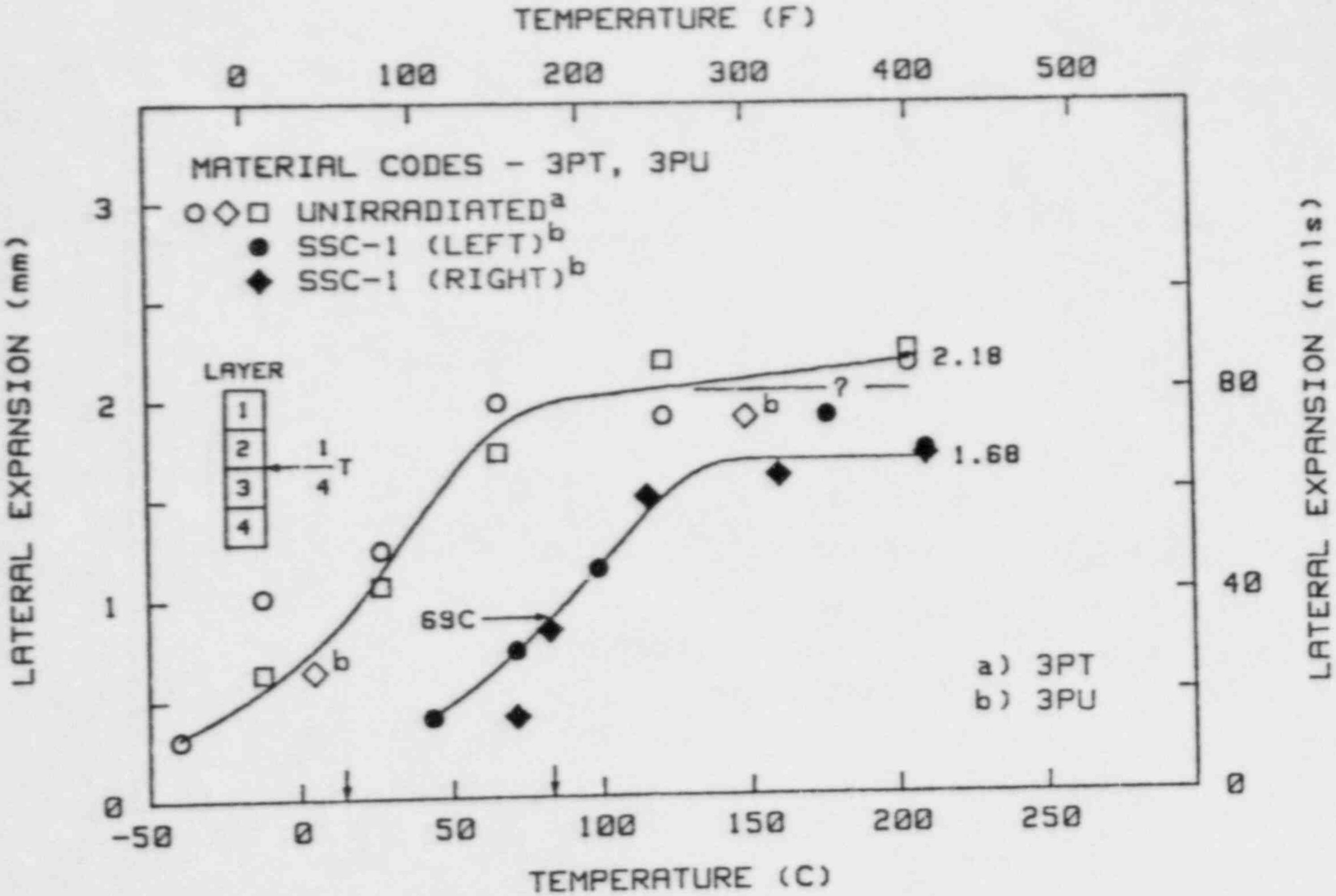

B.6 Charpy-V lateral expansion measurements for the A533-B reference plate before and after irradiation in Capsule SSC-1

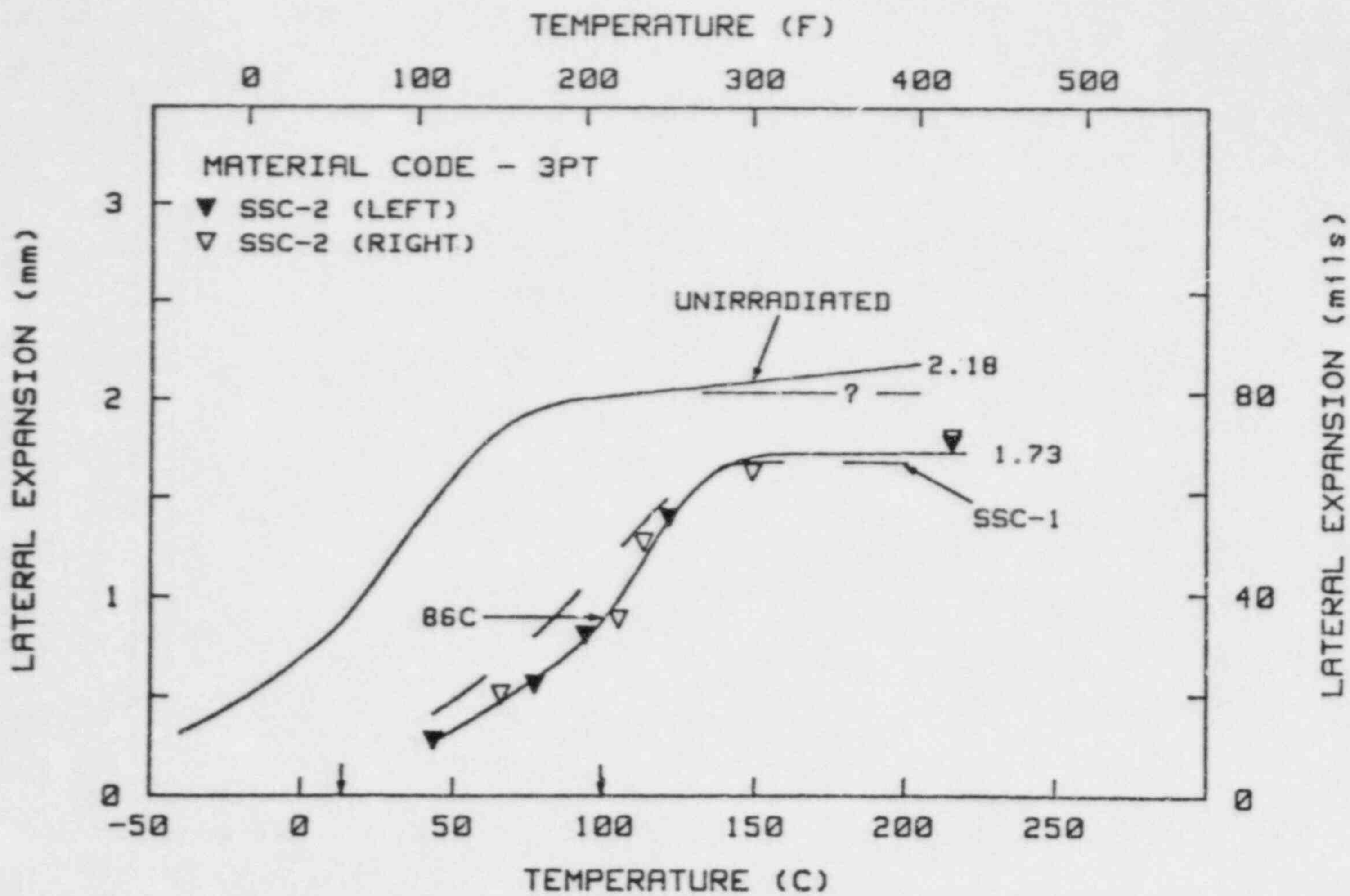

B.7 Charpy-V lateral expansion measurements for the A533-B reference plate before and after irradiation in Capsule SSC-2

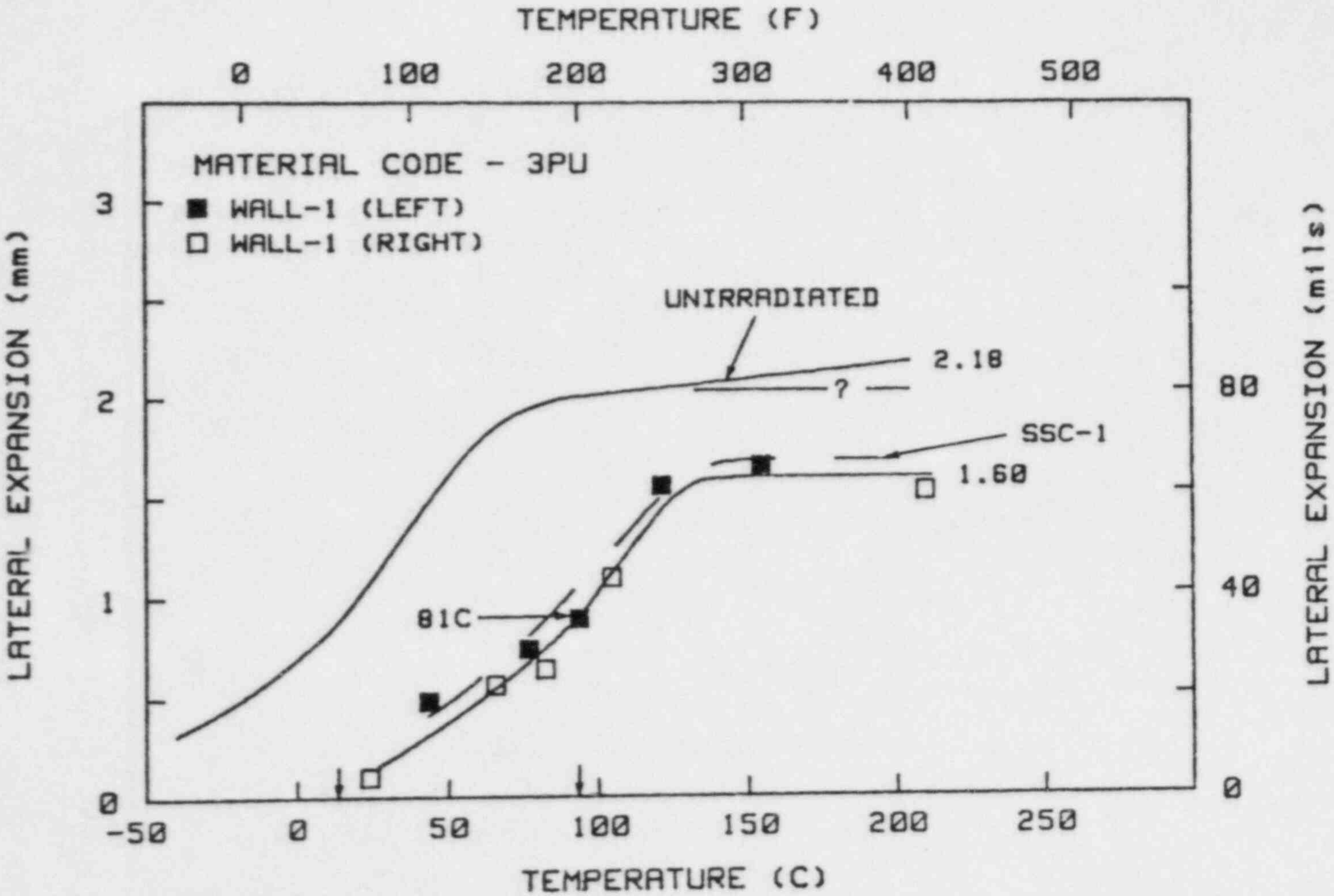

B.8 Charpy-V lateral expansion measurements for the A533-B reference plate before and after irradiation in Capsule Wall-1

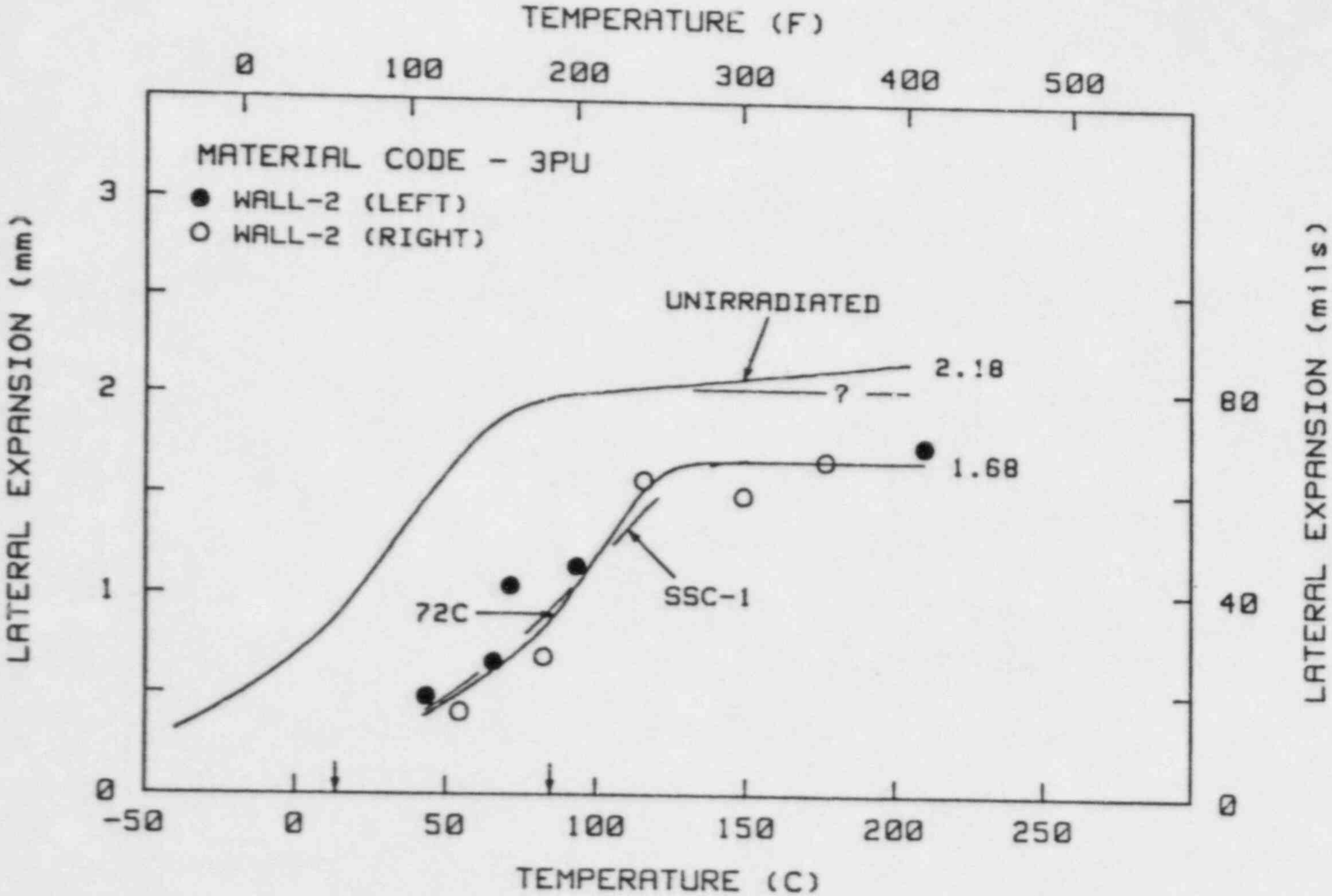

B.9 Charpy-V lateral expansion measurements for the A533-B reference plate before and after irradiation in Capsule Wall-2

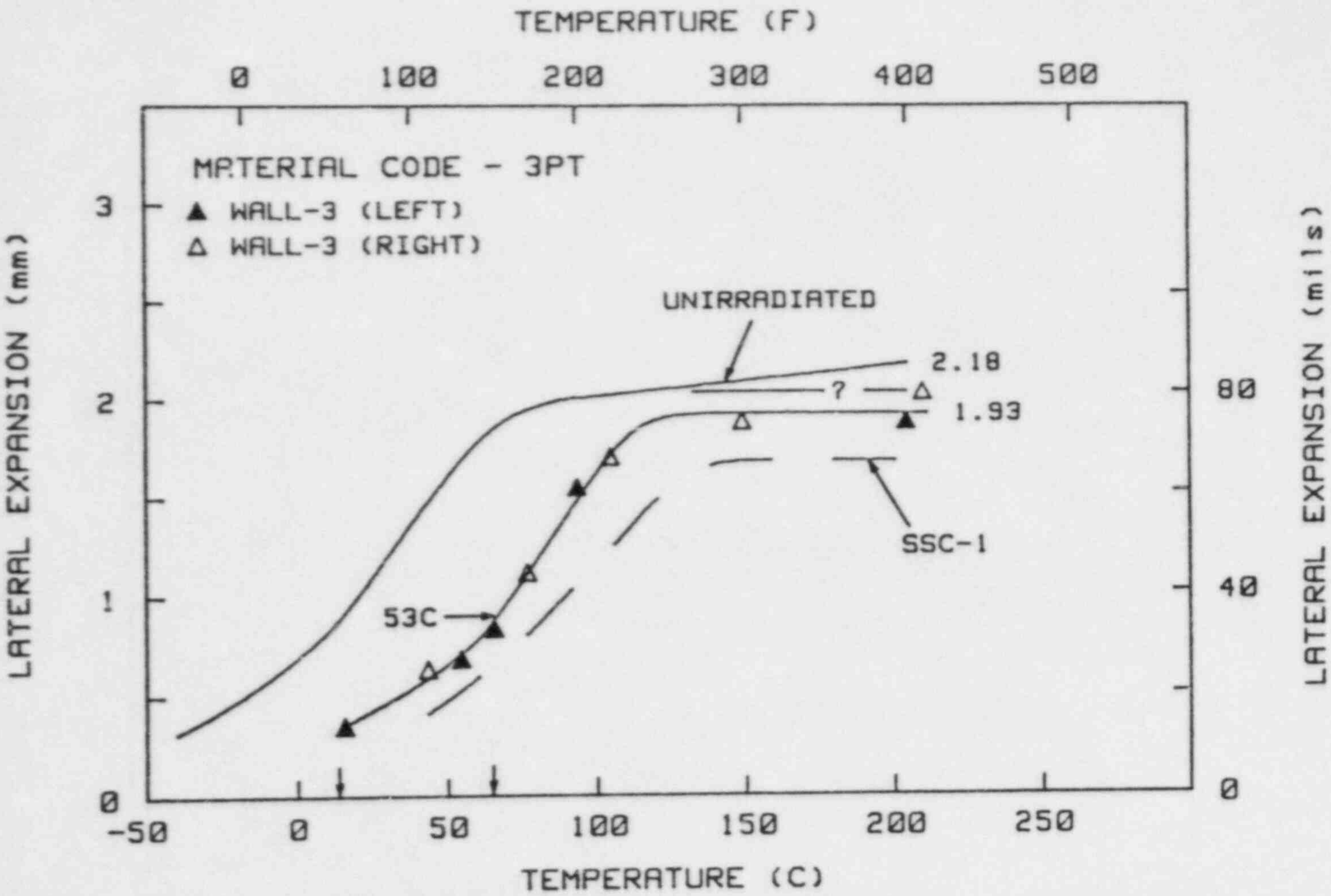

B.10 Charpy-V lateral expansion measurements for the A533-B reference plate before and after irradiation in Capsule Wall-3

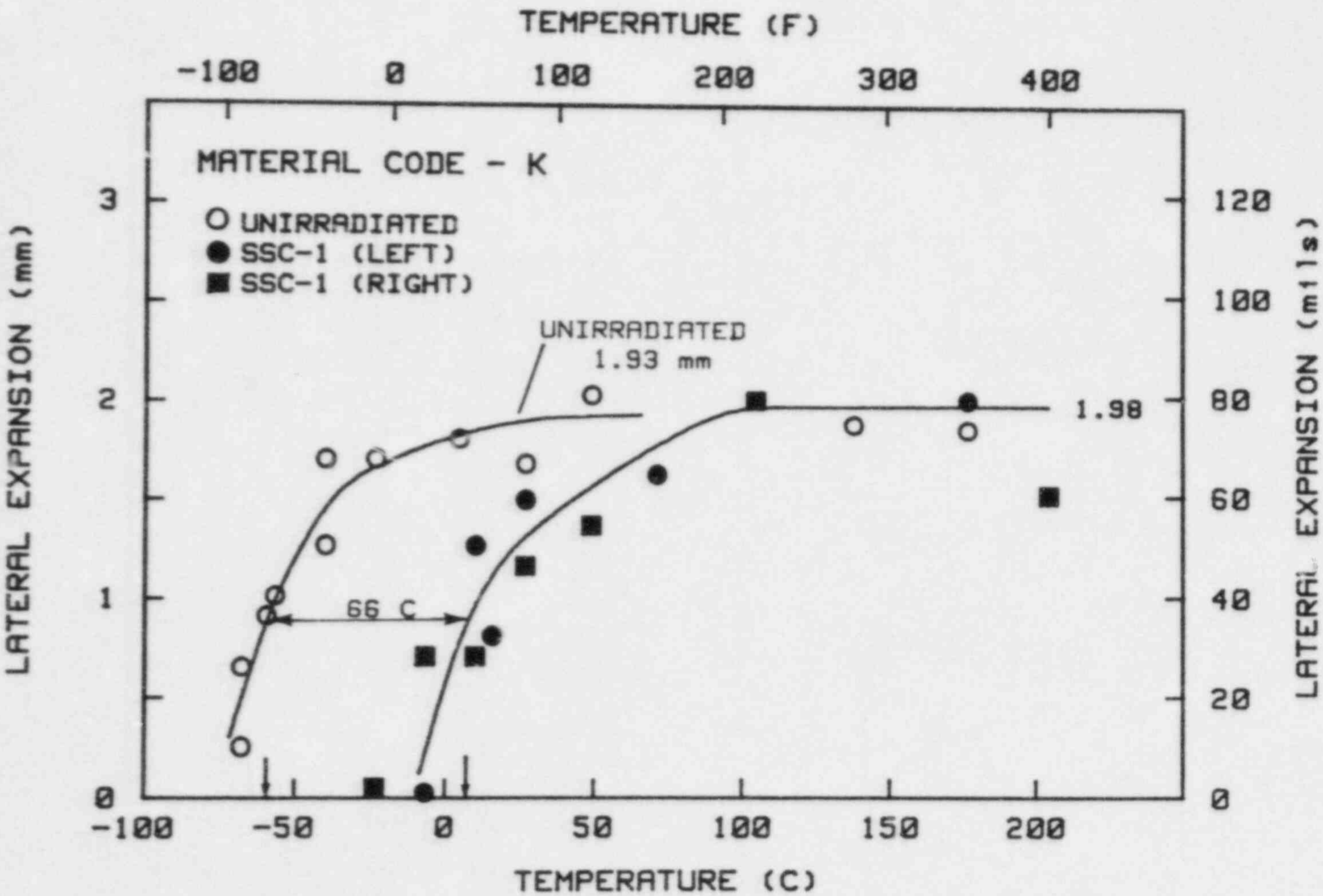

B.11 Charpy-V lateral expansion measurements for the 22NiMoCr37 forging before and after irradiation in capsule SSC-1

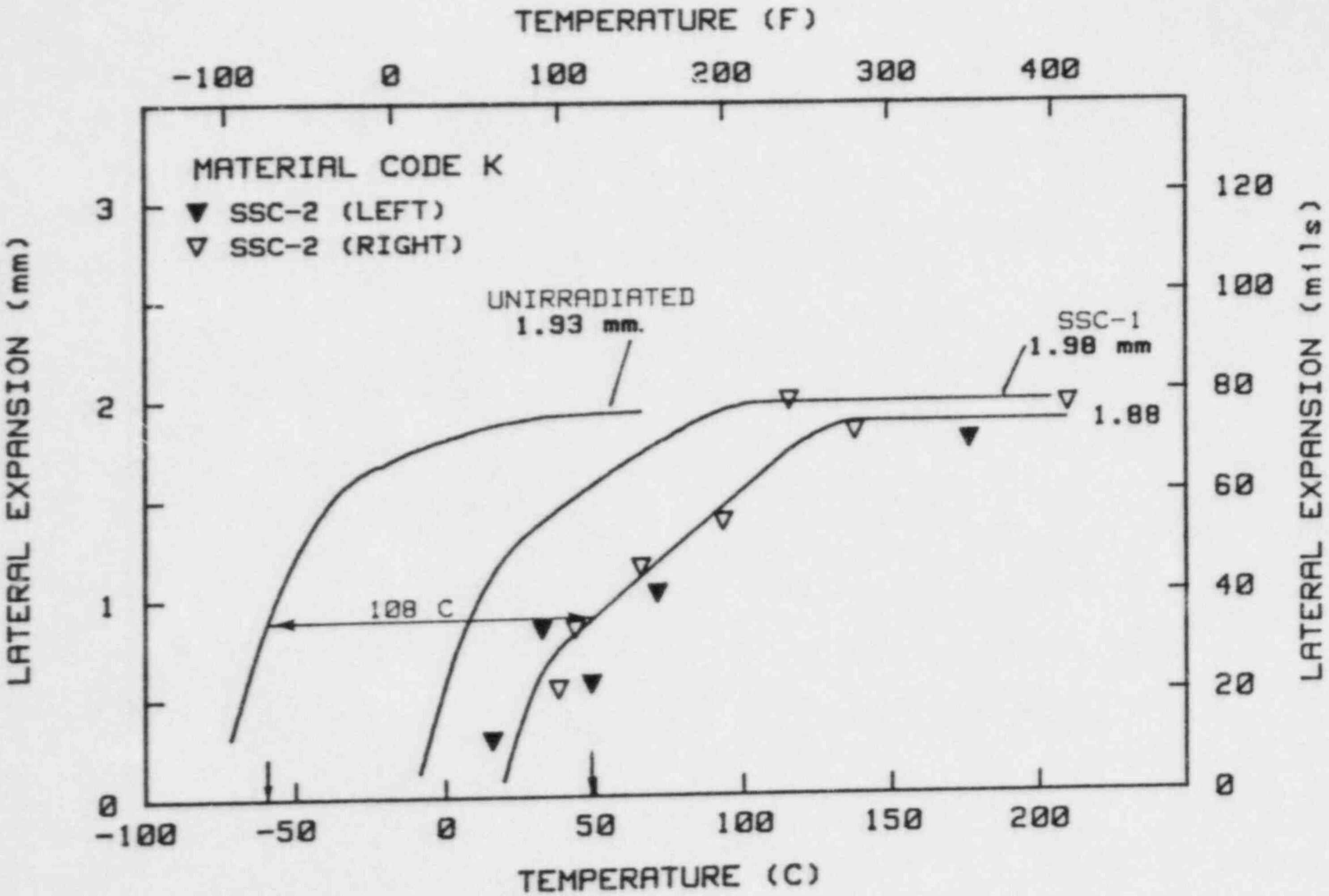

B.12 Charpy-V lateral expansion measurements for the 22NiMoCr37 forging before and after irradiation in capsule SSC-2

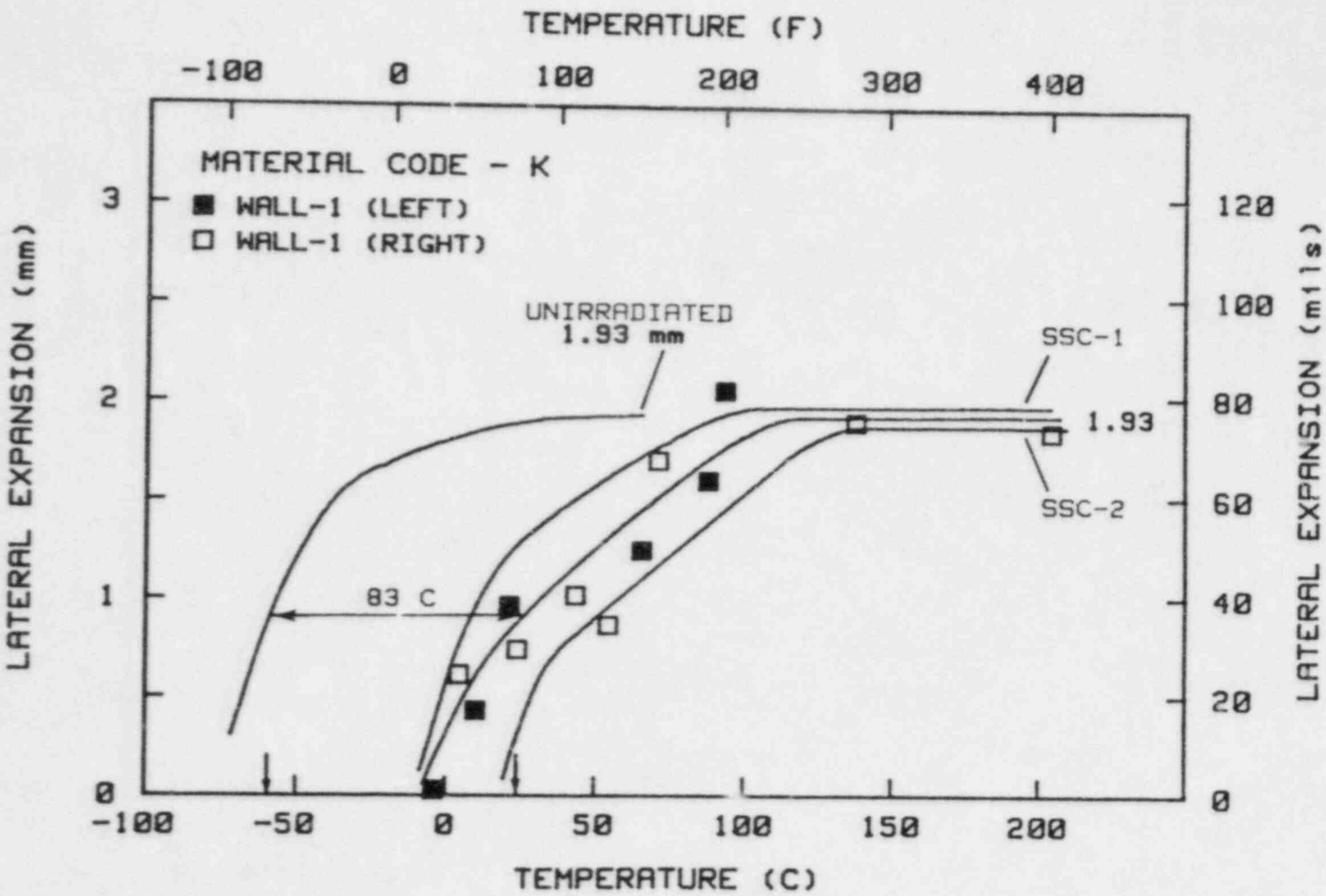

B.13 Charpy-V lateral expansion measurements for the 22NiMoCr37 forging before and after irradiation in capsule Wall-1

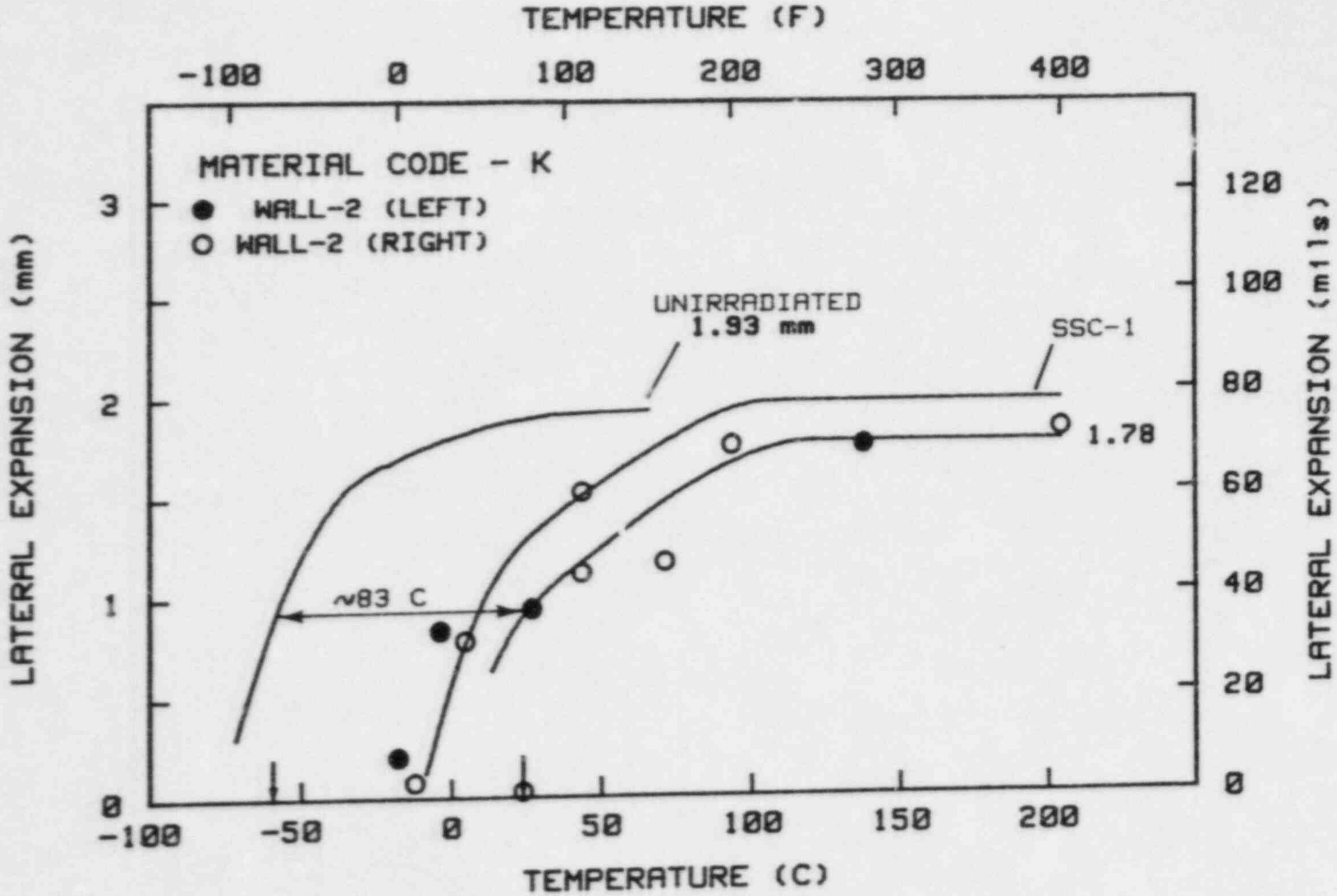

B.14 Charpy-V lateral expansion measurements for the 22NiMoCr37 forging before and after irradiation in capsule Wall-2

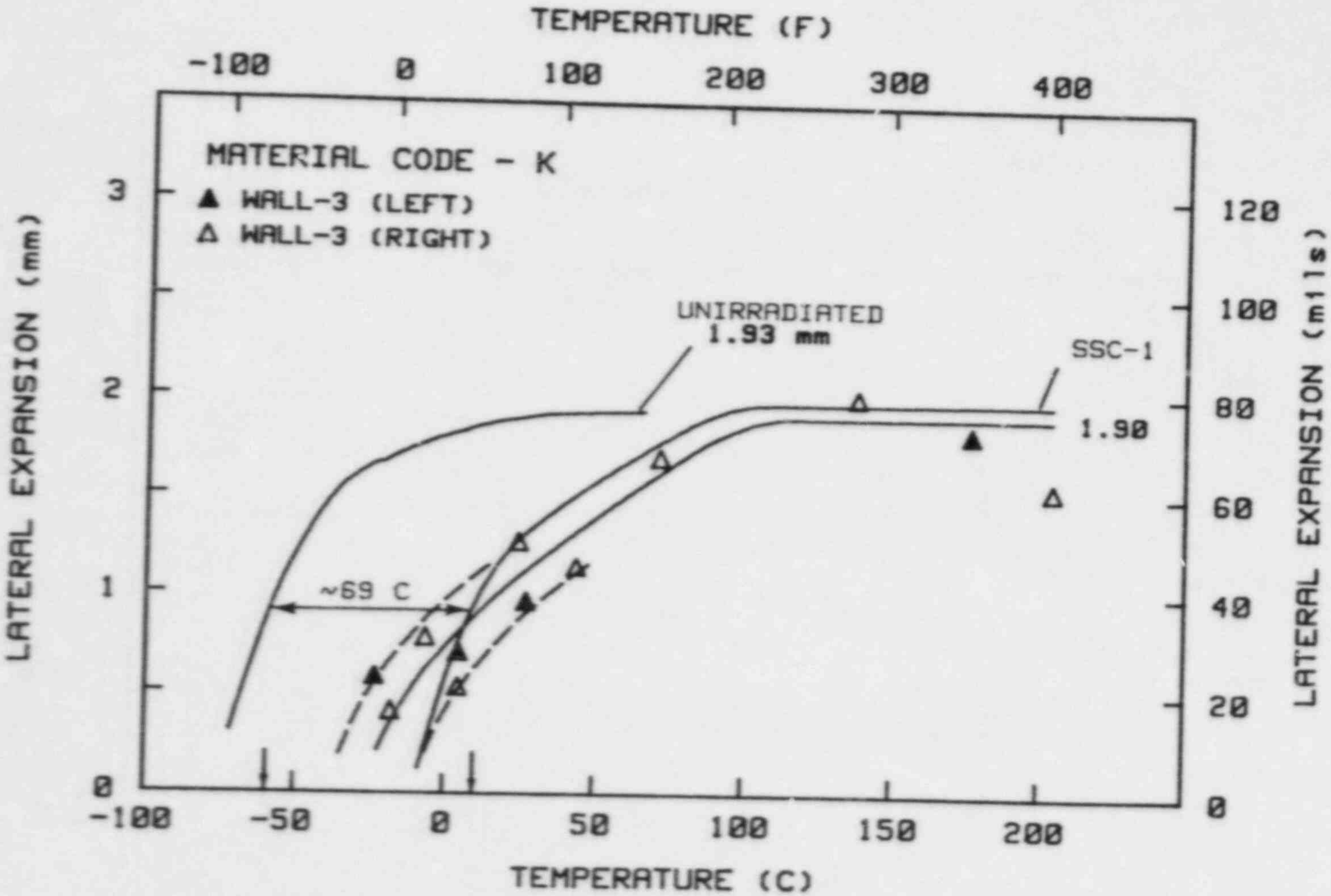

B.15 Charpy-V lateral expansion measurements for the 22NiMoCr37 forging before and after irradiation in capsule Wall-3

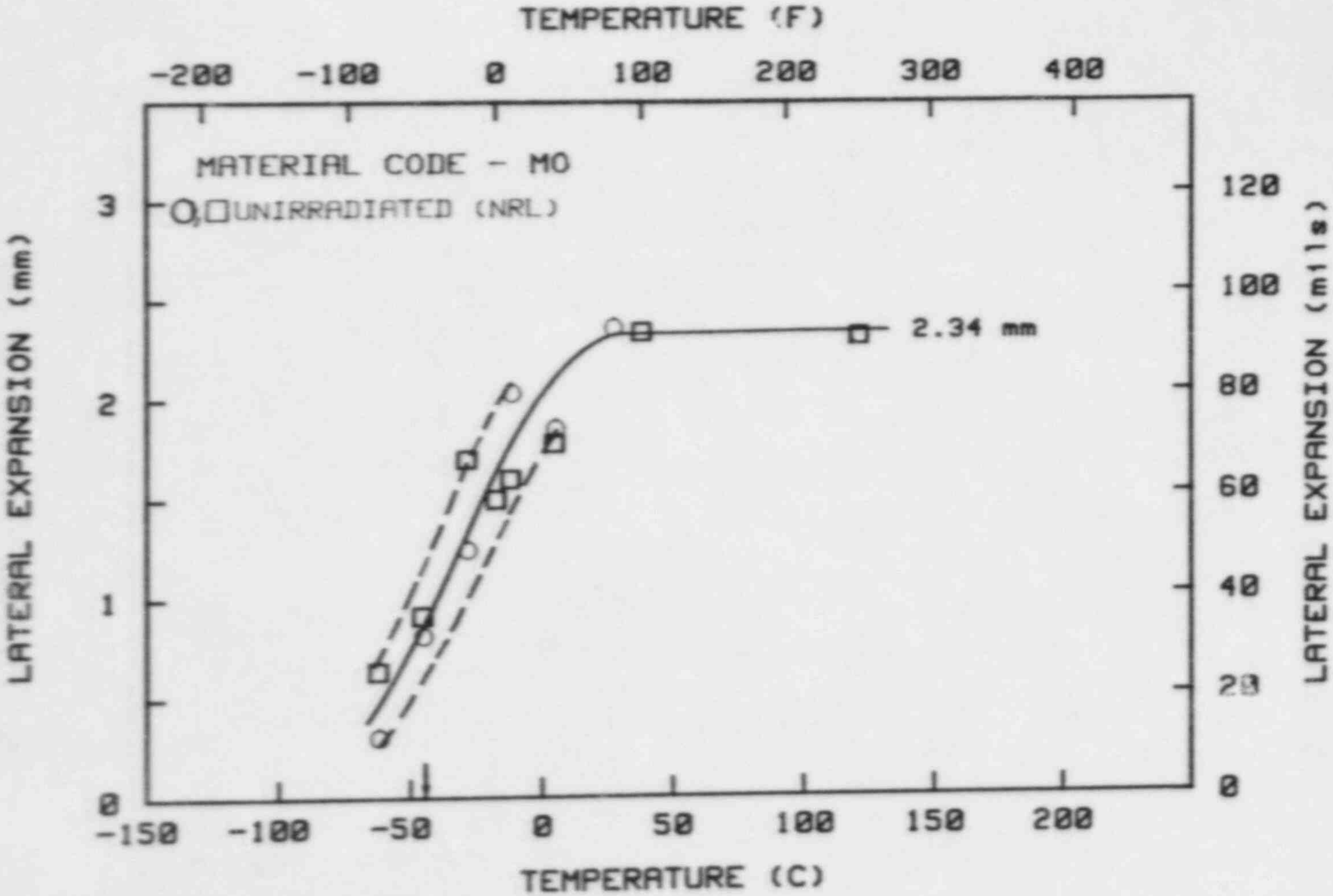

B.16(A) Charpy-V lateral expansion measurements for the A 508-3 forging before and after unirradiation in capsule SSC-1

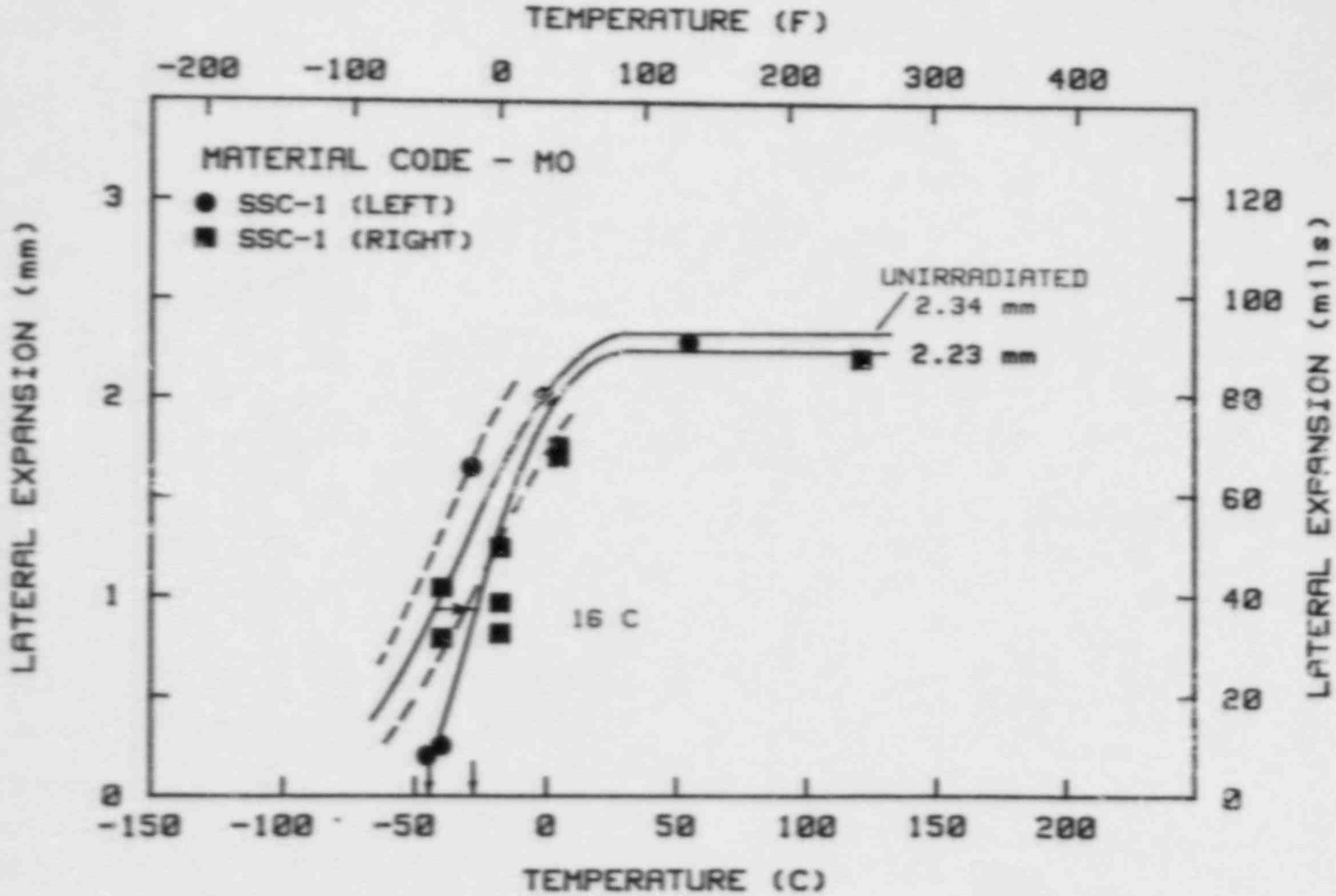

B.16(B) Charpy-V lateral expansion measurements for the A 508-3 forging before and after irradiation in capsule SSc-1

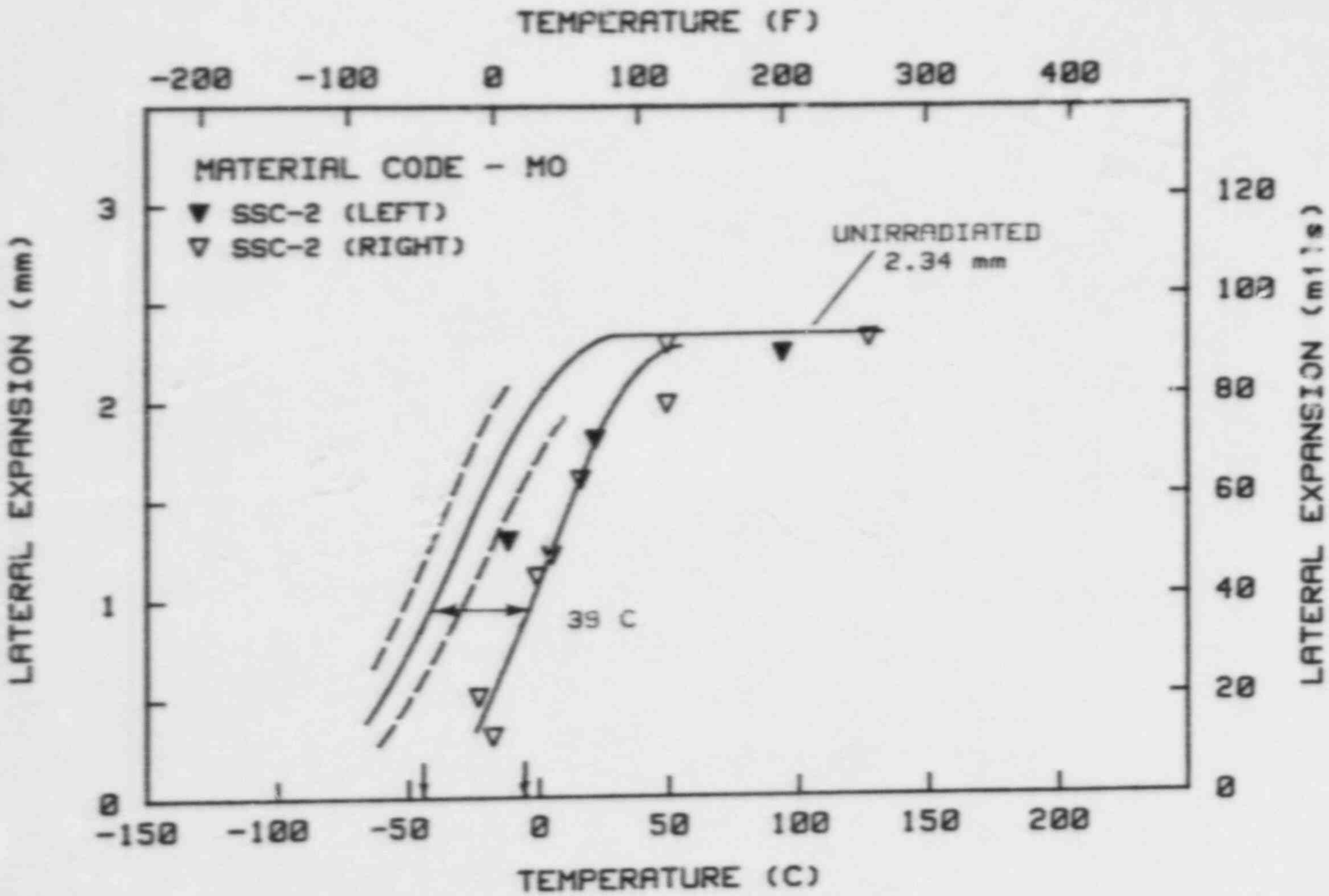

B.17 Charpy-V lateral expansion measurements for the A 508-3 forging before and after irradiation in capsule SSC-2

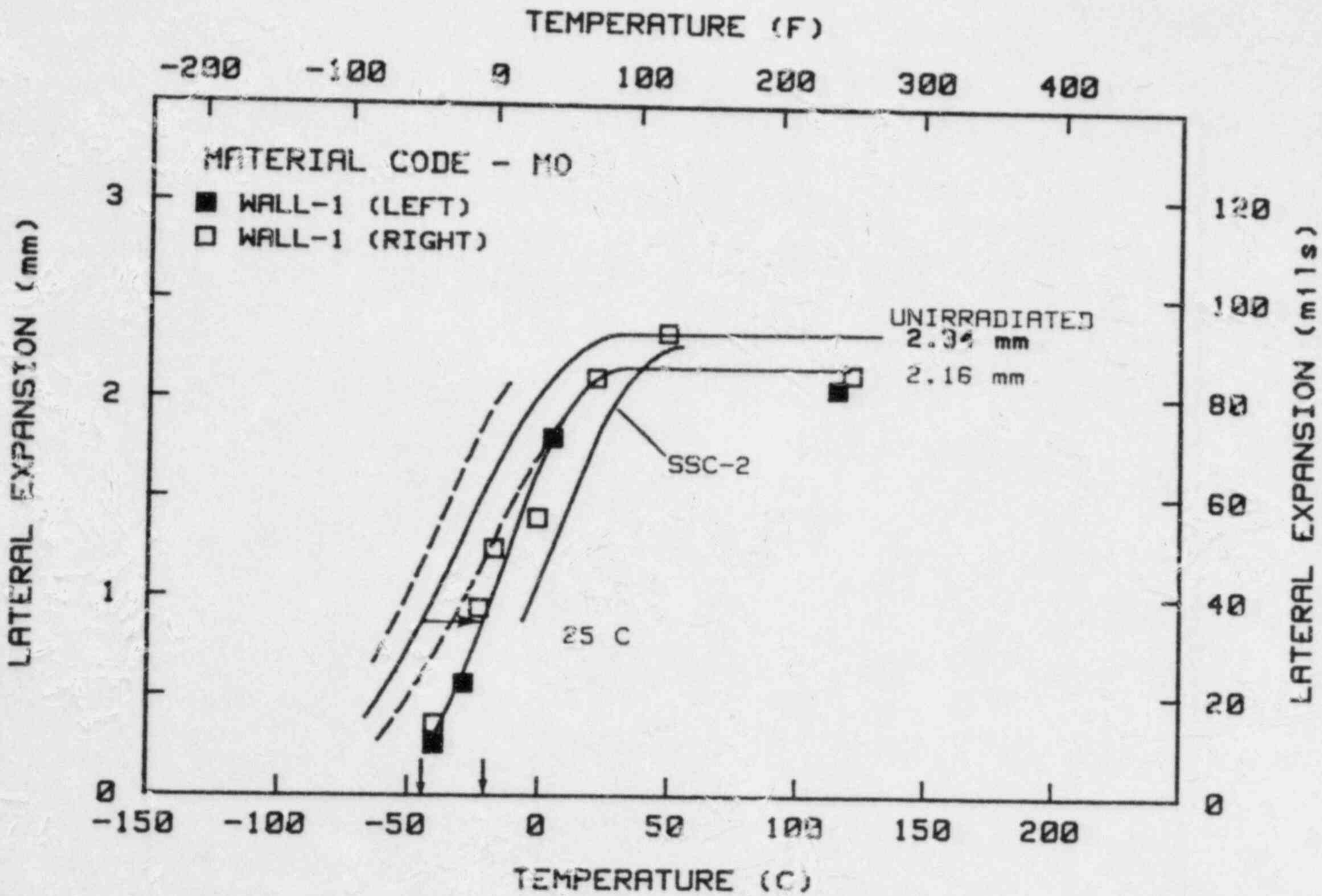

B.18 Charpy-V lateral expansion measurements for the A 508-3 forging before and after irradiation in capsule Wall-1

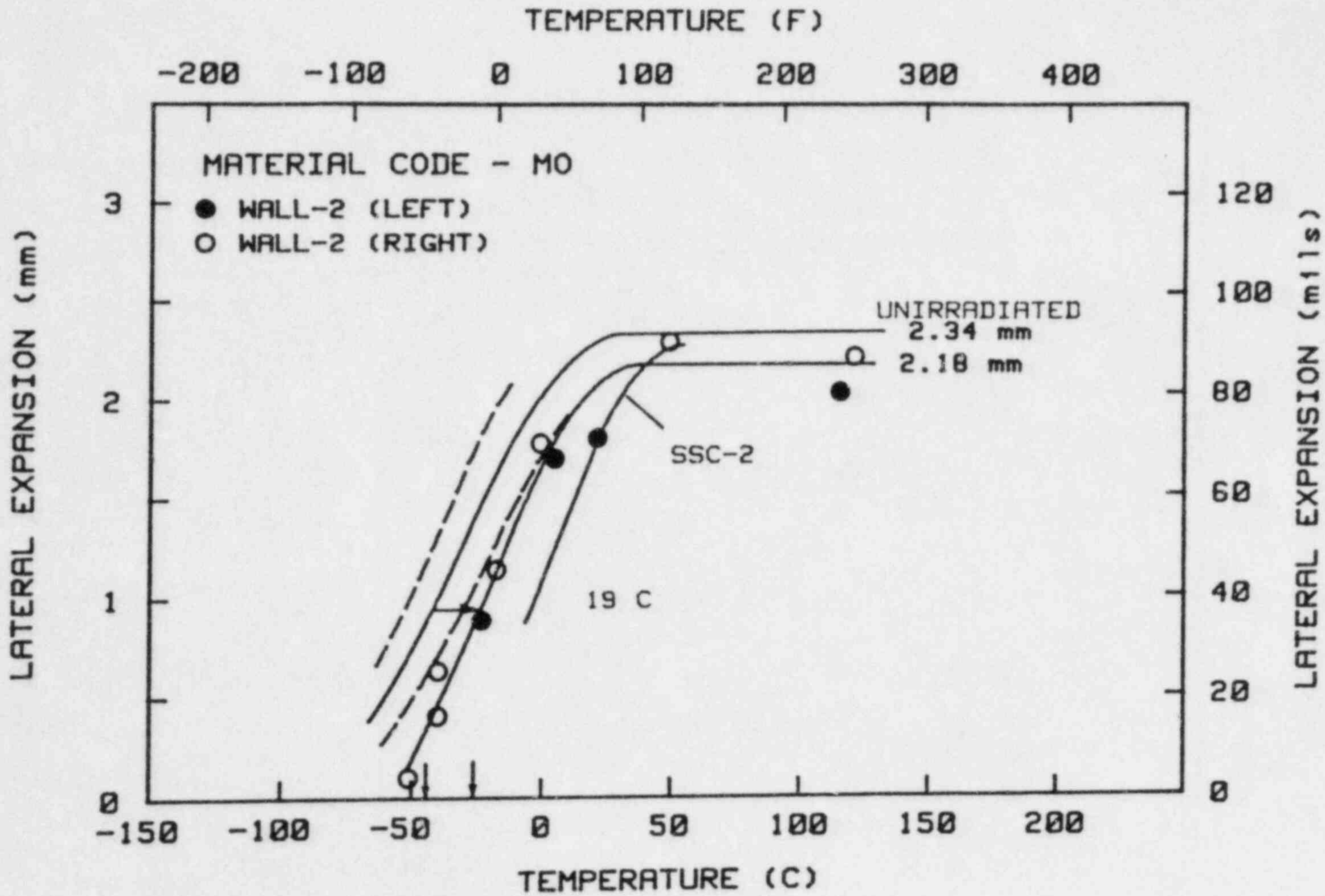

3.19 Charpy-V lateral expansion measurements for the A 508-3 forging before and after irradiation in capsule Wall-2

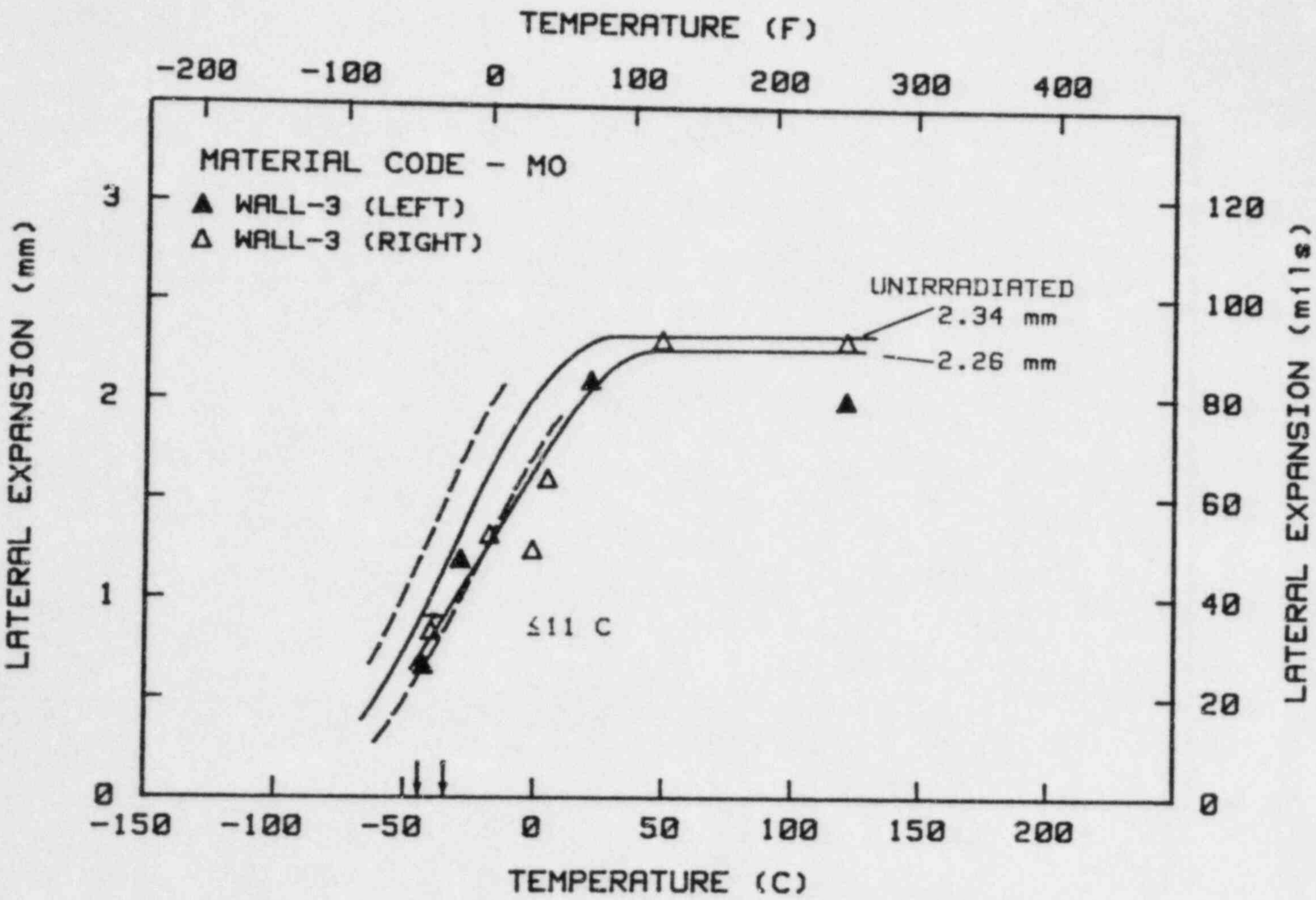

B.20 Charpy-V lateral expansion measurements for the A 508-3 forging before and after irradiation in capsule Wall-3

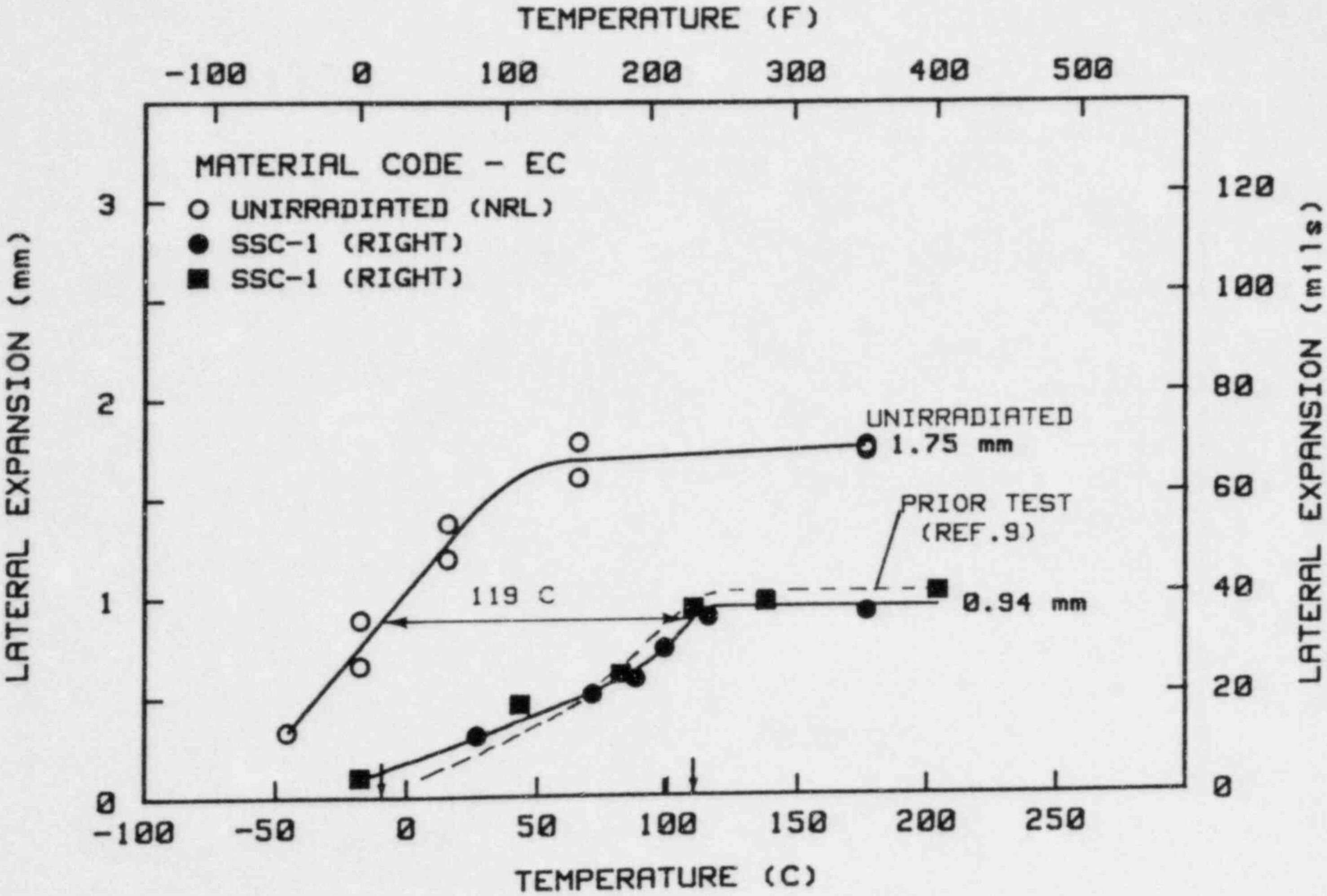

B.21 Charpy-V lateral expansion measurements for the submerged arc weld code EC before and after irradiation in capsule SSC-1

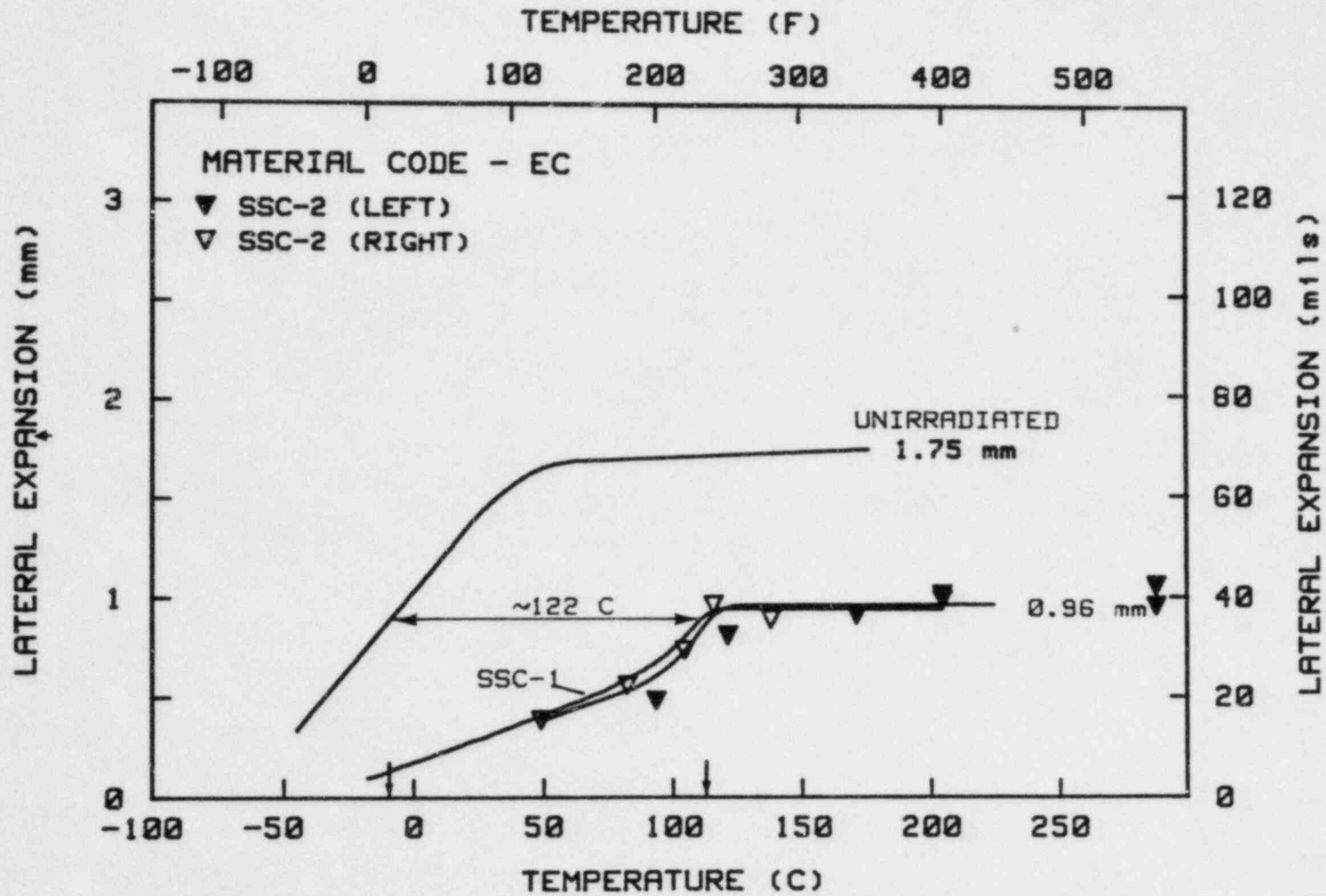

B.22 Charpy-V lateral expansion measurements for the submerged arc weld code EC before and after irradiation in capsule SSC-2

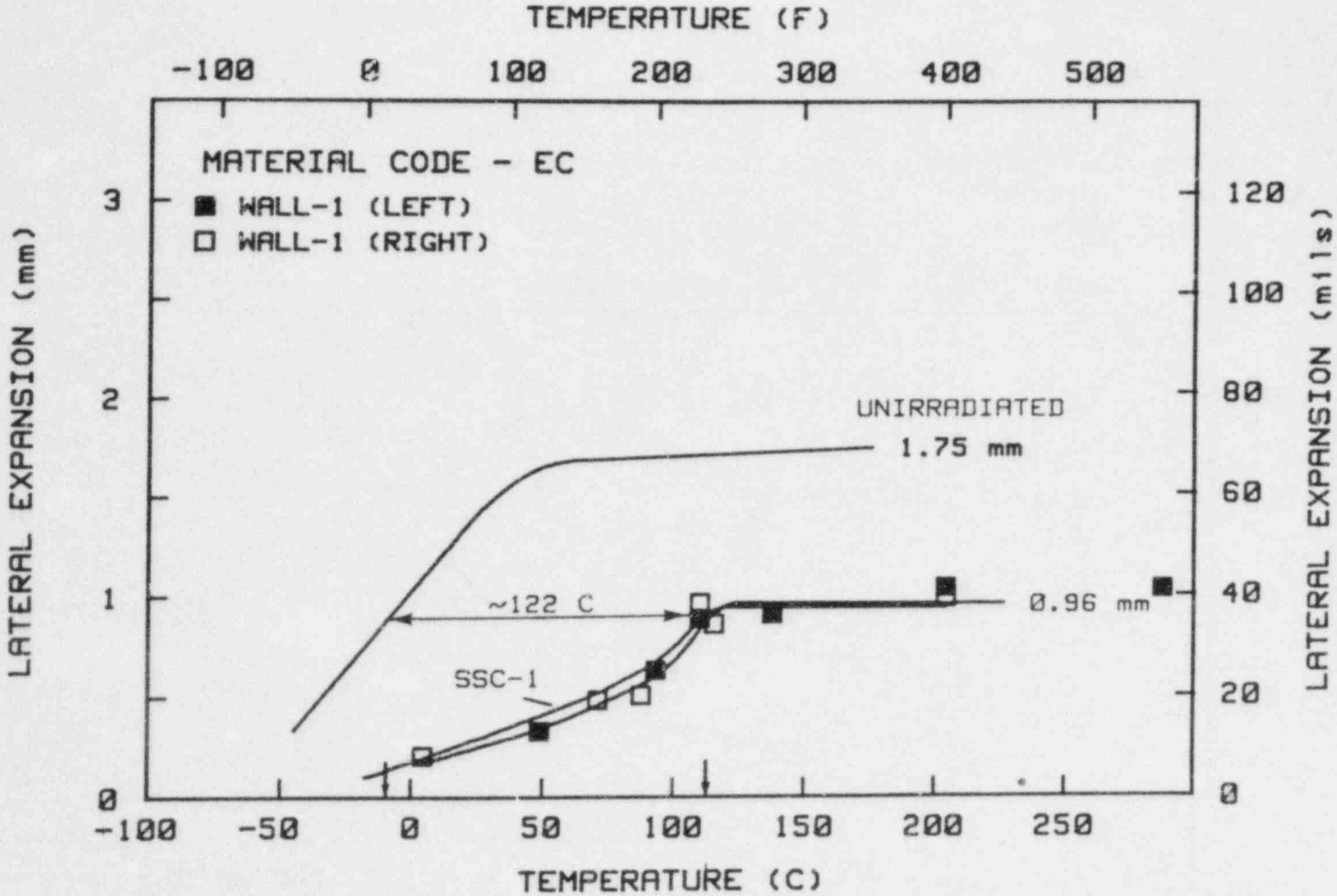

B.23 Charpy-V lateral expansion measurements for the submerged arc weld code EC before and after irradiation in capsule Wall-1

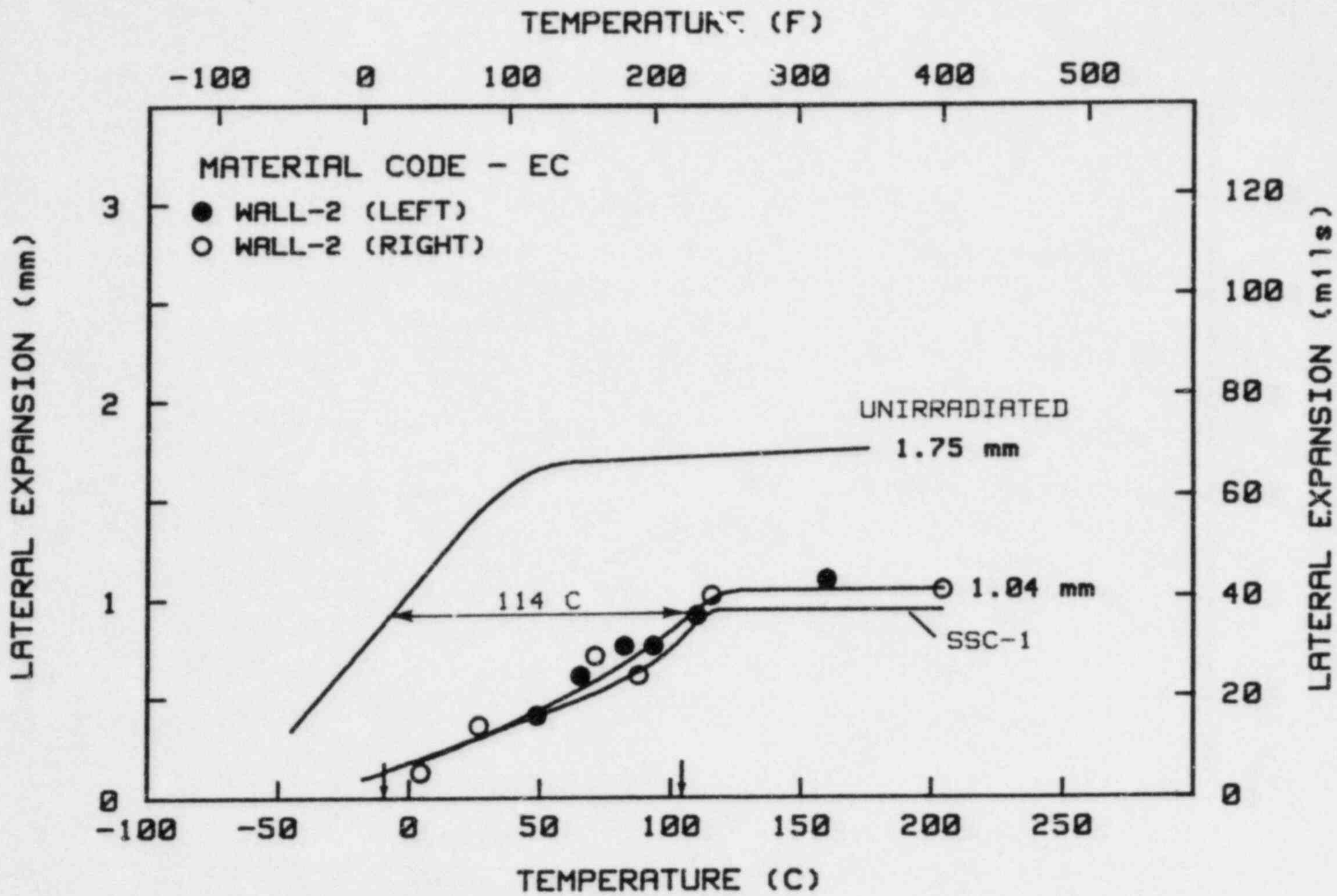

B.24 Charpy-V lateral expansion measurements for the submerged arc weld code EC before and after irradiation in capsule Wall-2

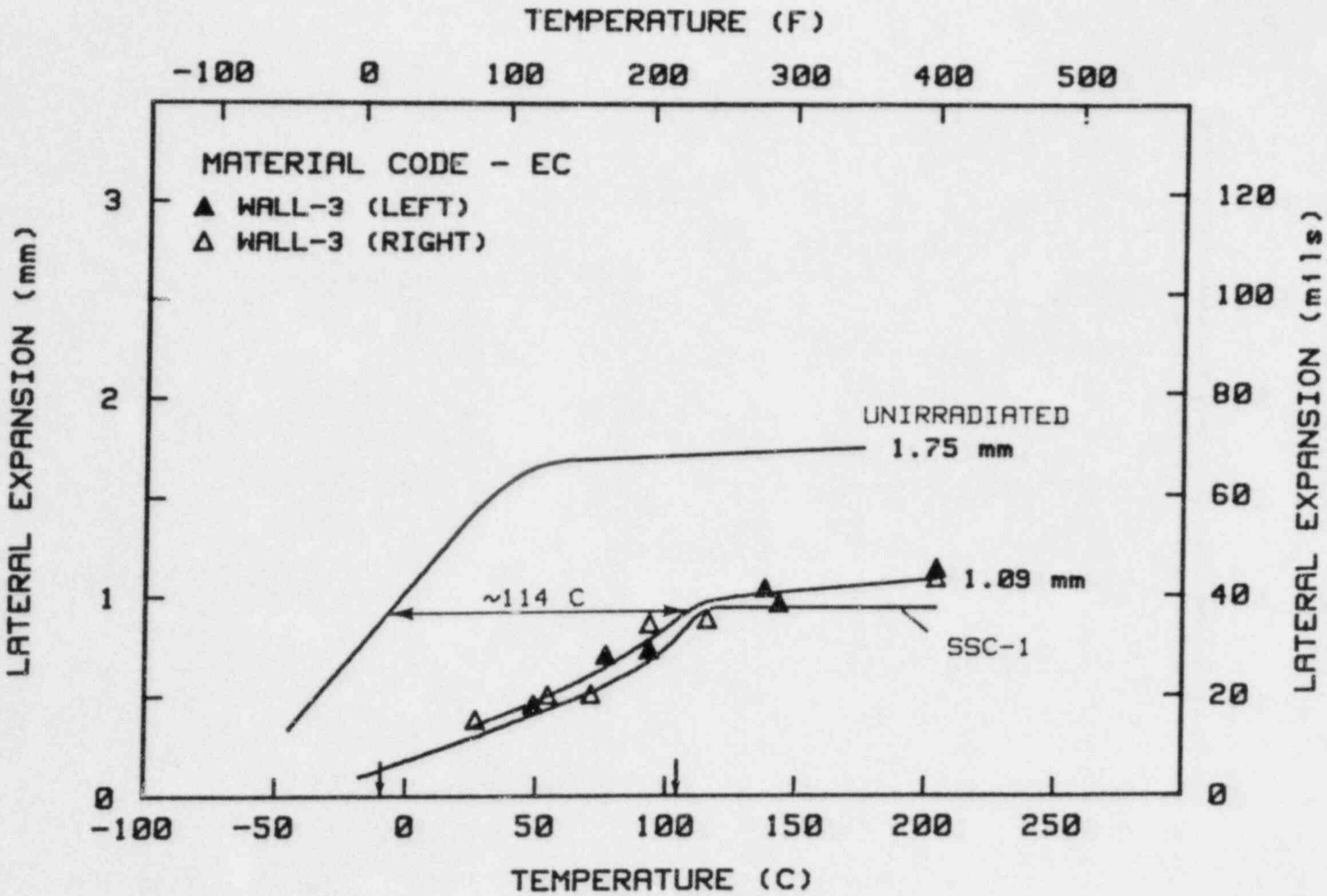

B.25 Charpy-V lateral expansion measurements for the submerged arc weld code EC before and after irradiation in capsule Wall-3

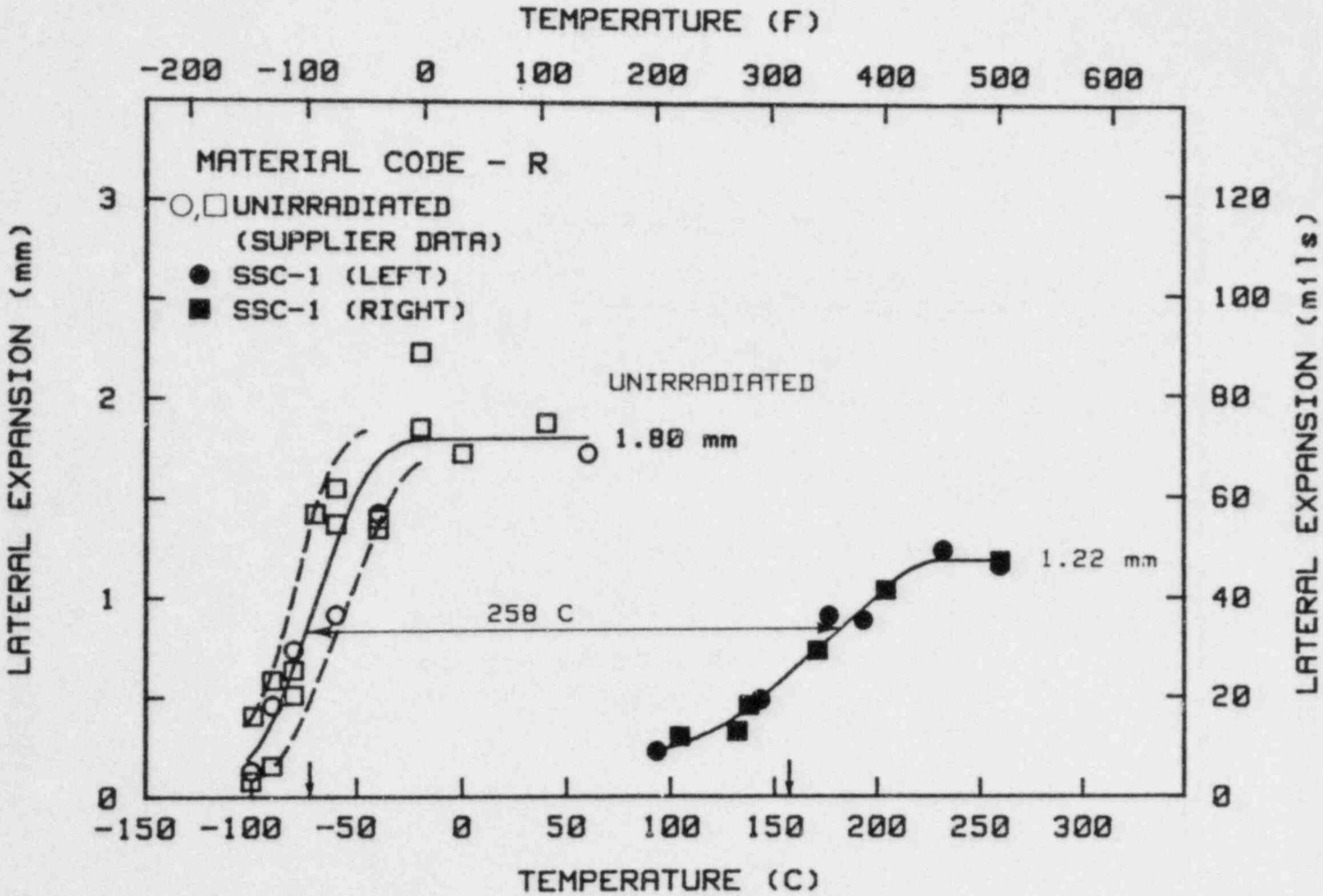

B.26 Charpy-V lateral expansion measurements for the submerged arc weld code R before and after irradiation in capsule SSC-1

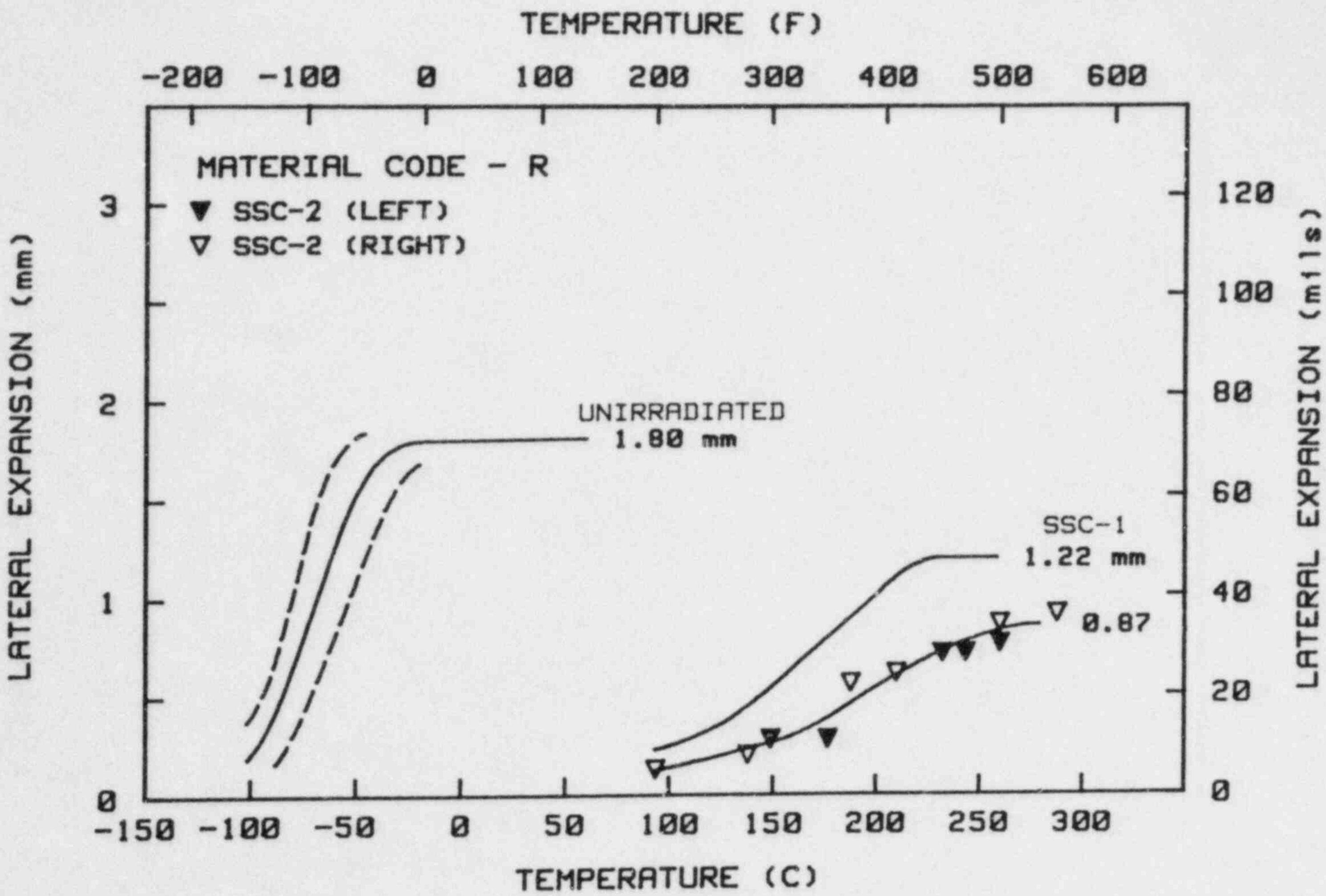

B.27 Charpy-V lateral expansion measurements for the submerged arc weld code R before and after irradiation in capsule SSC-2

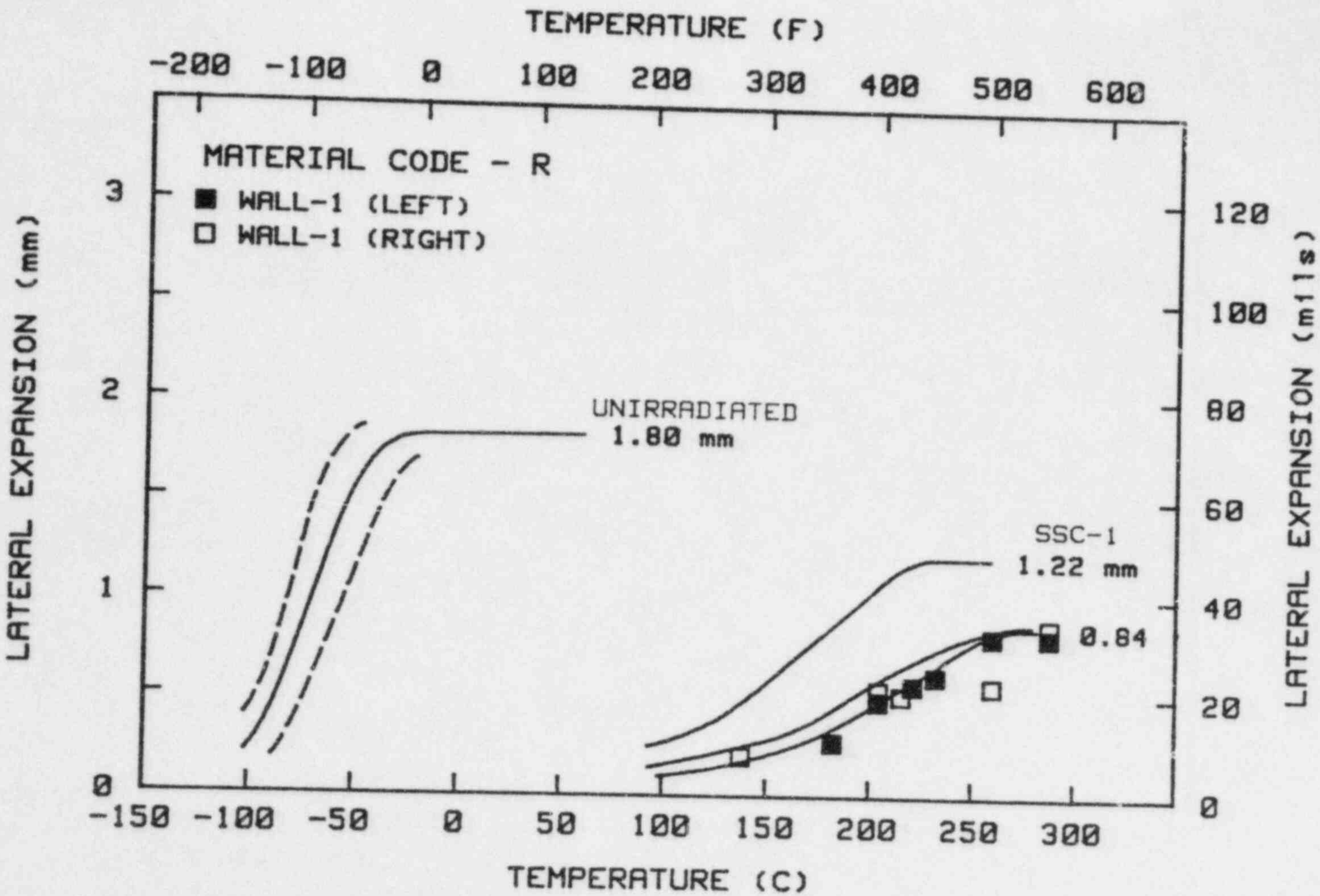

B.28 Charpy-V lateral expansion measurements for the submerged arc weld code R before and after irradiation in capsule Wall-1

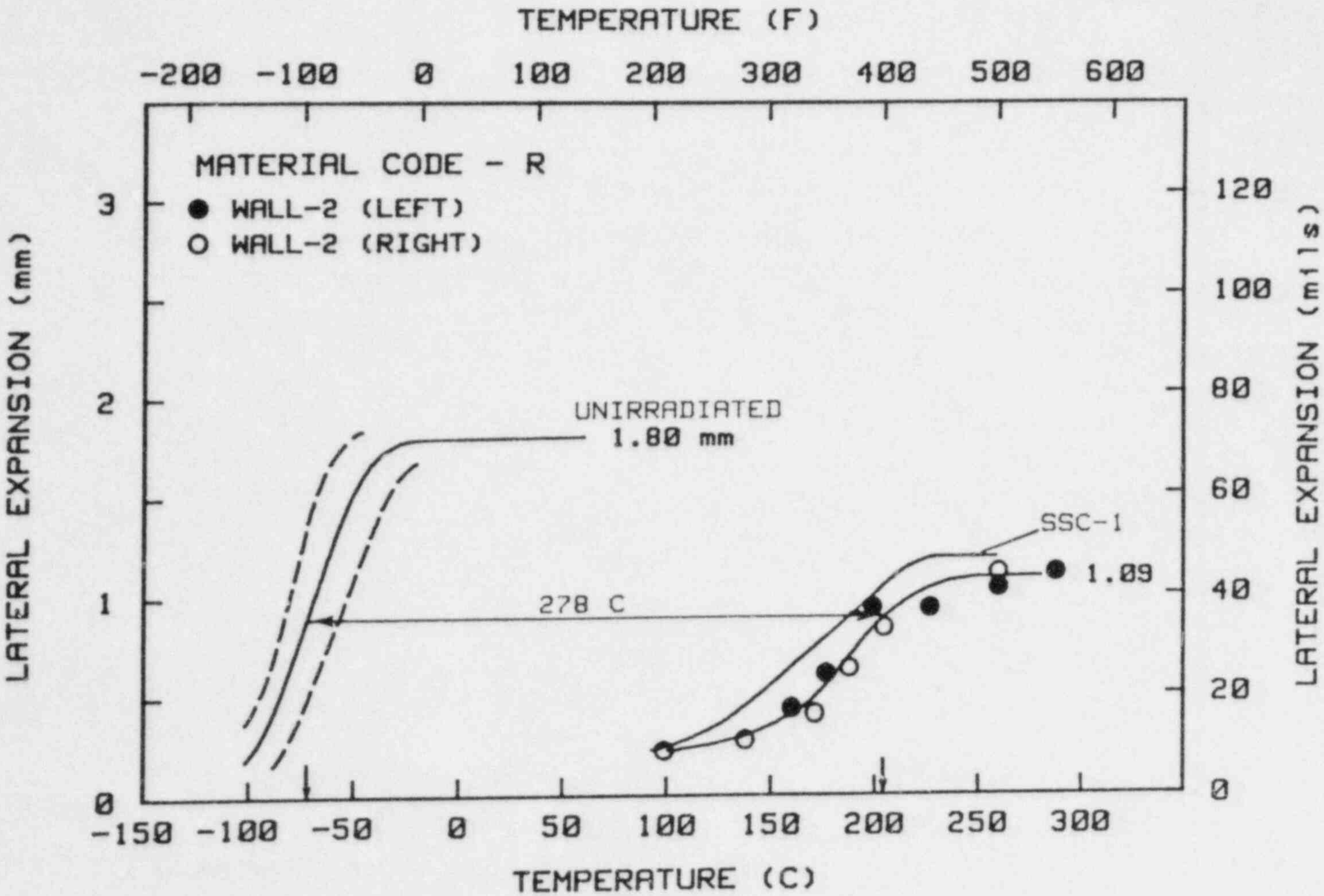

B.29 Charpy-V lateral expansion measurements for the submerged arc weld code R before and after irradiation in capsule Wall-2

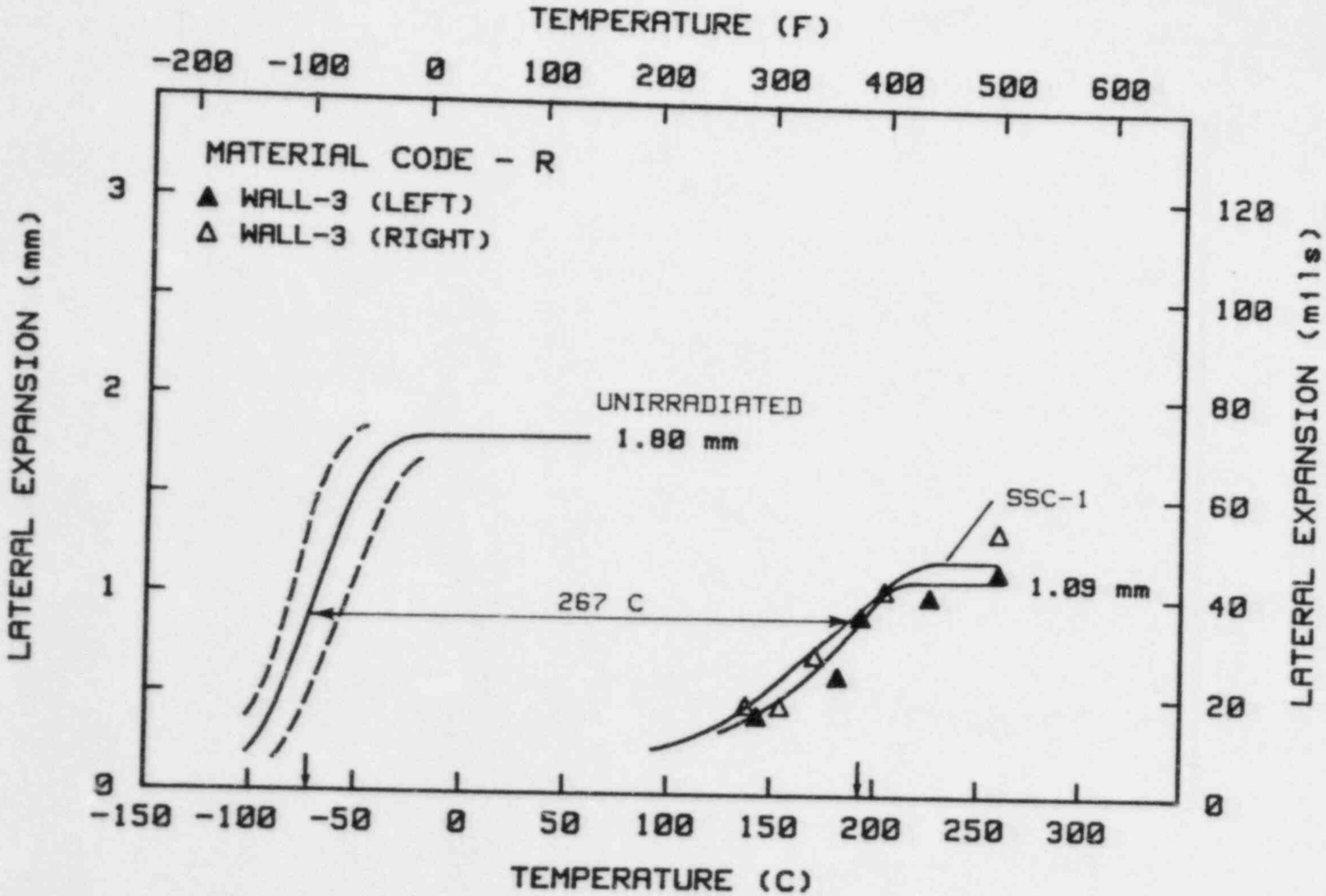

B.30 Charpy-V lateral expansion measurements for the submerged arc weld code R before and after irradiation in capsule Wall-3

NRC FORM 335
(11-81)

U.S. NUCLEAR REGULATORY COMMISSION

BIBLIOGRAPHIC DATA SHEET

1. REPORT NUMBER *(Assigned by DDC)*
NUREG/CR-3295
MEA-2017
Vol. 2

4. TITLE AND SUBTITLE *(Add Volume No., if appropriate)*
Light Water Reactor Pressure Vessel Surveillance Dosimetry Improvement Program: Postirradiation Notch Ductility and Tensile Strength Determinations for PSF Simulated Surveillance and Through-wall Specimen Capsules

2. *(Leave blank)*

3. RECIPIENT'S ACCESSION NO.

7. AUTHOR(S)
J. R. Hawthorne and B. H. Menke

5. DATE REPORT COMPLETED
MONTH: August YEAR: 1983

9. PERFORMING ORGANIZATION NAME AND MAILING ADDRESS *(Include Zip Code)*
Materials Engineering Associates, Inc.
9700B George Palmer Highway
Lanham, Maryland 20706

UNDER SUBCONTRACT TO:
ENSA, Inc.
3220 Bailey Avenue
Buffalo, New York 14215

DATE REPORT ISSUED
MONTH: April YEAR: 1984

6. *(Leave blank)*

8. *(Leave blank)*

12. SPONSORING ORGANIZATION NAME AND MAILING ADDRESS *(Include Zip Code)*
Division of Engineering Technology
Office of Regulatory Research
U.S. Nuclear Regulatory Commission
Washington, D.C. 20555

10. PROJECT/TASK/WORK UNIT NO.

11. FIN NO.
NRC FIN B8133

13. TYPE OF REPORT
Technical Report

PERIOD COVERED *(Inclusive dates)*

15. SUPPLEMENTARY NOTES

14. *(Leave blank)*

16. ABSTRACT *(200 words or less)*

The NRC's Light Water Reactor-Pressure Vessel Surveillance Dosimetry Improvement Program has irradiated Charpy-V (C_V) and tension test specimens of selected steels at 288°C in a pressure vessel wall/thermal shield mock-up known as the Pool Side Facility. Objectives include the study of through-wall toughness gradients produced by neutron irradiation and the relative irradiation effect at surveillance capsule vs. in-wall locations. This report presents properties data developed for six steels: the ASTM A 302-B reference plate, the HSST Program A 533-B Plate 03, A 508-3 and 22NiMoCr37 forgings, and two submerged arc weld deposits.

The radiation-induced toughness gradient between inner surface vs. mid-wall locations was small (31°C or less) for five of the six steels investigated. Tensile observations support the notch ductility trend indications. Simulated surveillance capsule irradiations reproduced well the embrittlement observed for vessel inner surface and quarter wall thickness locations in almost all cases. The primary exceptions to both trends were provided by a 0.23% Cu, 1.58% Ni weld deposit which showed the highest embrittlement sensitivity. Material irradiation sensitivity levels are in accord with predictions based on copper and nickel contents.

17. KEY WORDS AND DOCUMENT ANALYSIS

A 302-B Steel
A 508-3 Steel
A 533-B Steel
22NiMoCr37 Steel
Forgings
Fracture Resistance
Low Alloy Steels

17a. DESCRIPTORS

Notch Ductility
Nuclear Reactor Pressure Vessels
Radiation Embrittlement
Radiation Sensitivity
Reactor Vessel Surveillance
Submerged Arc Welds
Tensile Properties

17b. IDENTIFIERS/OPEN-ENDED TERMS

18. AVAILABILITY STATEMENT
Unlimited

19. SECURITY CLASS *(This report)*
Unclassified

20. SECURITY CLASS *(This page)*
Unclassified

21. NO. OF PAGES

22. PRICE
$

NRC FORM 335 (11-81)

UNITED STATES
NUCLEAR REGULATORY COMMISSION
WASHINGTON, D.C. 20555

OFFICIAL BUSINESS
PENALTY FOR PRIVATE USE, $300

FIRST CLASS MAIL
POSTAGE & FEES PAID
USNRC
WASH. D. C.
PERMIT No. G67

120555078877 1 1AN1RF1R5
US NRC
ADM-DIV OF TIDC
POLICY & PUB MGT BR-PDR NUREG
W-501
WASHINGTON DC 20555